EFFECT OF ALPHA7 NICOTINIC RECEPTOR ACTIVATION AND OVER-EXPRESSION IN BRAIN AND IN PC12 CELLS

By

KE REN

A DISSERTATION PRESENTED TO THE GRADUATE SCHOOL
OF THE UNIVERSITY OF FLORIDA IN PARTIAL FULFILLMENT
OF THE REQUIREMENTS FOR THE DEGREE OF
DOCTOR OF PHILOSOPHY

UNIVERSITY OF FLORIDA

2005

This document is dedicated to my parents: Xilin Ren and Aijuan Wang and my husband Jiang Liu.

ACKNOWLEDGMENTS

I would like to express my sincere appreciation and grateful thanks to Dr. Jeffrey A. Hughes for guiding me through the four years of Ph.D. study, giving me many excellent suggestions and supporting me in every respect. I am also extremely grateful for Dr. Edwin Meyer for providing a great environment in his laboratory and mentorship. He opened the door for me to explore the opportunities in research areas of nicotinic receptors and gene delivery. I would like to thank the members of my supervisory committee, Dr. Sean Sullivan and Dr. Sihong Song, for their valuable and kind advice throughout my doctoral research. I take this opportunity to express my gratitude to Dr. Mike King, Aaron Hirko, Craig Meyers, Jeffrey Thinshmidt and Dr. Yan Gong for all their help in conducting studies and in understanding them.

I also would like to extend my thanks to all the graduate students, exchange students, and post-doctoral fellows in the Department of Pharmaceutics who were my colleagues and friends for their support. Finally, I thank my husband Jiang, my parents and my sister for supporting me in many, many ways.

TABLE OF CONTENTS

LIST OF TABLES

Table page

LIST OF FIGURES

Abstract of Dissertation Presented to the Graduate School
of the University of Florida in Partial Fulfillment of the
Requirements for the Degree of Doctor of Philosophy

EFFECT OF ALPHA7 NICOTINIC RECEPTOR ACTIVATION AND OVER-EXPRESSION IN BRAIN AND IN PC12 CELLS

By

Ke Ren

December 2005

Chair: Jeffrey Hughes
Major Department: Pharmaceutics

Brain α7 nicotinic receptors are implicated in Alzheimer's disease through their actions on memory related behaviors, binding to beta-amyloid. α7 nicotinic receptors are calcium permeant and provide neuroprotection against many insults. The mechanism of α7 nicotinic receptors, intracellular calcium ions and downstream calcium channels in the protection were investigated. The α7 agonist GTS-21 prevented PC12 cell death induced by NGF + serum deprivation over a 3 day interval. This effect was blocked by the intracellular calcium chelator BAPTA-AM in a manner that did not appear to involve changes in receptor-density. BAPTA-AM blocked GTS-21 induced PKC activation, a necessary process for protection. The IP3 calcium channel blocker xestospongin C and the phospholipase C inhibitor U-93122 blocked protection and ryanodine receptor blocker ryanodine partially attenuated protection, but the L-type channel antagonist nifedipine had no effect. ERK1/2 but not JNK and p38 were activated by GTS-21, and the ERK phosphorylation inhibitors PD98059 and U0126 blocked protection. *In vivo*,

GTS-21 appeared to prevent cholinergic cell loss in septum following fimbria/fornix lesions in PS1 mice, but no protection in APP/PS1 and wild type mice.

Another approach to investigate the effects of α7 receptors on Alzheimer's disease-related processes involves elevating the levels of this receptor in the plasma membrane. We therefore took a somatic gene transfer approach to modify the expression of α7 nicotinic receptors in the brain. Recombinant adeno-associated virus (rAAV) was used. Vector containing rat α7 nicotinic receptors driven by the hybrid chicken beta actin/cytomegalovirus promoter was injected stereotaxically into wild type and α7 knockout mice hippocampus. Within three weeks, receptors were detected through binding assay and western-blots. The functional receptors were observed through electrophysiology response. rAAV 8/2-rat α7 nicotinic receptors gene transfer into wild type mice may improve acquisition performance in a dose-dependend manner.

In conclusion 1) IP3 calcium channel and ryanodine receptor are important for α7 nicotinic receptors mediated neuroprotection, but the L-type channel is not necessary for long term protection; 2) GTS-21 could prevent cholinergic cell loss in septum following fimbria/fornix lesions in PS1 mice; 3) rAAV-rat α7 nicotinic receptor could express functional receptors in rat, wild type and α7 knockout mice.

CHAPTER 1
INTRODUCTION

Alzheimer's Disease

Alzheimer's disease is an age related neuropathological disorder characterized by the presence of large numbers of neuritic plaques, neurofibrillary tangles and the progressive atrophy and loss of neurons. Aging is a major factor for this and many other neurodegenerative disorders. The United Nations population projections estimate that 50% of people older than 85 years of age are afflicted with AD (Allsop *et al.*, 2001). To date, the cause and progression of AD have not been fully elucidated. The "cholinergic hypotheses" was initially presented over 20 years age and suggests that a dysfunction of acetylcholine containing neurons in the brain contributes to the cognitive decline in AD (Terry and Buccafusco, 2003). Aging and AD have also been associated with degeneration of neurons of the ascending cholinergic pathway. The cell bodies of these neurons are located in the basal forebrain, and their axons innervate the amygdala, hippocampus and neocortex. Brain neuronal cholinergic transmission has not only been suggested to be affected in these pathologies, but also in human cognitive disorders associated with the normal process of aging. Among these are the age-related deficits in short- and long –term memory, impairment of attention, and delayed reaction time. Among several other observations relevant to the cholinergic systems, nicotinic acetylcholine receptors (AchR) binding sites have been reduced in number in the cerebral cortex of patients with AD (London *et al.*, 1989). The only FDA recognized therapies for

the disease are acetylcholinesterase (AChE) inhibitors such as aricept, tacrine, donepezil, rivastigmine and galantamine, and the NMDA antagonist memantine.

The rationale for using AChE inhibitors is to enhance cholinergic transmission in the brain by decreasing the metabolism of the neurotrasmitter acetylcholine. Basal forebrain cholinergic neurons that are important for memory related behavior are decreased in early AD, and this decrease becomes more evident as the disease progresses (Nordberg and Svensson, 1998). These basal forebrain neurons have their perikarya located primarily in the septum or the nucleus basalis. Septal cholinergic neurons send axons and nerve terminals to the hippocampus, providing the only cholinergic innervation of that region. Nucleus basalis cholinergic neurons send their projections throughout the cerebral cortex. This cerebral cortical innervation from nucleus basalis accounts for over 90% of the cholinergic activity in rodents; in humans, it accounts for about 60% of the cholinergic activity with the remainder due to intrinsic neurons in the neocortex. All of the AChE inhibitor drugs for AD are most effective in the early stages of the disease, presumably because there are more cholinergic neurons remaining for the drugs to act upon. Since AChE inhibitors protect acetycholine in the synapse, they increase all types of cholinergic transmission throughout the brain, including multiple muscarinic and nicotinic receptors. Which of these receptor subtypes collectively or individually are important for the beneficial effects of AChE inhibitors is an active area of study.

Several studies have shown that the expression and distribution of AChE in AD patients has changed (Kasa *et al.*, 1997; Talesa, 2001). AChE activity is lost in specific regions of the AD brain, such as the neocortex and hippocampus, which are important for memory-related behaviors. The relative proportions of different forms of AChE also

changed in this disease, suggesting changes in function. AChE has been found to co-localize with Abeta peptides, which appear to be involved in the disease as discussed below.

The rationale for using an NMDA antagonist in AD is to block the effects of elevated levels of glutamate that may lead to neuronal dysfunction. Glutamate receptors are already greatly reduced in this disease, and this is thought to be due to their excitotoxic properties. According to this model, excessive glutamate receptor activity in AD, especially that triggered by NMDA receptors, results in the excitotoxic loss of glutamate receptor expressing neurons. Memantine would prevent this toxicity, preventing further glutamate receptor loss and loss of neurons expressing these neurons. Memantine is the only one of the FDA approved drugs found to have efficacy in later stages of AD.

The "amyloid cascade" hypothesis is another of the central trends in AD research community (Allsop *et al.*, 2001). According to this hypothesis, neurodegeneration in AD begins with abnormal processing of the amyloid precursor protein (APP) and results in the production and aggregation of Abeta peptide-forming oligomers and amyloid fibrils that form the senile plaques. Less clear is whether these Abeta species trigger the formation of neurofibrillary tangles or eventually causes neuronal cell atrophy or death.

The amyloid cascade hypothesis has received considerable support from genetic studies into the early-onset familial forms of AD, for which mutations in APP or presenilin genes causing AD lead to an increase in Abeta production (Allsop *et al.*, 2001). Human APP mutations can cause amyloid plaques in transgenic in an age-related manner. These plaques are typically not seen until about 10 months of age, and become more

pronounced thereafter, especially in hippocampus and neocortex. Interestingly, transgenic mice with high levels of plaques exhibit only very modest decreases in memory related behaviors and few neuronal deficits. This suggests that AD may require more than just amyloid plaques.

Presenilins I and II were originally discovered and cloned through their involvement in genetic forms of AD. Subsequently, it was found that both of these gene products were involved in APP gamma secretase activity that leads to amyloidogenic peptides such as Abeta 1-42 (W., 2001). While once thought to be gamma secretase itself, presenilin was later shown to be a component of a multiprotein complex that has this enzymatic activity. Overexpression of mutant, AD-causing, human presenilin I in transgenic mice does not cause amyloid plaque formation. However, it does increase the levels of APP peptides and also causes modest behavioral changes. Further, double transgenic mice expressing mutant human APP and mutant presenilin I express amyloid plaques much more quickly than do single transgenics making mutant human APP alone.

Presenilins also appear to have a variety of additional cellular effects that may not be due to gamma secretase activity. These effects include the activation of multiple protein kinase pathways such as AKT and ERK1/2 that are involved in cell viability. It is possible that increased presenilin expression has complex effects on cell function, some reducing it (e.g., by increasing amyloid expression) and other improving it (increased kinase activity).

Important questions that remain are 1) how do mutations in presenilin or Abeta cause any of the symptoms seen in A? And 2) how do these mutations affect our ability to treat the disease pharmacologically? Recent studies suggest that both presenilin and

Abeta peptides affect pathways involved in cholinergic transmission, particularly involving nicotinic receptor mediated transmission.

A consistent and significant loss of some subtypes of nAChRs has observed in cortical autopsy brain tissue from AD patients compared to aged-matched healthy subjects. The neocortical nAChRs deficits significantly correlate with cognitive impairment in AD patients (Warpman and Nordberg, 1995). It was suggested that the nAChRs deficits in AD brains probably represent an early phenomenon in the course of this disease (Nordberg, 1994). Of the many nicotinic receptor subtypes found in the brain, the most attention has been focused on α7 nicotinic receptors because of their interactions with Abeta peptides, their importantance for memory related behaviors, their ability to be neuroprotective, and their loss of expression in AD.

α7 Nicotinic Receptors

AChRs exist as a variety of subtypes. Each of AChR subunits encoded by these genes is thought to have an extensive N-terminal domain positioned extracellularly, four transmembrane domains (MI-M4) that anchor these integral membrane proteins, and an extracellular C-terminus. nAChRs are ligand-gated ion channels that can be divided into two groups: muscle receptors and neuronal receptors. My research focuses on neuronal receptors because of their behavioral importance. Neuronal nicotinic receptors form a family of receptors that are differentially expressed in many regions of the CNS. nAChRs have many functions, such as cognition, sleeping, arousal, feeding behavior, neuronal development, and cell survival, but it remains to be determined which receptor subtypes are involved with which functions. Dysfunctions of nAChRs have been linked to a number of human diseases such as AD, Parkinson's disease and schizophrenia.

Nicotinic receptors consist of pentameric subunits that are either homemeric or heteromeric. Heteromeric brain nicotinic receptors consist generally of multiple α (mostly α2-4) and β (β2-4) subunits. The α4β2 combination is the most common combination of α and β subunits in the brain. α7 receptors, in contrast, are homomeric receptors. Mapping of AchR distribution at low resolution based on radioligand binding autoradiography is consistent with expression of some form of AchR in most of these "major" or "minor" cholonergic targets. Anatomic analyses also suggest that α4β2 and α7 (labeled using ^{3}H-labeled nicotinic agonists and ^{125}I-labeled Btx, respectively) have largely unique but sometimes overlapping distribution. Btx sites predominate in the septum, hippocampus, neocortex and hypothalamus, with lower density in the striatum. It has been suggested that α7 nicotinic receptors may play an important role in cognitive processes.

α7 receptors have a number of unique physiological and pharmacological properties among nicotinic receptors, including high permeability to calcium, rapid and reversible desensitization, and pronounced inward rectification. α7 receptors have a high affinity for the antagonists alpha-bungarotoxin and methyllycaconitine (MLA). The α7-receptor channel is highly permeable to calcium ions. Calcium acts as a second messenger inside the neuron and not only stimulates neurotransmitter release, but also stimulates signal transduction events through stimulation of protein kinases, calcineurins, nitric oxide synthetases and other enzymes (Kem, 2000).

α7 nicotinic receptors are located both pre- and post-synaptically (Albuquerque *et al.*, 1997). Their presynaptic location and ability to promote the conductance of calcium ions are consistent with an important role in the depolarization-dependent and calcium

ion-dependent release of neurotransmitters (Albuquerque *et al.*, 1997). These receptors have a very important postsynaptic location on gamma-aminobutyric acid-ergic (GABAergic) inhibitory tone (Adler *et al.*, 1998).

One of the difficulties in studying α7 receptor function is rapid desensitization (Seguela *et al.*, 1993). Selective agonists may act through receptor activation or subsequent desensitization. A standard approach to distinguish these possibilities is to use antagonists such as the non-selective mecamylamine, or the more selective MLA and α-bungarotoxin. If receptor-activation is required, these antagonists block the action; alternatively, their effects mimic antagonism if through desensitization. Nicotinic receptor antagonists that block α7 receptors interfere with memory related behaviors and block their neuroprotective properties. This indicates that agonist-activity is needed for these receptor functions.

α7 Nicotinic Receptors: Effects On Cell Viability *in vitro*

The pattern of activation of α7 nicotinic receptors by agonists is concentration dependent. Low concentrations of agonists induce a long term, low level and almost steady state increase in net cationic influx (Papke *et al.*, 2000). High concentrations of agonists, in contrast, cause a much larger spike in conductance that is also much shorter lived because of desensitization of the receptors. Only the longer term activation of the receptor by low agonist concentrations is associated with the neuroprotective effects of α7 receptor activation.

To date, α7 nicotinic receptor-mediated neuroprotection has been demonstrated in the following models: NGF- and serum-withdrawal from differentiated PC12 cells (Li *et al.*, 1999b); glutamate induced excitotoxicity in primary rat brain neuron cultures

(Shimohama *et al.*, 1998); Abeta amyloid exposure (Meyer *et al.*, 1998a); ethanol toxicity in primary neuronal cultures and PC12 cell (Li *et al.*, 1999a). In all these models, pretreatment with, and continued exposure to, agonist is necessary for neuroprotection. An overview of this subject recently concluded that nicotinic receptor mediated neuroprotection was attributable to α7 receptors (O'Neill *et al.*, 2002). For α7 receptors, the density of receptors and the binding affinity of the agonist could affect the extent of neuroprotection (Jonnala and Buccafusco, 2001). Even indirect activation of α7 nicotinic receptors by blocking cholinesterase activity is sufficient to be protective.

The mechanisms of α7 nicotinic receptor mediated neuroprotection *in vitro* have been studied with respect to several intracellular processes. Protein kinase C (PKC) activation, mitochondria membrane stabilization, reduced release of mitochondria cytochrome oxidase and increased BCL-2 expression have all been found to be involved in this neuroprotection (Li *et al.*, 1999a; Dajas-Bailador *et al.*, 2002a; Dajas-Bailador *et al.*, 2002c). α7 receptor mediated neuroprotection has also been found to require the Akt antiapoptic pathway (Shimohama and Kihara, 2001). However, many steps in the neuroprotection pathway are not known, starting with the role of calcium ions themselves, various calcium channels, other intermediary kinase systems, and even the level of α7-receptor density. It is also not known whether the pathways involved in neuroprotection depend on the model system.

While low levels of agonist activation are neuroprotective, high concentrations of agonists may be toxic to cells if applied quickly *in vitro* (Li *et al.*, 1999b). There is no evidence that this occurs *in vivo*, even at high doses of agonist. This may be due to the relatively slow delivery of drug through the circulation vs. rapid receptor desensitization.

However, it is a potential concern that must be addressed when considering any new approach that involves increased α7 receptor activity, since different approaches may affect the receptors and their interactions with cellular function differently.

α7 Nnicotinic Receptors: Neuroprotection Properties *in vivo*

The potential neuroprotective effects of α7 nicotinic receptors *in vivo* are not well understood. Pretreatment with the selective α7 receptor partial agonist GTS-21 was found to reduce the penumbral damage caused by focal ischemia in the rat cerebral cortex (Shimohama *et al.*, 1998). Dr. Meyer's laboratory suggested that GTS-21 could protect rat septal cholinergic neurons from partial fimbria-fornix lesions, though these lesions were minimal (fewer than 15% of the cholinergic neurons were lost even in controls). In a longer-term study of trans-synaptic cell loss, GTS-21 and nicotine were both found to protect cerebral cortical neurons from trans-synaptic loss or atrophy following lesioning of ascending nucleus baslis innervation (Meyer *et al.*, 1998b). This result was also seen in other nicotinic agonists (Socci and Arendash, 1996). However, no study has yet evaluated the neuroprotective effects of nicotinic receptor agonists in genetic models of AD such as the PS1 or APP/PS1 mouse.

3-benzylidene- and 3-cinnamylidene-anabaseine Compounds

Dr. Meyer's laboratory was the first to characterize families of 3-benzylidene- and 3-cinnamylidene anabaseine compounds as potential α7 receptor agonists for the treatment of brain disorders. While the 3-benzylidene anabaseine compounds (e.g., GTS-21) are typically selective partial agonists, the cinnamylidene anabaseines (e.g., 3-CA) are full or at least more efficacious agonists. Both types of compounds have been used to demonstrate neuroprotection through α7 nicotinic receptors. GTS-21 (also known as

DMXB) is 2,4- dimethoxybenzylidene anabaseine. It has been widely studied in preclinical animal models and evaluated in a Phase I trial for Alzheimer's disease (Kitagawa *et al.*, 2003). This drug has much lower efficacy for primate or human α7 nicotinic receptors than for rodent receptors. GTS-21 rapidly enters the brain after oral administration and improves memory related performance in nonhuman primates.

The pharmacokinetics properties of GTS-21 and 4OH-GTS-21 have been studied to a limited extent. Less than 1% of orally administered GTS-21 is recovered in the urine. Three-hydroxy metabolites are generated *in vitro* by rat hepatic microsomal O-dealkylation of the two methoxy substituents on the benzylidene ring. These metabolites are also found in plasma of rats after oral administration, but at significantly lower concentrations relative to the parent compound. However, the principal metabolite, 3-(4-hydroxy, 2-methoxy-benzylidene) anabaseine (4OH-GTS-21), displays a higher efficacy than GTS-21 on human as well as rat α7 nicotinic receptors (Figure 1-1). 4OH-GTS-21 has a similar level of efficacy for both rat and human α7 nicotinic receptors. The hydroxy metabolites are all more polar than GTS-21, derived from their octanol/water partition coefficients, and they enter the brain less readily than GTS-21 (Kem, 2000). However, they are behaviorally active when administered IP, indicating the ability to enter the brain at therapeutic levels.

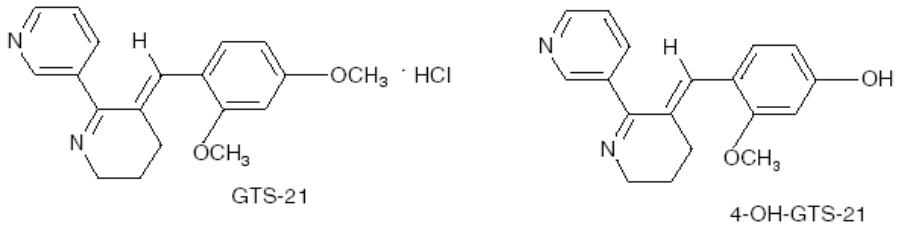

Figure 1-1. Chemical structures of GTS-21 and 4OH-GTS-21.

GTS-21 and 4OH-GTS-21 have been evaluated clinically. The pharmacokinetics of GTS-21 and 4OH-GTS-21 are shown in Table 1-1 and Table 1-2 (Kitagawa *et al.*, 2003).

Table 1-1. Mean ± SD Pharmacokinetic parameters for GTS-21 after oral adminstration of 25, 75 and 150 mg of GTS-21 for 5 Days

Parameter	25 mg	75 mg	150 mg
Cmax (ng/ml)	3.49± 0.09	12.8± 8.23	47.8± 28.4
Tmax (h)	1.19± 0.6	1.09± 0.28	1.02± 0.38
AUC	4.57 ± 2.62	32.7± 16.4	85.1± 32.9
t1/2 (h)	0.76± 0.38	0.93± 0.32	0.93± 0.19

Table 1-1. Pharmacokinetic parameters of GTS-21.

Table 1-2. Mean ± SD Pharmacokinetic parameters for 4OH-GTS-21 after oral adminstration of 25, 75 and 150 mg of 4OH-GTS-21 for 5 Days

Parameter	25 mg	75 mg	150 mg
Cmax (ng/ml)	2.71± 1.12	9.87± 5.19	32.9± 18.3
Tmax (h)	1.3± 0.58	1.23± 0.51	1.11± 0.48
AUC	7.49 ± 4.73	26.2± 5.72	71.3± 24.9
t1/2 (h)	0.81± 0.30	1.18± 0.41	1.15± 0.37

Table 1-2. Pharmacokinetic parameters of 4OH-GTS-21.

α7 Nicotinic Receptors and Memory Related Behaviors

α7 selective agonist such as GTS-21 improve several types of memory related behaviors, including spatial memory in the Morris water task (Meyer *et al.*, 1998a), passive and active avoidance behaviors in rats (Meyer *et al.*, 1997), radial arm maze in aged rats (Arendash *et al.*, 1995), delayed eye blink behavior in rabbits (Woodruff-Pak, 2003), hippocampal gating behavior in mice (Simosky *et al.*, 2001), and delayed pair

matching and word recall (Briggs *et al.*, 1997). In contrast, the selective antagonist MLA reduces performance in radial arm maze when injected directly into the hippocampus at low concentrations (Bettany and Levin, 2001). When injected peripherally, MLA also interferes with several memory related behaviors, though this effect is more obvious in ages, cognitively unimpaired rats than young adults rats or aged, impaired rats (personal communication; Dr. Greg Rose, Memory Pharmaceuticals). The less selective antagonist mecamylamine also interferes with memory related behaviors including the Morris water task in FFX-lesioned rats when administered peripherally (Brown *et al.*, 2001). As with many drugs that improve memory related behaviors in rodents, α7 nicotinic receptor agonists increase performance in lesioned or hypofunctional animals. Few reports show improvement in intact animals. However, GTS-21 was found to improve performance in delayed word match behavior in a small cohort of healthy adult humans (Kitagawa *et al.*, 2003). This observation suggests that these receptors may be effective for some behaviors even in normal individuals.

Models Of α7 Nicotinic Receptor Dysfunction: α7 Receptor KO Mice And Septohippocampal Lesions

α7 receptor knockout mice grow to normal size and show no obvious physical or neurological deficits. These animals do exhibit expected deficits in MLA-sensitive electrophysiological responses in hippocampus. This permits the knockout mouse to be used for α7 receptor gene delivery studies to demonstrate restoration of function.

Behavioral responses in α7 knockout mice also appear normal, except for anxiety-related behaviors in the open-field test. These observations may reflect developmental compensatory differences between normal and knockout mice, since, as noted above,

modulating α7 receptors function in wild type adults causes behavioral changes. Alternatively, it may be that some α7 receptors are modulatory but not necessary for neuronal function and thus, when present, are able to affect behaviors that do not depend on their presence. The α7 knockout mice were generated by introducing a 7 kb deletion into embryonic stem cells followed by transmission to the germline. The mutation deletes the last three exons (8-10) of the α7 locus. These exons encode the second transmembrane domain, forming the putative ion channel, and the third and fourth transmembrane domains and cytoplasmic loop (Orr-Urtreger *et al.*, 1997). Neuropathological examination of the brains of knockout mice revealed normal structure and cell layering, including normal neocortical barrel fields. The histochemical assessments of the hippocampus are also normal.

In contrast to the α7 knockout mice, mice expressing the α7 Leu250 point mutation show extensive apoptosis throughout the neocortex and most of them die within 24 hours of birth. This is probably due to the relative inability of this mutant to undergo desensitization. As previously suggested, the fast desensitization kinetics of wild type α7 nicotinic receptors, which limits large acetylcholine-elicited Ca^{2+} influxes, might protect against extensive neurodegeneration. The lack of additional neuroprotection in this α7 mutation relative to wild type mice suggests that a threshold Ca^{2+} level has to be reached for toxicity.

Another model of α7-receptor dysfunction involves lesions of the septohippocampal pathway, which reduce the cholinergic input to the hippocampus. The hippocampus has been organized to play a fundamental role in some forms of learning and memory, as shown since the early 1950s. The unusual shape of the human

hippocampus resembles that of a sea house, which is what led to its most common name (in Greek, hippo means “horse” and “kampos means “sea monster”) (Johnston *et al.*, 2003). It has been shown that damage to certain subregions of hippocampus can result in an enduring amnesic syndrome. Affected patients are incapable of recording everyday events and facts.

The hippocampus has been implicated in a number of neurological and psychiatric disorders, including epilepsy, AD and schizophrenia. Because of the important role of the hippocampus in learning and memory, it is not surprising that the hippocampus is functionally disconnected from the rest of the brain in this disease during later stages.

Lesioning the septal input to the hippocampus by ablating the fimbria-fornix pathway has recently been shown by Dr. Meyer and his colleagues to reduce α7 nicotinic receptor function as measured electrophysiologically in hippocampus in a manner that is overcome by chronic, twice-per-day injections of GTS-21 (Thinschmidt *et al.*, 2005). This reduction in function is paralleled by reductions in septal cholinergic density, but not changes in receptor binding density in the hippocampus. The effects of these fimbrial-fornix lesions on septal GABA neuronal survival are not known, but may be less than seen in the cholinergic system because only a small fraction of GABA neurons in septum project to the hippocampus. Selective lesions of either the cholinergic neurons or the GABA neurons in the septum are not enough to cause these receptor-function deficits. Instead, both types of neurons must be lesioned together such as by aspiration. Similarly, both types of neuron deficits are necessary for memory related behavioral impairments, with selective lesions in either type of nerve not causing much impairment (Yoder and Pang, 2005).

α7 Nicotinic Receptor And Beta Amyloid

There are data showing that 1) α7 nicotinic receptors are blocked by low concentrations of soluble Abeta 1-42 and other APP-derived peptides in a manner that is likely to be competitive (Liu *et al.*, 2001); 2) chronic oral treatment with nicotine reduces amyloid plaque accumulation in transgenic Swedish mutation overexpressing mice (Nordberg *et al.*, 2002); and 3) nicotine increases α-secretase products (APP soluble) (Efthimiopoulos *et al.*, 1996) while decreasing gamma-secretase products (Utsuki *et al.*, 2002). GTS-21 was also found to increase soluble APP in isolated rat brain nerve terminals, which would be expected to reduce amyloidogenic Aβ expression. These data suggested that a complex reciprocal interaction exists between nicotinic receptors and Aβ 1-42. Nicotinic receptor activation can be attenuated by the APP peptide but the levels of Aβ 1-42 and Aβ -containing plaques in turn can be reduced by nicotinic receptors activation. In my project, a selective α7 nicotinic receptor agonist, 4OH-GTS-21, was evaluated for neuroprotection in fimbria fornix (FFX)-lesioned mice of several genotypes: wild type, PSI only transgenic, and APP/PS1 double transgenic mice. The aspirative lesion used for the study affected both cholinergic and GABAergic neurons projecting to the hippocampus. This was the first time that an α7 nicotinic receptor agonist was tested for neuroprotection in this species, as well as in any combination model system consisting of both genetic changes and lesions.

I also investigated whether 4OH-GTS-21 could decrease the amyloid load in these mice. While it had been shown that nicotinic administered orally over a longer time interval was effective in reducing amyloid plaque load, it was not clear which receptor subtype or subtypes were mediated this effect. My study was designed to test the role of

α7 nicotinic receptors directly over a shorter interval (2 weeks), thereby testing the hypothesis that α7 nicotinic receptors could be targets for these components of this disease.

Memory Related Behavioral Tests

Morris water maze (MWM) is primarily designed to measure spatial learning and recall, and has become quite useful for evaluating the effects of aging, experimental lesions and drug effects (Jonasson *et al.*, 2004). MWM is a challenging task that employs a variety of sophisticated processes. These processes include the acquisition and spatial localization of relevant visual cues that are subsequently processed, consolidated, retained and retrieved. Several observations regarding the utility of the MWM are notable: 1) The functional integrity of forebrain cholinergic systems that are critical for efficient performance of that MWM appears to be consistently disrupted in patients who suffer AD (Perry *et al.*, 1999). 2) Neocortical and hippocampal projections from the nucleus basalis magnocellularis and septum are reproducibly devastated in AD. Accordingly, reductions in central cholinergic activity in rodents resulting from brain lesions and age reproducibly impair spatial learning in the MWM (McNamara and Skelton, 1993). 3) Other data implicated the hippocampus as an essential structure for place learning which is commonly atrophic in patients with AD (Terry and Katzman, 1983; Mann, 1991). 4) Anticholinergic agents that are used routinely to impair performance in the MWM also impair memory in humans and worsen the dementia in those with AD (Ebert and Kirch, 1998). 5) Spatial orientation, navigation, learning and recall are quite commonly disrupted in AD patients (Morris, 2003). However, the transgenic mice carrying human APP Swedish mutation and that develop amyloid

plaques, with or without mutant PSI co-expression, do not show large deficits in spatial learning and memory in MWM (Holcomb *et al.*, 1998).

The MWM procedure has several advantages as a means of assessing cognitive function in rodents when compared to other methods: 1) It requires no pre-training period and can be accomplished in a short period of time with a relatively large number of animals. 2) Through the use of training as well as probes, learning as well as retrieval processes can be analyzed and compared among groups. 3) Through the use of video tracking devices and the measures of swim speeds, behaviors can be delineated and motoric or motivational deficits can be identified. 4) By changing the platform location, both learning and re-learning experiments can be accomplished. This method is quite useful in drug development studies for screening compounds for potential cognitive enhancing effects.

rAAV Mediated Gene Transfer Into Brain

One of the approaches to increase receptor function without increasing agonist concentration, which as noted above is not always desirable in the case of α7 nicotinic receptors, is to increase receptor density by gene delivery. And one of the keys to successful gene delivery is the selection of the appropriate therapeutic genes and their molecular vehicle. A recombinant adeno-associated virus (rAAV) vector offers the advantage of the ability to infect non-dividing cells, affording a non-pathogenic, long-term transgene expression without a substantial inflammatory response when combined with appropriate promoters. One goal of my project was to develop α7 nicotinic receptors gene delivery systems for brain. This was hypothesized to provide safe, effective and long-term therapy to counteract α7 deficits.

rAAV is one of the most promising viral vectors for gene therapy due to its wide tropism and persistent transgene expression *in vivo*, and several clinical trials using rAAV to treat genetic disease have been carried out. rAAV is also a safe and effective means for studying transgene function in the brain.

AAV is a parvovirus with a diameter around 25 nm (Berns and Giraud, 1996). It is a single-strand 4.7 kb DNA (ssDNA) genome packaged into three viral capsid proteins: VP1 (87 kDa), VP2 (73 kDa) and VP3 (62 kDa). They form the 60-subunit viral particle in a ratio of 1:1:20 (Muzyczka *et al.*, 1984). The relatively high density of AAV particles allows us to be easily separated by CsCl density centrifugation from adenovirus helper particles whose density is approximately $1.35 g/cm^3$. The linear ssDNA contains two open reading frames flanked by two inverted terminal repeats of 145 nucleotides each (Sperinde and Nugent, 1998). The upstream open reading frame (ORF) encodes four overlapping nonstructural replication proteins (Rep), Rep78, Rep68, Rep52, and Rep40 (McLaughlin *et al.*, 1998). The downstream ORF codes for the capsid proteins. After entering host cells, the ssDNA genome of AAV is converted to the double-strand template in cell nuclei and finally integrated into the host genome at chromosome 19q13.3 in humans (Leopold *et al.*, 1998). This chromosome-selective integration is lost in rAAV vectors in which the Rep coding sequences are removed.

AAV has demonstrated a broad tropism of infection, including lung, brain, eye, liver, muscle, hematopoietic progenitors, joint synovium and endothelial cells (Miao *et al.*, 2000). The brain is a particularly good target for rAAV vector approaches because of the topic maps of neuroanatomical organization. rAAV vectors retain much of this tropism, with significant variations seen among serotypes depending on the tissue. These

serotypes differ in the composition of their capsid protein coat. rAAV serotype 2 (rAAV2) has been the most widely studied and best described among these. It binds to both heparan sulfate proteoglycans and fibroblast growth factor receptors as an essential step for cellular entry (Summerford *et al.*, 1999). Recently, rAAV5 and rAAV8 have also been investigated and found to bind to different cellular receptors. This probably accounts for their different biodistribution properties when injected in brain and other tissues. The mechanisms whereby other AAV serotypes enter host cells are actively being studied. Early studies showed that rAAV2 mediated transgene expression occurred in hippocampal interneurons, but not as strongly in hippocampal CA1 pyramidal neurons or dentate gyrus granul neurons. In my project, the rAAV8 vectors were also studied in hippocampus.

rAAV mediated transgene expression has persisted for up to 2 years after *in vivo* injection in rodent brains. rAAV-mediated expression is dose-dependent, but an accurate dose dependence of expression has not yet been established. It also depends on the kind of promoters chosen. Recently, we used the chick beta actin promoter/CMV enhancer, which provided very high, stable, and long term transgene expression. Staining for astrocytes or microglia following AAV-mediated transduction revealed no sign of gliosis or infiltration relative to vehicle injection. Given the lack of inflammatory response or pathogenicity, the reasonably high transduction efficiencies and the long persistence of transgene expression, rAAV has become a leading candidate vector for somatic gene transfer into brain *in vivo*.

AD is characterized by cholinergic deficits and degeneration of basal forebrain cholinergic neurons. Cholinergic degeneration correlates with loss of memory function.

Therefore, rAAV mediated α7 nicotinic receptor gene transfer may become a potential target for the treatment of AD.

Specific Aims

The goal of this project is to investigate the mechanism of α7 nicotinic receptors mediated neuroprotection and the potential of these receptors as targets for developing drugs for AD. I propose to evaluate α7 nicotinic receptors using selective α7 nicotinic receptors agonist such as GTS-21 and 4OH-GTS-21. Studies are focusing on three models: 1) cell cultures expressing α7 nicotinic receptors; 2) wild type and α7 knockout mice; 3) wild type, APP/PS1 and PS1 mice that have undergone FFX axotomy of the septohippocampal pathway. The specific aims of these projects are as follows:

1. Determine the roles of calcium, calcium channels, and several kinase-systems in α7 nicotinic receptor-mediated neuroprotection *in vitro*.
2. Test the hypothesis that the α7 nicotinic receptors agonist GTS-21 is efficacious in protecting septal cholinergic neurons from axotomy in wild type, PS1 overexpressing, and amyloid expressing mice.
3. Test the hypothesis that rAAV-rat α7 nicotinic receptor gene transfer increases receptor expression *in vitro* and *in vivo* without toxicity.

CHAPTER 2
MATERIALS AND METHODS

Construction of rAAV Plasmids

Vector plasmids used for these studies are pUF12-rat α7 with WPRE, pUF12-GFP, pUF12-rat α7 without WPRE were constructed from pUF12, which contains the chick β actin promoter with truncated cytomegalovirus (CMV) enhancer (CBA promoter). All plasmids had wild type AAV-2 terminal repeats (TR) and a poly (A) tail from bovine growth hormone. The mRNA stabilizer woodchuck posttranscriptional regulatory element (WPRE) was attached downstream to the α7 receptors in some rAAV2 vectors preparations. Rat α7 cDNA was subcloned into this plasmid using ClaI and verified using EcoRI and HindIII. GFP was subcloned into this plasmid using HindIII and verified with BamHI and BgIII. The DNA Core of the University of Florida analyzed both of the DNA sequences. The biological activities of the α7 nicotinic receptor-expression vectors were confirmed by western immunolabeling and binding assays following calcium phosphate transfection of rat pituitary tumor derived (GH4C1) cells. GH4C1 cells were incubated in 60 mm cell culture dishes in F-10 nutrient mixture (Ham) (Gibco BRL, Grand Island, NY) supplement with 10% fetal calf serum (FBS, Gibco, Invitrogen Corporation, CA) and 1% penicillin/streptomycin (Gibco, Invitrogen Corporation, CA) in a 5% CO_2 humidified atmosphere at 37^{o} C until 60% confluence. A mixture of 4 μg of plasmid DNA, 12.4 μl of 2 M $CaCl_2$ was prepared in a total volume of 100 μl filtered water. This mixture was added dropwise into equal volumes of 2 X HBS (280 mM NaCl,

10 mM KCl, 1.5 mM Na_2HPO_4 , 12 mM dextrose, 50 mM HEPES, pH 7.1). There were small precipitates at the bottom of dishes after two hours of transfection. The medium was changed after 8 hours of transfection and the cultures were incubated for up to 72 hours. For control groups, GFP was monitored in cells after transfection. Rat α7 expression was detected by western blot and binding assays at day 3 post-transfection.

Subcloning

A backbone was prepared of rAAV2- rat α7 vector. 20 µg of pUF12 was digested with Hind III at 37^o C for 1 hour. This digested reaction solution contained 6 µl Hind III, 6 µl NEB buffer 2, 20 µg DNA in 60µl water. The digested reaction solution was mixed with 12 µl 6 X DNA gel loading dye (30% glycerol, 6 mM EDTA, 0.06% bromophenol blue and 0.06% xylene cyanol FF) and loaded on the 1% agarose gel for a hour electrophorsis at 80 V. The larger size band was cut from the gel and extracted using an agarose gel extraction kit (Qiagen). The backbone was dephosphorylated using calf intestinal alkaline phosphatase (CIP, NEB). After dephosphorylation, the reaction was extracted with phenol-chloroform, followed by chloroform. The upper layer was collected. 2.5 volumes of 100% ethanol and one-tenth volume of 3 M NaAc pH 5.1 were added into the sample and mixed and precipitated at -80^o C for 2 hour. The sample was centrifuged at 5,000 g for 15 min. The supernatant was discarded. One ml of 75% ethanol was added to the pellet. The sample was centrifuged at 5,000 g for 15 min. The supernatant was removed and the pellet was air dried for 15 min and dissolved in 20 µl filtered water.

The second step was to add HindIII linker to rat α7 insert. Rat α7 insert was flanked by ClaI and blunt end ligated with T4 DNA polymerase. The blunt end reaction

contained 10 µl 10x Buffer T4 pol (NEB), 0.5 µl 25 mM dNTP (NEB), 3 µl T4 pol and 48 µl rat α7 insert and 38.5 µl water. The reaction was incubated at room temperature for 15 min. The whole reaction was mixed with 12 µl of 6-x DNA gel loading dye and loaded on the 1% agarose gel for a 1-hour electrophoresis at 80 V. The rat α7 insert band was cut from the gel and extracted using an agarose gel extraction kit (Qiagen). The insert was extracted by phenol-chloroform, then chloroform. DNA was precipitated by ethanol. The linker ligation reaction solution contained 17.5 µl rat α7 insert, 5 µl 5x DNA dilution buffer, 2.5 µl linkers (2.5 µg), 25 µl 2x ligation buffer and 2.5 µl ligase (Boehringer). The reaction mixture was incubated at room temperature for 5 min. The linker reaction was mixed with 6 µl of 6-x DNA gel loading dye and loaded on the 1% agarose gel for 1-hour electrophoresis at 80 V. At the same time rat α7 insert was loaded on the gel. The ligated linker shifted up a bit. The rat α7 insert linker band was cut from the gel and extracted using an agarose gel extraction kit (Qiagen). The fragment was extracted by phenol-chloroform, then chloroform. DNA was precipitated by ethanol. The pellet was dissolved in 10 µl water.

Gel electrophoresis was run to compare the relative concentrations of vector and insert. The third step was ligation. The ligation reaction contained approximately equimoloar concentration of backbone and insert, 2 µl 10 x ligation buffer and 2 µl T4 DNA ligase (NEB) and water. The total volume was 20 µl , which was added to a PCR tube. The ligation mixed was incubated in a PTC-200 DNA Engine Thermal Cycles (MJ Research) for overnight at 16^{o} C. The next day, 180 µl water was added into the ligation reaction. The ligation product was extracted by phenol-chloroform, then chloroform,

finally precipitated by ethanol. The pellet was dissolved in 10 µl H_2O. 2 µl of ligation product was used for transformation.

The next step was transformation. 2 µl of ligation product were transformed into 100 µl competent SURE cells (Stratagene, La Jolla, CA) using electroporation transformation methods. The cuvette was placed in the BioRad Gene Pulser II (Bio-Rad Laboratories). A single exponential decay pulse of 2.5 kV, 25 µF and 200 Ω were delivered. The whole reaction was added to 1 ml NZY (Fisher Scientific) without antibiotics and incubated in the shaker for 1 hour at 37^{o} C. 50 µl, 100 µl, 250 µl or 600 µl were added to 10 cm NZY/AMP (100 µg/ml) dishes and incubated at 37^{o} C overnight. Next day, six single colonies were selected and grown overnight. Minipreps of 6 single colonies were performed using Miniprep kit (Qiagen). The colonies were selected using restriction digestion and gel electrophoreses.

Plasmid Preparations

The plasmid was grown overnight in 5 ml of NZY/Amp (100 µg/ml) at 37°C on a shaking platform by pick a single colony. Next day, the culture inoculated into 2 L NZY/Amp (100 µg/ml) and incubated for 16-18 hour. The overnight culture was Spin down in 4 X 250 ml bottles at 5000 g for 15 min in a Sorvall RC-5B refrigerated superspeed centrifuge (DuPont Instruments). The pellets were resupsend in 20 ml of lysozyme buffer (25 ml Tris-HCl pH 8, 20 ml 0.5 M EDTA, 17.115 g of sucrose, dH_2O for a total volume of 1 liter). 12mg/ml of lysozyme (Sigma) was added, mixed and put on the ice for 5 min. 48 ml of solution II (20 ml 10% SDS, 4ml 10N NaOH, water for a total volume of 200 ml) was added, mixed and stored the bottles at room temperature for 4 min. 36ml of 3M NaAc (pH4.6-5.2) and 0.2 ml chloroform were added and mixed and

iced for 20 min. The mixtures were centrifuged at 5,000 g for 20 min. The clear supernatant was transferred into new 250 ml bottle through gauze. 33 ml of 40% PEG (Fishrs Scientific) was added, mixed and stored at -80^{o} C overnight. The mixtures were centrifuge at 5, 000g for 10min. The supernatant was removed and dissolved pellet in 10 ml of dH_2O. 10 ml of 5.5 M LiCl (Fisher Scientific) was added, mixed and iced for 10 min followed by centrifugation at 5,000 g for 10 min. 21 ml of supernatant were collected and transferred into 2 40 ml tubes. 6 ml isopropanol (Fisher Scientific) were added, mixed and iced for 20 min. The mixtures were centrifuged at 5,000 g for 10 min in small rotor. Each pellet was dissolved in 6.7 ml of TE buffer (10 mM Tris pH 8 and 1 mM EDTA). 8 g CsCl (Fisher Scientific) were added and mixed until dissolved. 0.44 ml of ethidium bromide (Fisher Scientific, 10 mg/ml) was added to each bottle. 8.9 ml of the solution were loaded into an Optiseal Beckman tube (Beckman Instruments). All tubes were loaded into a 70.1 Ti rotor and ultracentrifuged at 100,000 g in a Beckman L8-70M Ultracentrifuge for at least 19 hours at 20^{o} C. A hand held long wave UV 366 nm was used to estimate DNA density. There were two bands in the tube. The lower band was collected with 16 G needle (Becton Dickinson) and transferred to a 15 ml tube. The samples were extracted with equal volume of isoamyl alcohol (Fisher Scientific) until the sample was clear, then mixed and centrifuged at 3000 g for 2 min. 3 ml of the extracted sample were put into Corex tubes and 2.5 volume of H_2O was added, followed by 2 combined volumes of ethanol. The mixture was iced for 30 min. The mixtures were centrifuged at 5,000 g for 15 min. The supernatant was removed and the pellet dissolved in 400 µl of TE buffer in a 15 ml tube. It was washed with 400 µl of TE, which was pooled into the same tube. The sample was extracted with an equal volume of

phenol/chloroform (Amresco) until the interphase was clear, followed by chloroform extraction. The extracted sample (400 μl each) was transferred into 1.5 ml microfuge tubes. 40 μl of 3 M NaAc and 1 ml of ethanol were added, mixed and iced for 10 min, followed by microfuge for 5 min at max speed in a 5414 Centrifuge (Hamburg, German). The pellet was washed with 1 ml of 75 % ethanol, followed by 5 min at max speed. The supernatant was removed. The pellets were air dried for 15 min. Each pellet was dissolved in 200 μl sterile TE buffer. The DNA concentration was detected at 260/280 nm in a Beckman DU 650 Spectrophotometer. The plasmid was confirmed by restriction digestion and gel electrophoresis.

Packaging rAAV Vectors And Titration

The method used to package constructs and purify the rAAV was described by or modified from Zolotukhin et al (Zolotukhin *et al.*, 1999). HEK 293 cells at 70% confluence were transfected with two plasmids by the calcium phosphate method. One plasmid was pUF12-rat α7 or pUF12. The other was helper plasmid. The rAAV2 helper plasmid was pDG, which contained replication-deficient AAV genes for the rAAV protein coat and replication-defective adenovirus genes for helper function in packaging. The rAAV5/2 helper plasmid was pXYZ5. The rAAV8/2 helper plasmid was pXYZ8. These two plasmids were used in equal molar ratios for transfection. 10 cell culture dishes of 15 cm diameter were used. 1.25 ml of 2 M $CaCl_2$, 0.6 mg helper plasmid, 0.3 mg of pUF12-rat α7 or pUF12 and sterile water were mixed to the total volume of 10 ml for ten dishes. This mixture was added dropwise into equal volumes of 2x HBA while vortexing. This whole transfection mixture was added to 200 ml of warmed DMEM, which contain 10% FBS and 1% penicillin/streptomycin. 22 ml of this medium mixture

were added to each dish of HEK 293 cells. After a 6-hour transfection, the medium was removed and replaced with fresh DMEM. Seventy-two hours after the transfection, cells were harvested using cell a cell scraper (Corning Incorporated) and centrifuged at 3000 g at 4^{o} C for 20 min. The cells were resuspended in 15 ml of lysis buffer (150 mM NaCl, 50 mM Tris, pH 8.5). The suspension underwent 3 cycles of freeze thawing with dry ice/ethanol (10 min freeze, 15 min thaw, vortexing every 5 min). The samples were treated with benzonase (endonuclease, Sigma) to digest unpackaged DNA. 6 µl of 4.82 M $MgCl_2$ and 750 units of benzonase were added to 15 ml lysate and incubated at 37^{o} C for 30 min. The lysate was centrifuged for 30 min at 3,000 g at 4^{o} C. 15 ml of supernatant were collected in a 39 ml Optiseal tube through 16G needle. A Pump Pro (Watson-Marlow, UK) was set up as follows. 200 µl glass pipettes were used for intake and 100 µl glass pipettes were used for output. Pump speed was set at 37 rpm counterclockwise. The tube was rinsed with 40 ml water and 15 ml 15% iodixanol (IOD). The output pipette was loaded into Optiseal tubes. Pumping was started with 15% IOD (1:47 min), 25% IOD (1:15 min), 40% IOD (1:47 min) and 60% IOD (1:50 min). (180 ml of 15% IOD contained 45 ml of OptiPrep (Axis-Shield Poc AS, Norway), 36 ml of 5 M NaCl, 36 ml of 5x TD (5x PBS, 5 mM $MgCl_{2,}$ 12.5 mM KCl) and 63 ml water. 120 ml of 25% IOD contained 50 ml of OptiPrep, 24 ml of 5x TD, 46 ml of water and 300 µl of 0.5 % phenol red solution (Sigma). 100 ml of 40% IOD solution contained 68 ml of OptiPrep, 20 ml of 5x TD and 12 ml of water; 100 ml of 60% IOD contained 100 ml of OptiPrep and 250 µl of 0.5% phenol red solution). Tubes were sealed by heat and were untracentrifuged at 100,000 g in a Beckman L8-70M Ultracentrifuge for 2 hour at 18^{o} C. The rAAV band was located at the 1st interface (between 60% and 40%) from the

bottom of tube and up to 0.5 cm below the second interface; it was collected through a 16 G needle.

Heparin columns were used to purify AAV stereotype 2. Q sepharose was used for AAV serotypes 5 and 8. The heparin column was made as follows: the bottom of the Bio-Rad Econo-pac disposable chromatography column was snapped off and 6 ml of well-mixed heparin immobilized on cross-linked 4% beaded agarose (Sigma) were added to the column. The heparin column was equilibrated with 15 ml of 1xTD (1x PBS, 1 mM $MgCl_2$ and 2.5 mM KCl). The rAAV2 lysate was added onto the column, and then the column was washed with 20 ml of 1x TD. The rAAV2 was eluted with 15 ml of 1x TD/1 M NaCl. The 15 ml of eluted solution was collected into a 50 ml conical tube. The Q sepharose column was made as follows: the bottom of the Bio-Rad Econo-pac disposable chromatography column was snapped off and 5 ml of well-mixed Q sepharose (Sigma) were added into the column. The Q sepharose column was equilibrated with 20 ml of solution A (20 mM Tris/15 mM NaCl, pH 8.5) and the column was washed with 20 ml solution B (20 mM Tris/1M NaCl, pH 8.5) and again with 30 ml solution A. rAAV5/2 or rAAV8/2 sample was diluted with two times solution A and loaded to the column. After loading the sample, 50 ml of solution A were added to the column. The sample was eluted with 20 ml of solution C (20 mM Tris/355 mM NaCl, pH 8.5) and collected into a 50 ml conical tube. The sample was added into the concentrator (Minipore: Biomax-100K NMWL membrane) and centrifuged at 1,000 g for 5 min. The lysate was concentrated to 1 ml and diluted with 9 ml of Ringer's solution twice. The virus was concentrated to a final volume of 300 µl. Virus was collected into siliconized tubes (Fisher) and stored at -20^{o} C.

A dot-blot assay was used to determine the titer of rAAV virus based on total genomic particles. A 4 µl aliquot of the virus was treated with DNAse I (Roche) mixture for 1 hour at 37° C. This reaction contained 20 µl of 10X DNAse buffer (50 mM Tris-HCl, pH 7.5 and 10 mM $MgCl_2$), 2 µl of DNAse, 174 µl of dH_2O and 4 µl virus. After 1 hour, 22 µl Proteinase buffer (10 mM Tris-HCl, pH 8.0, 10 mM EDTA and 10% sodium dodecyl sulfate) were added and incubated for 1 hour at 37° C. An equal volume of phenol-chloroform was added to the sample, vortexed for 5 min and microfuged for 5 min at 14,000 g. This was followed by an extraction with an equal volume of chloroform and microfuging for 5 min at 14,000 g. The aqueous layer was transferred into a new microfuge tube to which was added 1/10 volume of 3 M NaAc (pH 5.2) and 2.5 volumes of ethanol. DNA was precipitated overnight at -80° C. Next day; the sample was microfuged at 14,000 g for 20 min. The supernatant was discarded. 0.5 ml of 75% ethanol was added to the pellet and microfuged at 14,000 g for 10 min. The pellet was air dried for 15 min and dissolved in 40 µl of water. The sample was quantified by a DNA slot blot assay using 1.7 kb EcoRI segment of pUF12 and a series of dilutions of pUF12 as standard curve. The dilution series of the pUF12 was started with 20-ng/µl and continued for 12 tubes. Each tube received 50 µl of water. 50 µl of DNA (20ng/µl) were pipetted from tube 1 to tube 2. Tube 2 was vortexed and 50 µl of DNA removed from tube 2 to tube 3. This dilution procedure was continued for all 12 tubes. A second set of tubes labeled 1-12 were set up behind the DNA dilution set. 200 µl of alkaline buffer (0.4 M NaOH, 10mM EDTA pH 8.0) were added to each tube. To each alkaline tube, 10 µl of DNA dilution set was added to each tube. For each virus sample, 10 µl of 1:10 dilution and 1:1 dilution each were added to 200 µl of alkaline buffer tube. The next step

was to set up the dot blotter (Bio-Rad). Two pieces of filter paper (Bio-Rad) were placed in water and then put on the dot blotter. Membranes (Bio-Rad, Zeta-Probe Blotting membranes) were put on the top of filter paper. The dot blotter was closed and 400 µl of water was added to each well. Vacuum was used to remove excess water. The standards of all 12 tubes (in alkaline buffer) and samples were boiled for 10 minutes. The standard curve tubes in alkaline buffer and samples were loaded to each well. The samples were aspirated slowly with vacuum until all samples disappeared. The vacuum was disconnected. 400 µl alkaline buffer were added to each well and allowed to stand for 5 min, followed by vacuuming remaining solution. The membrane was removed from the dot blotter and crosslinked by a UV crosslinker (UV Statalinker 1800, Strategene). The membrane was placed in a small Biometra bottle. Prehybridyzation buffer (7.5 ml, 7% SDS, 0.25 M $NaHPO_4$ pH 7.2, 1 mM EDTA pH 8.0) was added into the bottle and incubated at 65°C for 1 hour before labeling probe was added. 6 µl of biotinylated probe was diluted with 54 µl of 10 mM EDTA and denatured at 90°C for 10 min. The total 60 µl of denatured probe were added to the hybridization buffer and quickly mixed and incubated overnight at 65 °C in Biometra oven. A Brightstar Bio Detect kit (Ambion, TX) was used for detection. The membrane was placed into a staining container, then washed twice for 5 min in 1 X wash buffer (Ambion), followed by washing twice in blocking buffer (Ambion) for 5 min each. The membrane was then incubated for 30 min in blocking buffer. The membrane was incubated with 1 µl strep-alkaline phosphatase (Strep-AP) mixed with 10 ml blocking buffer for 30 min, followed by a 15-min incubation in blocking buffer. The membrane was washed 3 times for 5 min each in 1 X wash buffer and incubated with 1 X assay buffer for 2 min. The membrane was

incubated for 5 min in 5 ml of 1 X CDP-Star solution. The membrane was wrapped in a single layer of plastic wrap and exposed to film at room temperature in a dark room. The film exposure was for 15 mins. The blot was then scanned into computer and the intensity of the bands analyzed with NIH Scion image software (Scion Corporation, Maryland). The intensity of the bands for standard DNA was used to build a standard curve. The titers was calculated using the coefficients: 1 ng DNA = 4 x 10^{11} particles/ml. Vector stocks were ranged from 10^{12}-10^{13} genomic particles per ml, except for that containing the WPRE sequence (genomic lengths over 5000 kb) was 10^{7} genomic particles/ml.

Cell Transfections

GH4C1 cells were obtained from American Type Culture Collection (ATCC). The cells were grown in F-10 nutrient mixture containing 10% FBS and 1% penicillin/streptomycin at 37^{o} C in a 5% CO_2 and 90-92% humidity. The cells were split at a 1:3 ratio every 5 days, up to 10 passages. Cell confluence at the time of study was approximately 60%. The cell culture medium was removed. The cells were exposed to a 0.05% trypsin/0.53 mM EDTA solution for 5 min. After 5 min, the trypsin/EDTA was removed from the cells by transferring the cellular suspension to sterile conical tubes. These tubes were centrifuged at 3,000 g for 5 min. The supernatants were removed and the pellets were resuspended in 150 µl fresh medium. Increasing concentrations of 1.25 x 10^{9} /ml, 2.5 x 10^{9} /ml, 5 x 10^{9} /ml and 15 x 10^{9} /ml genomic particles were added to the medium and incubated for 30 min at 37^{o} C. After incubation, the cells were plated at the 60 mm dishes and added 2 ml of fresh medium was added to the dishes. 3-5 days after transfection, the cells were harvested for binding assays.

Stereotaxic Surgeries

Male Sprague-Dawley rats (~250g, 2 months old) were obtained from the Harlan Sprague Dawley Farm (Indiana). α7 heterozygous mice were obtained from the Jackson laboratory. They were housed and bred the in animal facility at the Health Science Center of the University of Florida. Rats or mice were anesthetized with 4% isoflurane/ oxygen. rAAV2-rat α7, rAAV2-GFP, rAAV8-rat α7 and rAAV8-GFP vectors were injected bilaterally into hippocampus or septum through a 27-gauge cannula connected via 26 gauge I.D. polyethylene tubing to a 10 μl syringe mounted to a CMA/100 microinjection pump. The pump delivered 2 μl virus (10^{10} genomic particles) at a rate of 0.15 μl /min. The injection coordinates for the hippocampus were –3.6 mm bregma, 2.2 mm medial-lateral, and 2.8 mm dorsal-ventral. For the medial septum, they were 0.7 mm bregma, 0.2 mm medial-lateral and 7.0 mm dorsal-ventral. The cannula was removed slowly removed after the injection. The skin was sutured. All animal care and procedures were in accordance with institutional IACUC and NIH guidelines. Two weeks or 6 months after injections, the animals were euthanized and their brains evaluated for receptor binding, immunohistochemistry, electrophysiology, or western blot.

High Affinity [^{3}H] MLA Binding Assay

Brain tissues or cell culture samples were prepared for nicotine-displaceable, high-affinity [^{3}H] methyllycaconitine (MLA) binding assay as follows. Septum or hippocampus was rapidly dissected from animals euthanized while fewer than 4% isoflurane/oxygen anesthesia and suspended in ice-cold Krebs Ringer buffer (KRH; in mM 118 NaCl, 5 KCl, 10 glucose, 1 $MgCl_2$, 2.5 $CaCl_2$, 20 HEPES; pH 7.5). Ice-cold

KRH was also used to wash, and then harvest culture cells. Brain tissues or cell culture samples were homogenized in ice-cold KRH buffer with a Polytron (setting 4 for 15 sec). After 2 1 ml washes with KRH at 20,000 g, the membranes were incubated in 0.5 ml Krebs Ringer with 2.3 nM [^{3} H] MLA (Tocris, Ellisville,MO), unless specified otherwise, for 60 min at 4^o C, plus or minus 5 mM nicotine. For determining the Kd and Bmax values, a range of total MLA was used from 0.5 nM to 50 nM for Scatchard analyses. Tissues were washed 3 times with 5 ml ice-cold KRH buffer by filtration through Whatman GF/C filters that were preincubated for 30 min with 0.5% polyethylenimine (Sigma). Liquid scintillation (EcoLite) counting of radioactivity was conducted in a Beckman LS1800. Nicotine-displaceable binding was calculated for each sample in triplicate in each experiment. Scatchard analyses are evaluated with the Statview program. ANOVA was performed for treatment effects.

In Bradford protein assay, 100 μleach of 0.1, 0.2, 0.4, 0.6 and 0.8 μg/μl of bovine serum albumin (BSA, Sigma) were used as standards to measure the protein concentration of the medium, brain samples and cell lysate samples. 50 μl of each samples were added into 5ml tubes containing 200 μl of 1 x KRH. Five ml of diluted (1:4 with water) BioRad protein assay dye reagent (Bio-Rad) was added to each tube, vortexed and sit for 30 min at room temperature. The O.D. of each tube was detected at 595 nm in a Beckman DU 650 Spectrophotometer (Beckman). A standard curve was prepared according to the concentrations and absorbance of the BSA standards at 595 nm and the protein concentration of each sample was determined using Prism software (GraphPad Software, Inc.CA).

Immunohistrochemistry

Animals anesthetized with 4% isoflurane/oxygen were perfused with 100 ml of cold phosphate-buffered saline (PBS), followed by 400 ml of cold 4% paraformaldehyde (Sigma) in PBS. The brain was removed and equilibrated in a cryoprotectant solution of 30% sucrose/PBS and stored at 4^{o} C. Coronal sections (50 μm thick) were cut on a sliding microtome with freezing stage. Antigen detection was conducted on floating sections by incubation in a blocking solution (2% goat serum/ 0.3% Triton X-100/ PBS) for 30 min at room temperature, followed by primary antibody incubation overnight at 4^{o}C. Primary antibodies used were: anti-α7-antibody mAb 306 (1:500, Sigma), 6E10 (1:1000, Signet, Dedham MA), glial fibrillary acidic protein (GFAP) (1:2000, Chemicon, Temecula, CA), NeuN (1:1000, Chemicon), anti-Chat (1:1000, Chemicon) and anti-parvalbumin (1:1000, Chemicon). To optimize α7 immunohistochemistry, 250 μl of 50% ethanol were added to each section and incubated for 30 min before added anti-α7 antibodies. The sections were washed in PBS 3 times for 5 min each and then incubated with biotinylated anti mouse IgG or anti rabbit IgG (1:1000, Dako, Carpinteria, CA) for 1 hour at room temperature. The sections were then washed with PBS three times for 5 min each and labeled with ExtrAvidin peroxidase (HRP) conjugate (1:1000, Sigma) for 30 min at room temperature. Development of color was conducted with a solution of 0.67 mg/ml diaminobenzidine (DAB, Sigma)/0.1 M sodium acetate/8 mM imidazole/2% nickel sulfate/0.003% H_2O_2. The sections were mounted on Fisher Superfrost Plus slides and air dried for 30 min. They were passed through water, 70% ethanol, 95% ethanol and 100% ethanol, and then the slides were xylene dehydrated. The slides were coverslipped with Eukitt (Calibrated Instruments,NY).

Some sections were used with fluorescent secondary antibody. After incubating with primary antibody, sections were washed in PBS 3 times and incubated with fluorescein (FITC)-conjugated anti-mouse (Jackson Immunoresearch, 1:1000) secondary antibody overnight at 4° C. Sections were washed in PBS and then mounted on Fisher Superfrost Plus slides, air-dried and coverslipped with glycerol gelatin (Sigma).

FluoroJade Staining

FluoroJade staining is a method to stain degenerating neurons. Floating brain sections prepared as describe above were treated with 100% ethanol for 3 min, followed by 70% ethanol and dH_20 for 1 min each, 0.06% potassium permanganate for 15 min, and a wash with dH_20 for 1 min. The sections were treated in the dark with 0.001% Fluoro-Jade for 30 min and then mounted on slides, air-dried and coverslipped with glycerol gelatin.

Western-blot

Septum or hippocampus was rapidly dissected from animal's euthanized under 4% isoflurane/oxygen anesthesia. Ice-cold sodium phosphate buffer (50 mM sodium phosphate, 50 mM NaCl, 2 mM EDTA, 2 mM EGTA, and 1 mM phenylmethysulfonyl fluoride, pH 7.4) was used to harvest cells. Fresh brain tissues or cell culture samples were homogenized with ice-cold 50 mM sodium phosphate buffer and centrifuged at 60,000 g for 60 min at 4 ° C. The supernatant was discarded. The pellets were resuspended in an ice-cold buffer containing 2% Triton X-100 and protease inhibitor cocktail (Sigma). The suspension was mixed for 2 hour at 4°C and then centrifuged at 100,000 g for 60 min at 4°C. The supernatants were used for western blot analysis. Protein contents in the fraction were assayed with the Bio-Rad protein assay kit. 25 μg each sample protein were mixed with 2x Laemmli sample buffer (Bio-Rad) and fresh 5%

2-mercaptoethanol. Samples were boiled for 5 min. Each sample was separated on 10% sodium dodecyl sulfate-polyacrylamide (SDS) gels by electrophoresis (150 V for 60 min). The proteins in the gel were blotted onto polyvinylidene difluoride membranes using a transfer unit (Bio-Rad) (120 V for 2 hour) at 4^{o}C. The membrane was blocked with 5% nonfat dry milk/ PBS buffer containing 0.05% Tween 20 for 60 min at room temperature. The membrane was incubated with monoclonal anti-α7 antibody (Sigma, mAb 306, 1:500) overnight at 4^{o}C, then washed three times with PBS/ 0.05% Tween 20 for 5 min each. The membrane was incubated with secondary antibody horseradish peroxidase-conjugated anti-mouse IgG (Amersham, 1:10,000 dilution) for 60 min at room temperature. The membrane was washed 3 times with PBS/ 0.05% Tween 20 for 5 min each. The membrane was exposed to ECL PLUS reagent (Amersham) for 1 min and the membrane was exposed to Hyper Performance Chemiluminescence film (Amersham). α7 nicotinic receptor band (MW 38,000) was quantified with the NIH Image program.

Morris Water Task

Morris water maze tests were performed to test the spatial learning and memory of mice injected rAAV2-rat α7 vectors. These tests were conducted using a specially designed water tanks (1 m) for mice with a fixed platform hidden just below (~ 1.0 cm) the surface of the water. The platform was rendered invisible by adding powdered milk to render the water opaque. Various geometric images (e.g., circles, squares, triangles) were placed in the testing room or hung on the wall in order that mice can use these visible objects as a means of navigating in the maze. Mice received 2 blocks of training trials (4 trials/block) daily for 8 days. With each subsequent entry into the maze the mice progressively become more efficient at locating the platform. The ninth day was for

probe trials. The mice had 60 seconds to search for the platform and they were hand guided to the platform if they did not reach it during that interval. The mouse was allowed 30 seconds on the platform. For each trial, latency to find the platform, path length to the platform, and swim speed were recorded by a video-tracking/computer-digitizing system (HVS Image, Hampton, UK). On day 9, animals were given a probe test in which the platform was removed and the rats had 60 seconds to search for the platform. The swim distance and percentage of time spent in each quadrant were recorded. The total time required for each animal to reach the platform was determined for the 8 days training period, and these values were compared among the treatment group by ANOVA. ANOVA was also used to compare probe (retention and recall) performance among the treatment groups.

Electrophysiological Recordings

Fresh horizontal slices (300 μm) were prepared using a vibratome (Pelco, Redding, CA). Slices were incubated at 30°C for 30 min and then maintained submerged at room temperature. The artificial cerebral spinal fluid (ACSF) used for cutting and incubating slices contained in mM: 124 NaCl, 2.5 KCl, 1.2 NaH_2PO_4, 2.5 $MgSO_4$, 10 D-glucose, 1 $CaCl_2$, and 25.9 $NaHCO_3$, saturated with 95% O_2 / 5% CO_2. Following incubation, slices were transferred to a recording chamber where they were superfused at a rate of 2 ml/min with ACSF at 30°C containing in mM: 126 NaCl, 3 KCl, 1.2 NaH_2PO_4, 1.5 $MgSO_4$, 11 D-glucose, 2.4 $CaCl_2$, and 25.9 $NaHCO_3$, saturated with 95% O_2 / 5% CO_2. Individual neurons were identified with infrared differential interference contrast microscopy (IR DIC) using a Nikon E600FN microscope (Nikon, Inc.). Whole-cell patch-clamp recordings were made with pipettes pulled on a Flaming/Brown electrode puller (Sutter

Instruments, Novato, CA). Pipettes were typically 3-5 MΩ when filled with an internal solution that contained in mM: 140 Cs-$MeSO_3$, 8 NaCl, 1 $MgCl_2$, 0.2 EGTA, 10 HEPES, 2 mg ATP, 0.3 Na_3GTP, and 5 QX-314. This solution blocked all action potentials and allowed stable voltage-clamp recording at depolarized membrane potentials. All internal solutions were pH adjusted to 7.3 using additional CsOH or KOH and volume adjusted to ~285 mOsm.

For experiments involving fluorescence microscopy, GFP-expressing neurons were visualized using light from a mercury lamp filtered at 510-560 nM. For all local application experiments, a picospritzer (General Valve, Fairfield, NJ) was used to apply ACh (1 mM) from pipettes identical to those used for whole-cell recording or from double-barreled pipettes made using theta tubing (Sutter Instruments, Novato, CA). An Axon Multiclamp 700A amplifier (Axon Instruments, Union City, CA) was used to amplify voltage and current records. The data were sampled at 20 kHz, filtered at 2 kHz, and recorded on a computer via a Digidata 1200A or 1321 analogue-to-digital converter using Clampex version 8-8.2 (Axon Instruments). Data were analyzed using Clampfit version 8-8.2 (Axon Instruments), OriginPro v. 7.0 (OriginLab, Boston, MA) and Graphpad Prism v. 3.0 (Graphpad Software, San Diego, CA).

Fimbria Fornix Lesions And 4OH-GTS-21 Injections

Wild type (Swiss Webster) and APP/PS1 (B6/D2 x Swiss Webster; a gift from Dr.Karen Duff) or PS1 (Taconic Swiss Webster x B6D2F1 crosses) mice are anesthetized with sodium 2-6% isoflurane/oxygen gas. Depth of anesthesia was determined by toe pinch and corneal reflex. Body temperature was maintained at 37^{o} C with an isothermal pad. The skull was exposed, and the bone from the region overlaying the septal area was

removed. A modified Pasteur pipette (pulled to a tip-diameter of 0.4mm) was lowered under visual control with a surgical microscope and mild vacuum applied to remove the fornix and small amounts of surrounding neocortical tissue. Stereotaxic coordinates for the lesion sites in mice were A.P. 0.1mm, M.L. $\pm$ 0.5mm, D.V.-2-3.8mm. Following the lesioning procedures, a piece of gel foam was placed in the skull hole, antibiotic powder was sprinkled over the skull, and the scalp was closed with tissue clamps. Animals were returned to their cages after fully reaching consciousness. 4OH-GTS-21 (1mg/kg) or 0.9% saline diluents was injected IP 2x daily (8AM or 6 PM) for two weeks post-lesion, with the first injection 30 min prior to the lesion.

Differentiation Of PC12 Cells

PC12 cells were obtained from American Type Culture Collection (ATCC). The cells were grown in RPMI Medium 1640 containing 10% heat-inactivated horse serum, 5% FBS and 1% penicillin/streptomycin at 37^{o} C in a 5% CO_2 and 90-92% humidity. The cells were plated in culture plates that had been pre-coated with collagen (BD Biosciences) for 3 hours. The cells were split at a 1:4 ratio every 3 days, up to 10 passages. Cell confluence at the time of study was approximately 60%. Cultures were maintained for 7 days in serum-supplemented media with 100-ng/ml nerve growth factor (NGF, BD Biosciences), which had been added at day 1 and day 3. On the day 7 of differentiation, the medium was replaced with one of the following conditions: serum medium with 100 ng/ml NGF, serum-free medium with or without NGF or serum-free medium containing specified concentrations of various drugs. 10 μM of 1,2-Bis (2-aminophenoxy) ethane-N,N,N$'$,N$'$- tetraacetic acid (BAPTA-AM, Molecular Probles Eugene), 500 nM of nifedipine (Sigma), 10 μM of xestospongin C (Calbiochem), 10 μM

of ryanodine (Sigma), 10 μM of PD98059 (Calbiochem), 10 μM of U0126 (Cell Signaling), 10 μM of U-73122 (Calbiochem), 100 nM of MLA (RBI, South Natick,MA) were added at specified time point in 100 μl sterile water immediately after medium replacement. 10 μM GTS-21 was added in 50 μl sterile water. Three days after NGF+ serum removal, five random photographs were taken in each plate with a Nikon inverted microscope. Images were analyzed in a blinded manner for cell density using the NIH Immage 1.55 program. There were 6 plates per treatment group. Cell counts are expressed as a mean$\pm$ SEM. Only the cells attached to the bottom of the dishes were analyzed.

Protein Kinase C (PKC) Assay

The total PKC activity was measured in membrane and soluble fractions of cell lysates obtained by probe sonication using a kit purchased from Amersham. The medium was removed from each well and replaced with HEPES-PO_4 buffer (137 mM NaCl, 5.4 mM KCl, 0.3 mM Na_2HPO_4, 0.4 mM KH_2PO_4, 1 mg/ml dextrose, 20 mM HEPES, 1mM $CaCl_2$,pH 7.2) and incubated for 10 min. The HEPES-PO_4 buffer was removed and 40 μl of kinase assay buffer (KAB) was added. 50 μg/ml digitonin, 200 μM MBP [4-14] substrate peptide, 100 μM NaATP and 30 μCi/ml (γ^{32} P) ATP were added immediately. The enzyme activity was measured for 10 min. The reaction was terminated with 10 μl of 25% trichloracetic acid. 45 μl of the acidified assay mixture from each well were spotted onto 2 x 2 cm Whatman P-81 phosphocellulose filter paper. Phosphorylated MBP [4-14] was quantified by liquid scintillation spectrophotometry in a Beckman LS1800 counter.

Tail DNA Extraction And Genetype

Mice homozygous for the *Chrna7*^{tm1Bay} mutation are viable and fertile, but are inconsistent breeders, producing small litters. The heterozygous *Chrna7*^{tm1Bay} mutation breeder mice were obtained from Jackson laboratory. Two-week-old mouse-tails were cut off at the tip (2-5 mm) and were transferred to a pre-labeled tube. 700 µl of lysis buffer (50 mM Tris, 100 mM EDTA, 0.05% SDS and 20 µg/ml proteinase K) were added to the tube. The tubes were incubated at 55^{o} C overnight. The tubes were removed from 55^{o} C and 150 µl 5 M NaCl were added. An equal volume of phenol-chloroform was added to the sample, vortexed for 5 min and microfuged for 5 min at 14,000 g. This was followed by an extraction with an equal volume of chloroform and microfuging for 5 min at 14,000 g. The aqueous layer was transferred into a new microfuge tube to which was added 2.5 volumes of ethanol. DNA was precipitated at -80^{o} C for 30min. The sample was microfuged at 14,000 g for 20 min. The supernatant was discarded. 0.5 ml of 75% ethanol was added to the pellet and microfuged at 14,000 g for 10 min. The pellet was air dried for 15 min and dissolved in 50 µl of water. 4 µl tails DNA were added to the 46 µl mix of the components for PCR amplification (9 µl 10X PCR buffer, 4 µl 2.5 mM dNTP, 2.5 µl 20 µM 1002 primer, 1.25 µl 20 µM 1003 primer, 1.875 µl 20 µM 1004 primer, 1 µl Taq DAN polymerase and 31.5 µl ddH_2O). The PCR reaction product was loaded to 1.5% agrose gel (Figure 2-1). The size of the α7 KO mouse band is 750 bp. The sizes of α7 bands for heterozygous is 440 bp and 750 bp. The size of wild type mice is 440 bp.

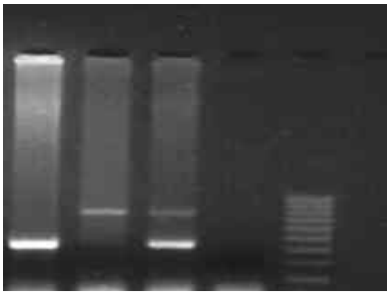

Figure 2-1. The α7 genotype of mice. 1: wild type mouse; 2: α7 knockout mouse; 3: α7 heterozygous mouse; 4: negative control; 5: 100 bp marker.

Statistical Analyses

Statistical analyses involved one way or multiple ANOVA for comparisons of parametric populations, using the Statview program. For non-parametric analysis, such as groups that undergo multiple treatments that may be interactive, resulting in a non-normal population, using a rank order test on the Statview program (acquisition behavior Morris water task).

CHAPTER 3
MECHANISMS UNDERLYING α7 NICOTINIC RECEPTOR NEUROPROTECTION IN PC12 CELLS

Introduction

PC12 cells and SK N SH cells were being chosen in this aim study. Both of them express endogenous α7 nicotinic receptors. It had shown that NGF-differentiated PC12 cells would undergo apoptosis following removal of both NGF and serum. NGF-deprivation is hypothesized to occur in AD in septal cholinergic neurons. SK N SH cells line is very sensitivity to exposure Abeta. We therefore used these two models to test the cytoprotective action of α7 nicotinic receptors.

Several groups including ours have demonstrated that GTS-21 and 4OH-GTS-21 α7 agonists increase intracellular calcium concentrations (Gueorguiev *et al.*, 2000; Li *et al.*, 2002). They also activate the calcium-sensitive transduction processes such as protein kinases A (PKA)(Dajas-Bailador *et al.*, 2002b) and C (PKC), inositol triphosphate (IP-3) kinase (Kihara *et al.*, 2001), ERK (Dajas-Bailador *et al.*, 2002b; Bell *et al.*, 2004), and janus kinase (Salehi *et al.*, 2004). PKC (Li *et al.*, 1999c), IP-3 kinase (Kihara *et al.*, 2001) and janus kinase (Salehi *et al.*, 2004) are each essential for α7 mediated protection against one or more apoptotic insults, while the roles of the other kinase pathways have not been studied. This protection through calcium-sensitive kinases suggests a protective role for the increased intracellular calcium ion concentrations observed following treatment with α7 agonists. However, there remains no direct demonstration that α7 receptor mediated protection or kinase activation depends

on intracellular calcium ions. We tested this hypothesis by investigating the effects of intracellular calcium ion chelation on both protection and PKC activation in NGF-differentiated rat pheochromocytoma (PC12) cells. These cells undergo apoptosis following NGF- removal and may provide a model for the dysfunction of ascending basal forebrain neurons associated with decreased NGF-transport seen in Down's syndrome and Alzheimer's disease (Kerwin *et al.*, 1992; Scott *et al.*, 1995; Cooper *et al.*, 2001; Salehi *et al.*, 2004). They also express α7 nicotinic receptors and are protected from apoptosis by prolonged treatment with α7 receptor agonists

Activation of α7 receptors can increase calcium accumulation both directly as well as through activation of downstream L-type voltage sensitive channels, IP-3 channels, and ryanodine channels (Vijayaraghavan *et al.*, 1992; Gueorguiev *et al.*, 2000; Shoop *et al.*, 2001; Dajas-Bailador *et al.*, 2002a), analogous to what is seen with metabotropic glutamate receptors (Fagni *et al.*, 2000). L-type channels are activated by depolarization triggered by the influx of sodium ions and calcium ions through these receptors, while the intracellular calcium channels are likely activated through calcium-influx through both α7 receptors and L-type channels. Blocking IP-3 channels with xestospongin C attenuates the long term increase in calcium accumulation following α7 receptor activation almost completely in PC12 cells, implicating these channels in neuroprotection (Gueorguiev *et al.*, 2000). An analysis of the calcium elevations triggered by nicotine in SH-SY5Y cells indicated that xestospongin C-sensitive IP-3 channel activation appeared to be more important than nifedipine-sensitive L-type channels or ryanodine-sensitive channels for the long term effects of α7 receptors (Dajas-Bailador *et al.*, 2002a). We therefore hypothesized that these three channels may be differentially important for the

long term cytoprotective actions of α7 receptors, which we tested in PC12 cells that express each of these calcium channels (Gafni *et al.*, 1997; Tully and Treistman, 2004)).

A third goal of this study was to evaluated the role of the calcium-sensitive MAP kinases ERK1/2, p38, and JNK in the α7 receptor mediated neuroprotection, since they are also differentially involved in the cytoprotective effects of other anti-apoptotic agents (Hetman and Xia, 2000; Hsu *et al.*, 2004; Kyosseva, 2004). ERK1/2 phosphorylation has been reported to be essential for the antiapoptotic effects of a wide variety of drugs (Hetman and Xia, 2000; Kyosseva, 2004). It was therefore a likely candidate for involvement in α7 receptor mediated protection, along with the other kinases mentioned above. Two other MAP kinase pathways, p38 and JNK, which are more frequently involved in stress responses than cytoprotection (Hsu *et al.*, 2004; Kyosseva, 2004), were also evaluated following α7 receptor activation to determine their potential involvement in the protective effects of these receptors.

Results

PC12 cells were plated in 60 mm culture dishes and differentiated for 7 days in the presence of 100 ng/ml NGF (Figure 3-1). NGF and serum were withdrawn from the medium at that time. The cells were treated with different concentrations of GTS-21 (0, 3 μM, 10 μM and 30 μM) for 72 hours. Cell density was measured after 3 days by the NIH Image system program (Figure 3-1). This figure demonstrates that NGF and serum withdrawn caused approximately a 50% cell loss. 3 μM and 10 μM GTS-21 induced protection and provided 80-90% cell survival. But 30 μM GTS-21 cause even more extensive cell loss.

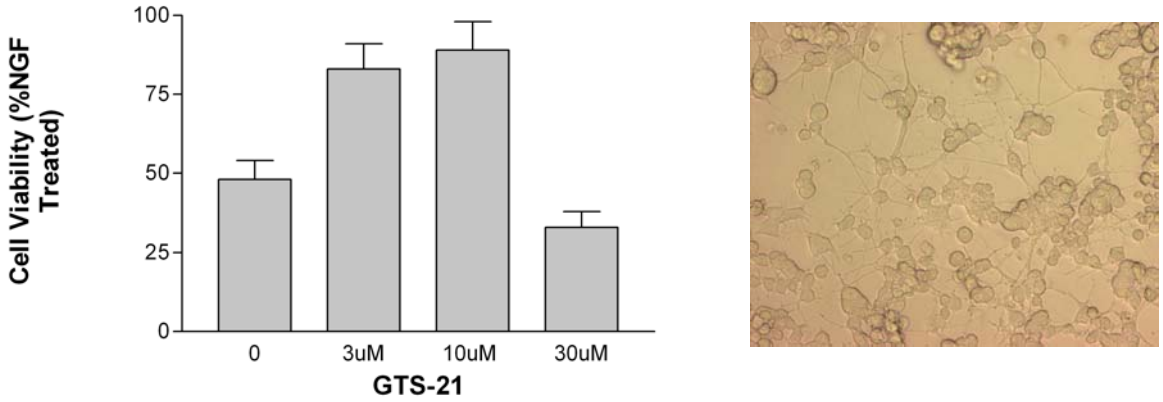

Figure 3-1. GTS-21 induced protection of PC12 cells during trophic factor deprivation. PC12 cells were plated in the 60 mm culture dishes and differentiated with NGF for 7 days. Cells were rinsed and the media was replaced with fresh media containing the treatment indicated above. Cell density was measured 3 days later and expressed as the mean ± SEM of 6-8 plates/group from 3 experiments. Three random areas were counted per plate and these 3 values were averaged to yield one value per plate. *$p < 0.05$ compared to untreated group (one way ANOVA).

In order to evaluate the role of intracellular calcium ions and α7 receptors in this cytoprotection. 10 μM BAPTA-AM and 100 nM MLA were added either 30 min before (pretreatment) or 30 min after (posttreatment) GTS-21. Treatment with BAPTA alone had no effect on cell survival during NGF + serum removal or in the presence of NGF, though it blocked the cytoprotective action of 10 μM GTS-21 when added 30 min prior to or 30 min after the receptor agonist. MLA similarly blocked the GTS-21 induced protection when added at both time points (Figure 3-2).

None of the treatments affected the Kd for high affinity MLA binding to α7 receptors (range: 1.6-2.3 nM). Removal of NGF + serum reduced the density of α7 receptors over the 3 day but not 30 min interval (Table 3-1); this reduction was not seen with addition of 100 ng/ml of NGF. Addition of BAPTA to the NGF + serum deprived

medium had no acute effect on α7 nicotinic receptor binding density, but also modestly increased density over the 3 day interval compared to cells without the chelator. Neither GTS-21 nor GTS-21 + BAPTA preserved receptor density in this manner.

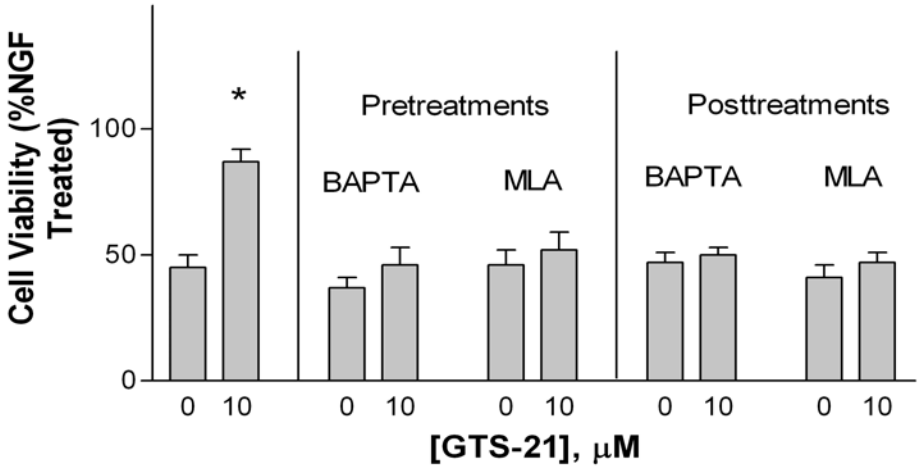

Figure 3-2. Effects of intracellular calcium chelation on GTS-21 induced protection of PC12 cells during trophic factor deprivation. Cells were differentiated for 7 days with 100 ng/ml mouse NGF and then exposed to serum-free medium containing either BAPTA-AM (10 μM), GTS-21, or MLA (100 nM). BAPTA-AM and MLA were added either 30 min before (pretreatment) or 30 min after (posttreatment) the GTS-21. Cell density was measured 3 days later and expressed as the mean ± SEM of 6-8 plates/group from 3 experiments, normalized to the NGF-treated values for each experiment. *$p < 0.05$ compared to untreated group (one way ANOVA).

10 μM of BAPTA also blocked the concentration-dependent GTS-21 induced elevation in PKC membrane translocation seen in these NGF and serum withdrawn differentiated PC12 cells (Figure 3-3).

Table 3-1. Effects of BAPTA and GTS-21 on α7 receptor binding density in PC12 cells

Treatment	High affinity MLA binding (Bmax in fmol/mg protein)	
	30 min	3 days
NGF+serum removal	152 ± 11	107 ± 10^
+ NGF (100 ng/ml)	165 ± 18	172 ± 15*
+ BAPTA (10 μM)	167 ± 13	144 ± 13*
+ GTS-21 (10 μM)	155 ± 17	101 ± 14^
+ BAPTA + GTS-21	172 ± 16	98 ± 12^

Table 3-1. PC12 cells were differentiated for 7 days with 100 ng/ml NGF and then exposed to NGF + serum withdrawal. Specified concentrations of NGF, BAPTA, or GTS-21 were added and high affinity [^{3}H] MLA was measured 30 min or 3 days later. Each value is the mean ± SEM of three samples, each assayed in tripicate. *$p < 0.05$ compared to same time point, no drug-treatment (two way ANOVA); ^$p < 0.05$ compared to 30 min interval, same treatment.

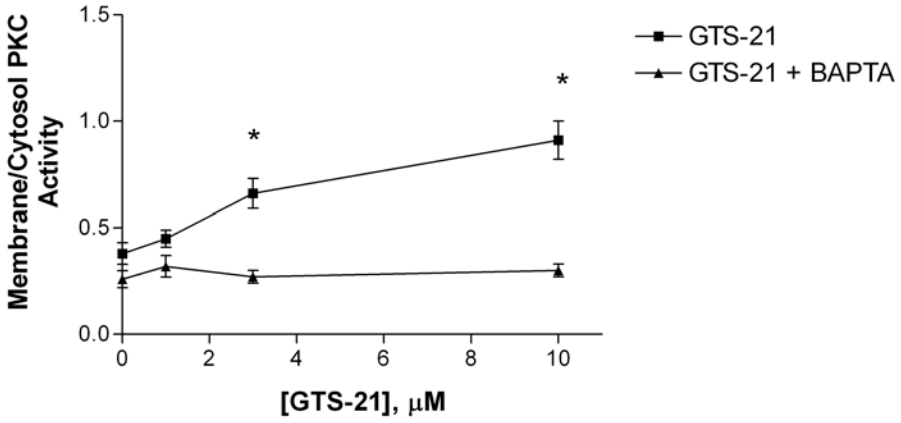

Figure 3-3. Effects of intracellular calcium chelation on PKC activation by GTS-21 in PC12 cells. Cells differentiated as in Figure 3-1 were simultaneously exposed to serum and NGF removal, as well as to specified concentrations of GTS-21 in the presence or absence of 10 μM BAPTA-AM. 15 min later, cells were fractionated to membrane and soluble portions, each of which was assayed for phorbol-stimulated PKC activity/mg protein. Values are expressed as the ratios of membrane/soluble PKC activity; N = 6 plates/group from 3 separate experiments. *$p < 0.05$ compared to BAPTA-treated group, same GTS-21 concentration.

Effects of 4OH-GTS-21 on PKC isozyme translocation were tested. Different concentrations of 4OH-GTS-21 were used in serum and NGF withdrawn differentiated PC12 cells. 3 μM and 10 μM 4OH-GTS-21 increased PKC alpha translocation (Figure 3-4). But 30 μM 4OH-GTS-21 decrease the membrane/soluble ratio of PKC alpha. PKC delta membrane/soluble ratios were decreased at higher concentrations of 4OH-GTS-21. PKC gamma was unaffected.

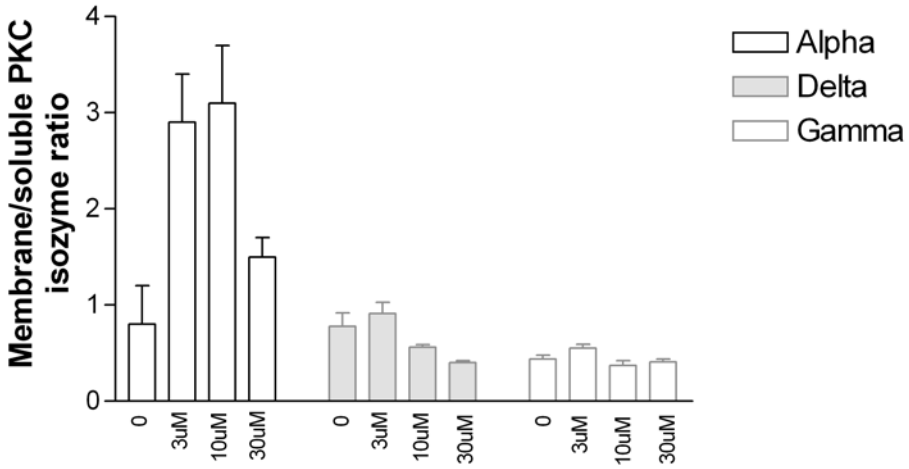

Figure 3-4. Effects of 4OH-GTS-21 on PKC isozyme translocation. Neuroprotective concentration of 4OH-GTS-21 increased the membrane/soluble ratio of PKC alpha, a measure of its activation. PKC delta membrane/soluble ratios were decreased, but over a higher concentration range. No effect was seen on translocation of PKC gamma.

In order to determine the roles of different calcium channels in α7 receptor induced neuroprotection, some cells were treated either with L-type channel blocker nifedipine, ryanodine receptor blocker ryanodine, IP3 channel antagonist xestospongin C, phospholipase C inhibitor U-73122 with or without 10 μM GTS-21. The voltage sensitive L-type calcium channel blocker nifedipine had no effect on cell viability when applied alone or when with GTS-21 (Figure 3-5). Ryanodine partially attenuated the GTS-21 induced protection, also without direct effect alone, indicating that only some

cells appeared to depend on this channel activation for survival in this model. Xestospongin C, the IP3 channel antagonist, completely blocked α7 receptor mediated protection and had no effect on cell density when applied alone.

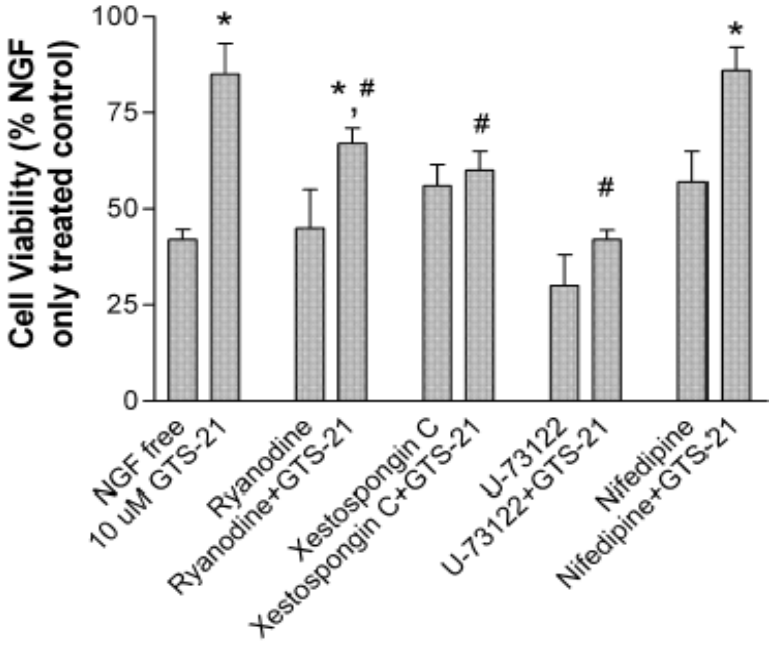

Figure 3-5. Effects of calcium channel antagonists on GTS-21 induced cytoprotection in NGF-deprived PC12 cells. Cells differentiated as in Figure 1 were treated with 10 μM GTS-21 immediately after NGF + serum removal, with or without 10 μM ryanodine, 10 μM xestospongin C, 10 μM U-73122 or 500 nM nifedipine. Each value is the mean ± SEM of 6-8 plates/group from 3 separate experiments. *$p < 0.05$ compared to same treatment without GTS-21;#$p < 0.05$ compared to GTS-21 only treatment group (one way ANOVA).

Serum and NGF were withdrawn from differentiation PC12 cells and 10 μM GTS-21 was added to cells. ERK1/2, p38 and JNK-phosphorylation were measured at 5 and 180-minute time interval. ERK1/2-phosphorylation was increased by 10 μM of GTS-21 within 5 minutes, and this effect increased by 3 hours (Figure 3-6). Increased ERK1/2 phosphorylation was blocked by 500 nM MLA applied 5 minutes before GTS-21 addition (not shown). p38- and JNK-phosphorylation were unaffected by GTS-21 at either time interval.

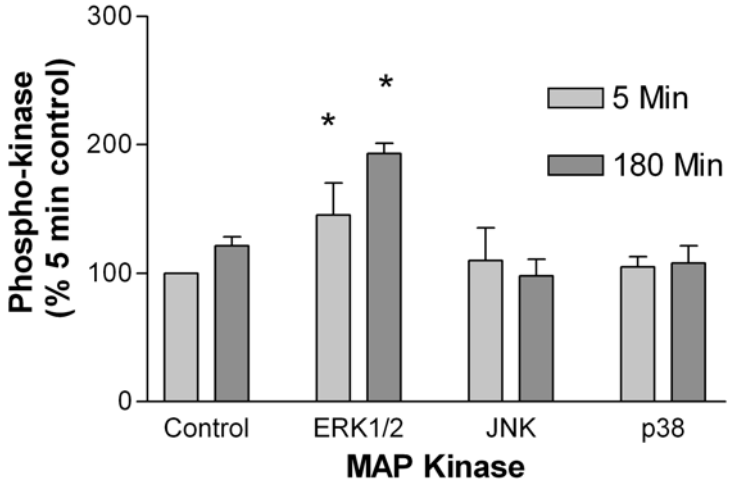

Figure 3-6. Effects of GTS-21 on the phosphorylation of several MAP kinases in PC12 cells. Cells differentiated as in Figure 1 were treated with 10 μM GTS-21 for the specified interval upon removal of the NGF + serum. Whole cell extracts were assayed for phospho-ERK1/2, phospho-JNK and phospho-p38 by western blotting and expressed as the mean ± SEM of 4 samples/group, normalized to the 5 minute control value for that experiment. Each gel contained two lanes from the same 5-minute control sample that were averaged and used for normalization. *$p < 0.05$ compared to control from same time point (one way ANOVA).

Four different concentrations of GTS-21 (0, 0.5,3 and 10 μM) were used to test ERK1/2 phosphoration (180 minutes later). Some of groups pretreated with 100 nM MLA. The effect of GTS-21 on ERK1/2 phosphorylation was concentration dependent. This effect was blocked by MLA, demonstrating the role of α7 receptors (Figure 3-7).

GTS-21 mediated neuroprotection was blocked by either pretreatment with the PKC blocker BIM or the ERK1/2 blocker U0126 and PD98059 (Figure 3-8).

Various kinase inhibitors were tested on the effects of 4OH-GTS-21 on differentiation PC12 cells. α7 antagonist MLA (1 μM), PKC antagonist BIM1 (100 nM), ERK1/2 inhibitor PD98059 (20 μM) and PKA inhibitor H89 (1 μM) blocked 4OH-GTS-21 provided cytoprotection (Figure 3-9).

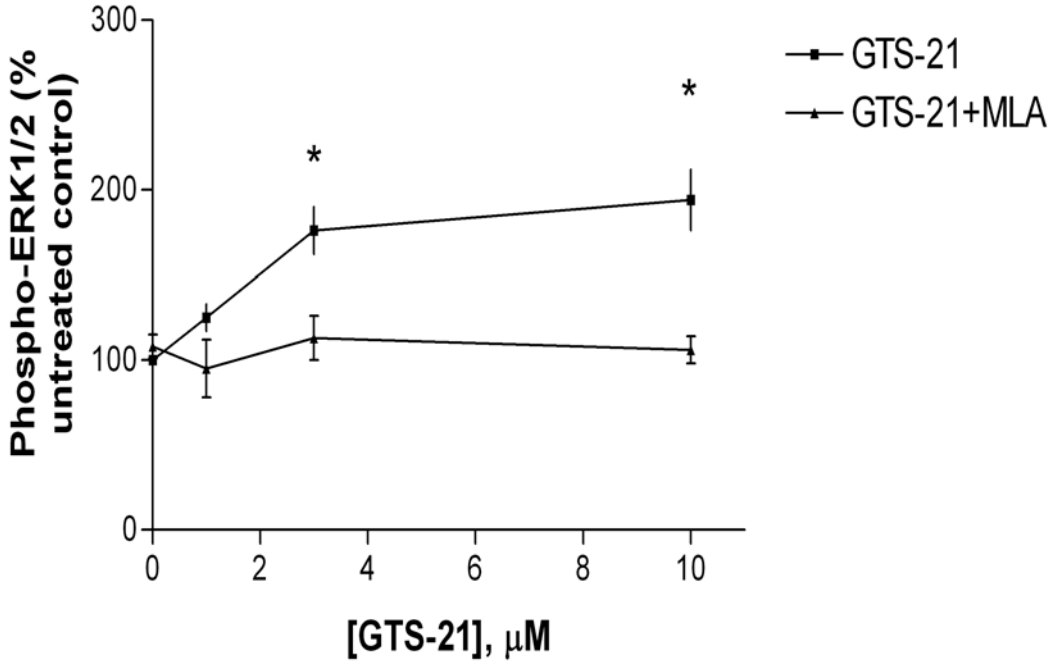

Figure 3-7. MLA blocks the ERK1/2 phosphorylation triggered by GTS-21. Cells were treated as in Figure 4, except with varying concentrations of GTS-21 for 180 minutes, plus or minus 100 nM MLA. Phospho-ERK was assayed and expressed as the mean + SEM of 4 samples/group, normalized to untreated control values on the same gel. *$p < 0.05$ compared to either the corresponding MLA treatment group.

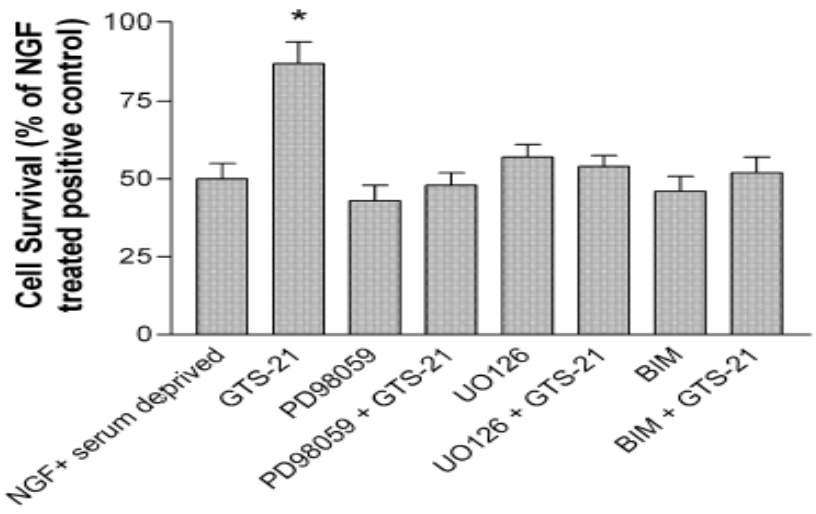

Figure 3-8. GTS-21 induced cytoprotection is dependent on ERK phosphorylation and PKC activation. Differentiated PC12 cells were treated with10 μM GTS-21 for 3 days upon NGF + serum removal, with or without 10 μM PD98059, 500 nM bis-indole maleimide (BIM) or 10 μM U0126. Cell densities are expressed as the mean ± SEM of 6 plates/group from 3 experiments; *$p < 0.01$ compared to untreated control (one way ANOVA).

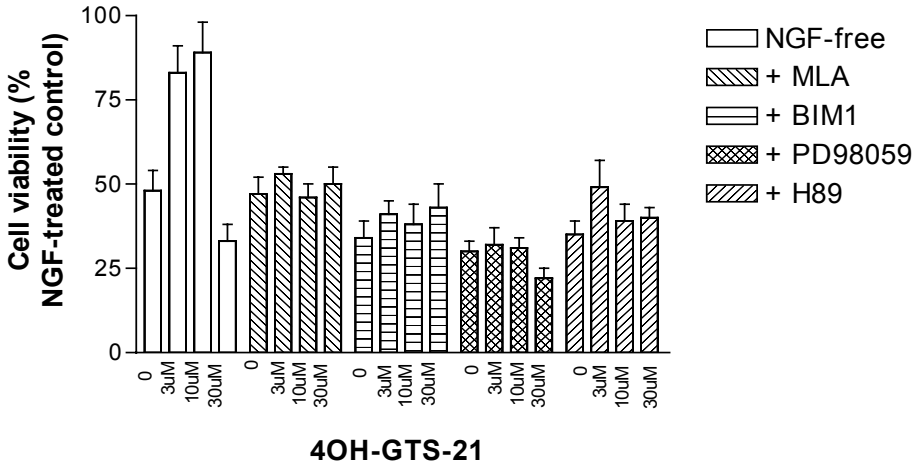

Figure 3-9. Effects of 4OH-GTS-21 and various kinase inhibotor on PC12 cells. NGF and serum were removed 1 hour before agonist treatment. 1 μM α7 antagonist MLA, 100 nM PKC antagonist BIM1, 20 μM ERK1/2 inhibitor and 1 μM PKA inhibitor H89 were added 15 minutes prior to 4OH-GTS-21. Cell density was measured 3 days after NGF-removal. Values are means + SEM of 4 plates/group.

Various kinase inhibitors were also tested on the protective effects of 4OH-GTS-21 against an amyloid peptide in human SK N SH cells. Abeta 25-35 (20 μM) caused a significant reduction in cell density alone, which was partially blocked by 4OH-GTS-21 in a concentration dependent manner. At 30 μM 4OH-GTS-21, additional toxicity was seen over that with Abeta peptide alone. The α7 antagonist MLA (1 μM), PKC antagonist BIM1 (100 nM), ERK1/2 inhibitor PD98059 (20 μM) and PKA inhibitor H89 (1μM) all blocked this 4OH-GTS-21 provided cytoprotection (Figure 3-10). However, only MLA blocked the additional toxicity caused by 30 μM 4OH-GTS-21.

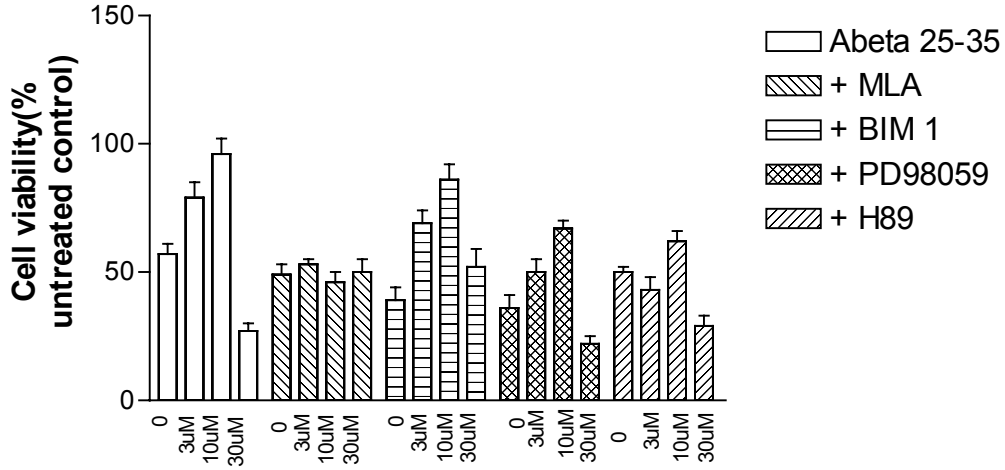

Figure 3-10. Effects of Abeta 25-35, 4OH-GTS-21 and various kinase inhibitor on SK N SH cells. All cells were treated with specified concentrations of 4OH-GTS-21 for 1 hour prior to adding 20 μM Abeta 25-35. 1 μM α7 antagonist MLA, 100 nM PKC antagonist BIM1, 20 μM ERK1/2 inhibitor and 1 μM PKA inhibitor H89 were added 15 minutes prior to 4OH-GTS-21. Cell density was measured 3 days after NGF-removal. Values are means ± SEM of 4 plates/group.

Discussion

Previous studies have demonstrated GTS-21-induced calcium elevations (Gueorguiev *et al.*, 2000; Li *et al.*, 2002) and have suggested the importance of multiple calcium-activated processes for α7 receptor-induced neuroprotection (Li *et al.*, 1999c;

Kihara *et al.*, 2001; Dajas-Bailador *et al.*, 2002b; Bell *et al.*, 2004; Salehi *et al.*, 2004). The present results show for the first time that chelation of intracellular calcium ions blocks GTS-21-induced, α7 mediated neuroprotection, demonstrating a direct role for these divalent cations in the receptor-modulation of cell viability. This is consistent with previous studies that chelated or removed extracellular calcium ions to attenuate α7-mediated protection or kinase-activation (Donnelly-Roberts *et al.*, 1996; Dajas-Bailador *et al.*, 2002b). The concentration of BAPTA-AM used in our study was selected for its ability to prevent nicotine-induced elevations in both cytoplasmic calcium and tyrosine hydroxylase activity in PC12 cells (Gueorguiev *et al.*, 1999). It therefore appears that the calcium-elevations triggered by α7 receptor activation have important roles both for the phenotypic properties of these cells as well as for their long-term viability in the presence of toxic insults. It is interesting to note that a careful study of intracellular calcium chelation in hippocampal neurons recently concluded that modest increases in intracellular calcium-concentrations were also associated with improved viability (Bickler and Fahlman, 2004). It remains to be determined to what extent BAPTA-treatment reduces calcium concentrations in mitochondria, smooth endoplasmic reticulum, and other storage sites under our experimental conditions.

The effects of α7 receptor activation on cell viability and their blockade by BAPTA were seen without any acute change in α7 nicotinic receptor binding density and a modest increase in receptor density by 3 day. These observations are significant because α7 binding density was recently found to modulate the neuroprotection seen in PC12 cells (Jonnala and Buccafusco, 2001). The reduction in α7 receptor binding density over three days of NGF + serum removal is probably related to the observation that NGF

increases this receptor subunit expression in PC12 cells(Takahashi *et al.*, 1999). GTS-21 has not been reported to increase α7 receptor expression or lead to PC12 cell differentiation, which may account for its inability to prevent the loss of α7 receptor density over the 3-days of NGF-deprivation. The lack of effect of GTS-21 on α7 receptor binding density following the 3 days of NGF + serum deprivation was a surprising result since the less selective agonist nicotine was found to increase α7 receptor expression in these cells (Jonnala and Buccafusco 2001). MLA also increases α7 receptor density in PC12 cells (Jonnala and Buccafusco 2001), which might be expected with GTS-21 if it acted by desensitizing most α7 receptors. One possibility is that selective, low level activation of α7 receptors is insufficient to increase their density, which is consistent with the lack of effect of chronic GTS-21 administration on α7 receptor density in neocortex *in vivo* (Meyer *et al.*, 1997). Alternatively, GTS-21 may preserve a population of PC12 cells that expresses fewer α7 receptors, while simultaneously increasing their α7 receptor expression, resulting in no net change in density under these conditions.

Our results indicate that the cell viability effects of BAPTA are likely due to processes downstream from the receptor activation, since there was no decrease in binding density that would be expected to interfere with the actions of GTS-21. This is consistent with the observation that BAPTA exposure attenuated GTS-21 induced PKC activation. PKC-translocation and activation were previously found to be essential for α7 mediated protection in this apoptotic model (Li *et al.*, 1999c). This increase in PKC activity occurs within 15 minutes; during the interval that neuroprotection is BAPTA-sensitive, suggesting that the kinase activation may be one of the relatively early steps in the protective process.

The antiapoptotic effect of GTS-21 in PC12 cells requires extended activation of α7 receptors, since MLA blocks this cell survival when administered up to 1 hr post-agonist (Li *et al.*, 1999c). The ability of BAPTA to block protection when applied 5 min after GTS-21 suggests that a protracted elevation in intracellular calcium ions is also essential for protection. Whether this is due to a slow or rapid increase in calcium is not clear. We previously demonstrated that neuroprotective concentrations of GTS-21-caused a long term, near steady state calcium influx through α7 receptors, without the desensitization of the overall receptor population seen at higher, non-protective agonist concentrations (Papke *et al.*, 2000). However, while it is likely that this low-level receptor activation provides an early calcium-transient that is important for triggering the cytoprotective pathway, it appears that downstream calcium channel activation is important as well.

The multichannel modulation of intracellular calcium by voltage sensitive L-type calcium channels, intracellular IP3 channels, and intracellular ryanodine channels provides a potentially complex mechanism for α7 receptors to affect cellular function and viability (Vijayaraghavan *et al.*, 1992; Gueorguiev *et al.*, 2000; Shoop *et al.*, 2001; Dajas-Bailador *et al.*, 2002a; Dajas-Bailador *et al.*, 2002c). Activation of the intracellular IP3 calcium channel, and to a lesser extent the ryanodine receptor, are necessary for complete α7 mediated protection in this model, based on sensitivity to antagonists. This is consistent with the protective actions of metabotropic receptors such as bradykinin (Yamauchi *et al.*, 2003) and mGluR4s (Maj *et al.*, 2003) that also act on IP3 receptors. The concentration of xestospongin C used in the present study was found previously by our group to block IP3 receptors and reduce GTS-21 induced calcium accumulation in PC12 cells for as long as it was assayed (45 min)(Gueorguiev *et al.*, 2000). This

dependence on IP3 channels for most of the long term elevation in intracellular calcium triggered by α7 receptors is consistent with their involvement in cytoprotection, which similarly depends on long term receptor activation (Li *et al.*, 1999c). Inhibition of phospholipase C with U-73122 (Kokoska *et al.*, 1998), which blocks IP3 production, also attenuates GTS-21 induced protection, providing additional support for a role of IP3 receptors.

Ryanodine channels were also involved in the protection of some NGF + serum deprived PC12 cells, though this effect was less dramatic than that seen with IP3 channel attenuation. Since ryanodine may only partially attenuate α7 mediated calcium elevations (Gueorguiev *et al.*, 2000), it is not surprising that some cells remained sensitive to GTS-21 in the presence of this channel blocker. There are multipe types of ryanodine receptor that are differentially expressed in various tissues, however, so it is conceivable that this result may be difficult to extrapolate to other neuronal models (Berridge *et al.*, 2000). In brain neurons, ryanodine receptors are primarily localized to the endoplasmic reticulum of postsynaptic entities, from which they release calcium in response to increased cytoplasmic calcium. Recently, however, they have been found presynaptically and may be involved in modulating transmitter release (Bouchard *et al.*, 2003), another well characterized function of α7 receptors.

The nifedipine-sensitive voltage sensitive L-type channel also underlies a significant amount of the calcium accumulation seen following α7 receptor activation. Although extracellular calcium is necessary for neuroprotection, as noted above, it appears that the channels other than L-type channels are involved in this action, probably the α7 receptors themselves. The observation that L-type channels are not essential for

protection may be due to multiple factors. First, L-type channel openings may be for a shorter duration than is necessary for protection, e.g., if the voltage-dependent channel openings is attenuated over time through calcium-activated potassium channels. Alternatively, the calcium entry through these channels may be physically removed from the transduction processes essential for cytoprotection. A third possibility is that the intracellular calcium channels may provide sufficient calcium for protection even in the absence of voltage sensitive calcium channel activation.

Our results indicate for the first time that the ERK1/2 MAP kinase pathway is required for α7 receptor mediated protection, based on its GTS-21 induced phosphorylation and attendant activation, as well as the ability of the ERK1/2 inhibitor PD98059 to block protection. ERK1/2 phosphorylation has been associated with cytoprotection in a variety of model systems e.g., (Hetman and Xia, 2000; Kyosseva, 2004), and with other anti-apoptotic processes found to be triggered by α7 receptors, including bcl2 elevations, increased mitochondrial membrane potential, and reduced cytochrome C release (Li *et al.*, 1999c). Our results indicate therefore that calcium accumulation triggered by α7 receptor activation is necessary for this chain of kinase-mediated anti-apoptotic events. In contrast, neither the p38 nor the JNK pathway was apparently activated by a protective concentration of GTS-21. It is interesting to note that activation of ERK has been reported with very low concentrations amyloid peptides, suggesting that this may provide a dose-dependent protective role for the peptides and receptors under appropriate conditions, perhaps even in the sparing of α7 receptor expressing cells in Alzheimer's disease.

In summary, α7 receptor activation provides cytoprotection against trophic factor deprivation and triggers PKC translocation through a mechanism that appears to involve intracellular calcium ion elevations (Figure 3-11). Among the several calcium channels triggered by α7 receptor activation, IP3- and, to a lesser extent ryanodine-receptor calcium channels are likely mediators of these calcium-elevations and are essential for cytoprotection. Downstream ERK1/2 phosphorylation is also essential for protection, while other MAP kinases JNK and p38 are not. It now becomes important to determine the role of these various pathways in the protective actions of α7 receptors in brain *in vivo*.

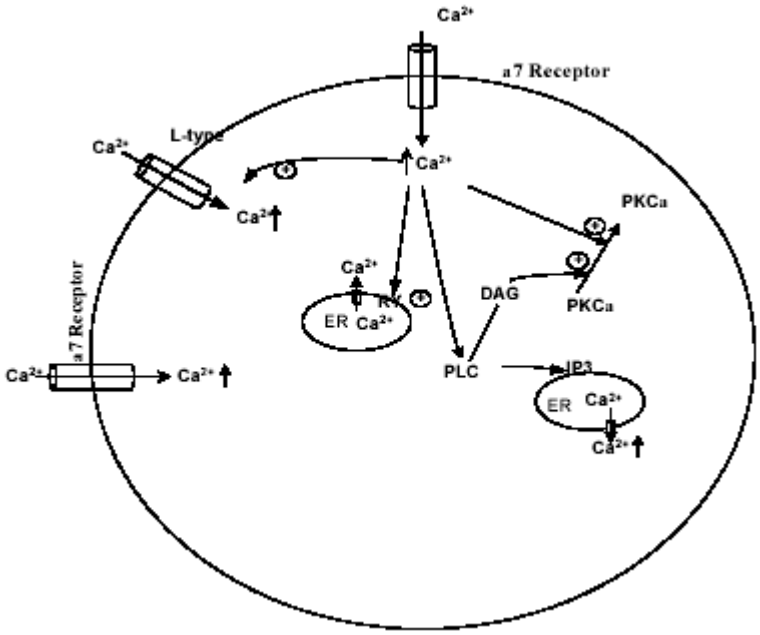

Figure 3-11. The potential mechanism of α7 nicotinic receptors mediated cytoprotection.

CHAPTER 4
NEUROPRECTIVE AND ANTI-AMYLOIDOGENE EFFECTS OF THE α7 PARTIAL AGONIST 4OH-GTS-21 IN FIMBRIA FORNIX LESIONED MICE OF DIFFERENT GENOTYPES

Introduction

While α7 nicotinic receptors are neuroprotective in a variety of models, little is known about their protective properties in models of neuronal dysfunction related to AD *in vivo*. There is presently no animal model that mimics every aspect of AD, though various lesion and genetic manipulations have been used. Combinations of these approaches, however, are much less common.

Investigations of genetic linkage and transgenic animal models have shown that no single genetic defect that accounts for all the features of AD. A certain number genes have been identified to be involved in the progressive neuron degeneration of this disease. Most AD cases have mutations in the genes encoding for APP, presenilin 1 (PS1) or PS2. All of these mutations have been shown to alter APP metabolism and increase the Aβ peptide levels in the brain.

Transgenic mice expressing mutated human genes that are associated with familial AD offer a powerful model to study Aβ. The present study employed either single human mutated PS1-M146L transgenic mice or double transgenic mice expressing both human APP Swedish mutant K670N/M671L and PS1-M146L mutations (APP/PS1). Both types of transgenic APP/PS1 mice have elevated levels of fibrillogenic Aβ 42 peptide in their brains, though only the APP/PS1 mice develop amyloid plaques starting

around the age of 4 months of age. By 6 months of age, the amyloid plaque load is comparable to that of 12-month-old single APP K670N/M671L mice. This demonstrates that APP/PS1 mice develop amyloid plaques earlier than the APP-only transgenic mice. However, neither type of transgenic mice shows neurofibrillary tangles. These mice do have deficits in spatial memory in selected paradigms, notably the radial arm task in the Morris water paradigm, though not in the classic Morris water protocol. Mutations in PS1 may act synergistically with Swedish mutant APP to cause some pathology reminiscent of the AD brains.

PS1 and PS2 play a critical role in mediating gamma secretase cleavage of the APP. Gamma secretase is one step in the formation of amyloidogenic Aβ 1-42 or Aβ 1-40. In addition, PS1 deficiency leads to alter intracellular Ca^{2+} homeostasis involving endoplasmic reticulum Ca^{2+} stores. PS1 transgenic mice that overexpress the mutant AD protein have been found to elevate levels of endogenous Abeta 1-42, but not Abeta1-40. Abeta1-42 levels are significantly elevated in the mutant PS1 mice, presumably by enhancing cleavage of APP at a gamma-secretase site. Evidence from *in vitro* studies also indicates that PS1 itself might either act as gamma-secretase or mediate the catalytic activity of the enzyme (De Strooper and Annaert, 2000). These PS1 transgenic mice do not form amyloid deposits upon aging, presumably because the levels of Abeta do not reach the level required to start the aggregation process in mice (McGowan *et al.*, 1999). Mutated PS1 mice also do not show overt AD-like pathology or spatial learning deficits in the Morris water maze test. The densities of α7 nicotinic receptor-binding sites are unaltered in transgenic PS1 mice compare to non-transgenic controls.

A recent study showed that no significant differences in size or number of cholinergic nerve terminals in the hippocampus or neocortical areas of mice overexpressing M146L PS1 (Wong *et al.*, 1999). Conversely, studies from the double transgenic mice APP/PS1 mice have been found to display an extensive loss of cholinergic synapses in the frontal cortex and hippocampus (Vaucher *et al.*, 2002). It was suggested that overexpression of human Aβ peptide combined with a shift toward longer forms of Aβ terminating at residues 42 or 43 due to mutation of PS1 is required to elicit cholinergic deficits in mice (Bronfman *et al.*, 2000). Vaucher et al. showed that mutation of the human PS1 gene might alter sensorimotor activity and long-term retention of object recognition memory but not ChAT enzymatic activity or cholinergic receptor binding sites (Vaucher *et al.*, 2002). Whether this cognitive deficit is due to an alteration in APP processing of the endogenous mouse APP holoprotein by the PS1 mutation or related to altered functions of other neurotransmitters is not known.

A non-genetic approach to model AD involves lesions of neuronal pathways affected by the disease. One of the early effects of AD is the degeneration of basal forebrain cholinergic neurons, which results in loss of cholinergic function in the neocortex and hippocampus. The septo-hippocampal pathway has been the most thoroughly investigated basal forebrain cholinergic pathway. This pathway carries the acetylcholine and GABA as neurotransmitters in axons that project to the hippocampus. Fimbria fornix lesion (FFX-lesion) can result in partial or near-complete loss of cholinergic activity in the hippocampus and impairment in behavioral tasks, depending on the extent and type of lesion. For example, the aspirative lesions used in my studies affect from 50-90% of the cholinergic and GABA neurons projecting to the

hippocampus. Following these lesions, animals become deficient in septal cholinergic neuronal density, memory related behavior and, as was recently reported, in hippocampal α7 nicotinic receptor functions.

The cholinergical deficits in septum following FFX lesions may be due to the loss of retrograde axonal NGF transport from the hippocampus, based on the observations that: 1) NGF is typically transported in this manner by these cells retrograde; and 2) that NGF-administration can protect septal cholinergic neurons from the effects of the lesion. Since NGF-deprivation in differentiated PC12 cells is toxic in a manner that is protected by α7 nicotinic receptor agonists, my hypothesis was that the α7 nicotinic receptors partial agonist 4OH-GTS-21 would also be able to protect cholonergic neurons *in vivo* from axotomy. However, this protection was not expected in amyloid expressing mice such as the APP/PS1 double transgenic because of the α7 nicotinic receptor blockade by amyloid peptides.

Mapping of cholinergic pathways based on choline acetyltransferase (ChAT) immunohistrochemistry could be considered to define the limits of nicotinic cholinergic signaling systems in the mammalian CNS. ChAT immunohistochemical maps identify major cholinergic projection from loosely-delimited nuclei of heterogeneous neurotransmitter phenotype in the medial septum (Mesulam, 1995). However, since α7 nicotinic receptors are also activated by choline, a natural byproduct of phosphatidylcholine metabolism and a circulating nutrient, it is possible that these cholinergic signals do not require and are not marked by ChAT staining.

A small fraction (10-20%) of septal GABAergic neurons are intermingled with cholinergic neurons projecting to the hippocampus, although estimates about the number

of GABAergic neurons in this region vary across different studies and species. Septal GABA neurons have morphologies similar to those of ChAT- positive neurons, with a somewhat different topography. GABAergic neurons have been demonstrated a roughly similar number to the cholinergic neuron in rats, though a smaller fraction project to the hippocampus in at least some mouse stains (Sarter and Bruno, 2002). Interestingly, while these septohippocampal GABA neurons project alongside cholinergic neurons, they are not adversely affected by AD even as cholinergic neurons are lost. This may be due to the differential need of these cell types for NGF, since the GABA neurons do not posses NGF receptors.

It has been reported that both septal GABA and cholinergic neurons possess α7 nicotinic receptors, but whether these receptors are protective for both populations is not known. One possible mechanism to account for α7 nicotinic receptor mediated neuroprotection is an increase in NGF expression. Nicotinic receptor activation was found to increase NGF levels and NGF-receptor levels, so this is a possibility. If so, then the α7 nicotinic receptor agonist treatment will likely be protective only for cholinerhic neurons and not GABA neurons. Alternatively, if α7 nicotinic receptors are protective more directly, then it would more likely that both types of neurons were protected by α7 nicotinic receptor agonists. I investigated these possibilities by comparing the neuroprotective actions of 4OH-GTS-21 in both populations of neurons following FFX lesions.

While multiple studies have evaluated the effects of potential therapeutic agents in either transgenic mice or lesioned animals, no study has yet combined these two model systems. One of my project goals was therefore to test whether an α7 nicotinic receptor

agonist could provide neuroprotection in a combination transgenetic and lesion model involving FFX lesions of wild type, APP/PS1 and PS1 transgenic mice.

Another potential beneficial effect of α7 nicotinic receptor activations for AD may be reducing amyloid plaque density. Nicotine has been found recently to reduce amyloid plaque density in mutant APP transgenic mice over a period of several months of PO treatments. While it is not clear which of the nicotinic receptor subtypes cause this effect, my hypothesis was that α7 nicotinic receptors may be involved based on the observations, as noted in Chapter 1, that these receptors can stimulate APP α-secretase activity, which would be expected to reduce substrate availability for Abeta amyloidogenic peptides.

One method to determine the role of α7 nicotinic receptors in the nicotinic-induced reductions in amyloid density is to use selective agonists for the receptor. I addressed this possibility with the partial agonist 4OH-GTS-21 in double transgenic APP/PS1 mice.

Results

Mice receiving FFX- lesions appeared to be no different from unlesioned animals with respect to body weight gain or visual assessments of health. In a preliminary study, AChE staining was used to verify the extent of the lesion relative to the loss of cholinergic innervation of the hippocampus. Aspirative FFX-lesions were performed unilaterally on male adults SD rat. The lesion resulted in a nearly complete loss of the hippocampal AChE-positive fibers on the lesion side. High levels of AChE staining were observed in the unlesioned side (Figure 4-1).

Figure 4-1. Aspirative FFX-lesion of the septal hippocampal cholinergic pathway. The lesioned side hippocampus AChE staining is over 90% lost.

Wild type C57/B16/J mice (9 month), PS1 mice (9 month) and APP/PS1 (9 month) also had significant, 55-60%, reductions in septal hippocampal cholinergic neuronal density following FFX-lesion as measured by septal ChAT staining two weeks post-lesion (Figure 4-2). There was no difference in the extent of this ChAT staining loss among the three groups when expressed as a percent of unlesioned, contralateral cell density. This normalization procedure of expressing neuronal density as a percent of the contralateral control side was used to control for inter-animal differences in perfusion, sectioning and staining. To what extent the loss of cholinergic neuron density was due to neuronal death versus phenotypic change is not known. There was also a significant reduction in the size of the septal cholinergic perikarya caused by this lesion.

In order to evaluate the effect of chronic $\alpha 7$ nicotinic receptors activation on this septal cholinergic dysfunction, wild type, PS1 and APP/PS1 mice were injected IP twice/per day for two weeks (first injection 15 minutes prior to lesion) with either 0.9% saline vehicle or 1 mg/kg (salt weight) 4OH-GTS-21 (Figure 4-2 and 4-3). None of the strains appeared to be adversely affected by this dose of 4OH-GTS-21 based on weight

gain, animal appearance, or gross behavior or physiology. For wild type and APP/PS1 mice, there was no apparent difference in septal ChAT staining between the 4OH-GTS-21 (1mg/kg) and 0.9% saline treatment groups. However, the PS1 mice treated with this 4OH-GTS-21 regimen retained more ChAT staining perikarya on the lesion side compared to the wild type and APP/PS1 mice. This stereological evaluation indicated that 4OH-GTS-21 could provide some protection of cholinergic neurons in PS1 mice, under conditions in which it did not affect APP/PS1 or wild type mice.

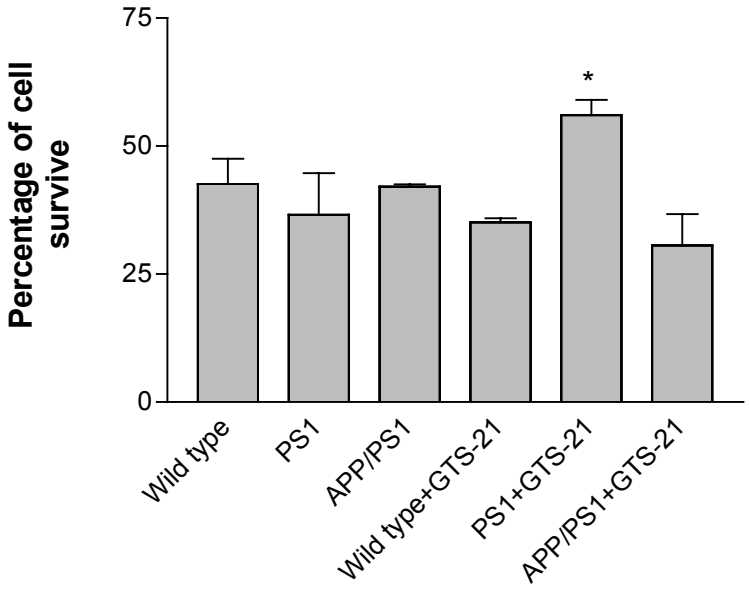

Figure 4-2. Septal ChAT neuron staining in 9 month old mice. 4OH-GTS-21 injected 2x daily (1 mg/kg IP) for 2 weeks increased septal ChAT staining neurons in unilaterally lesioned PS1 mice. 4OH-GTS-21 had no protective effect in 9 month old APP/PS1 and wild type mice. * $P<0.05$ compared to other group (one way ANOVA).

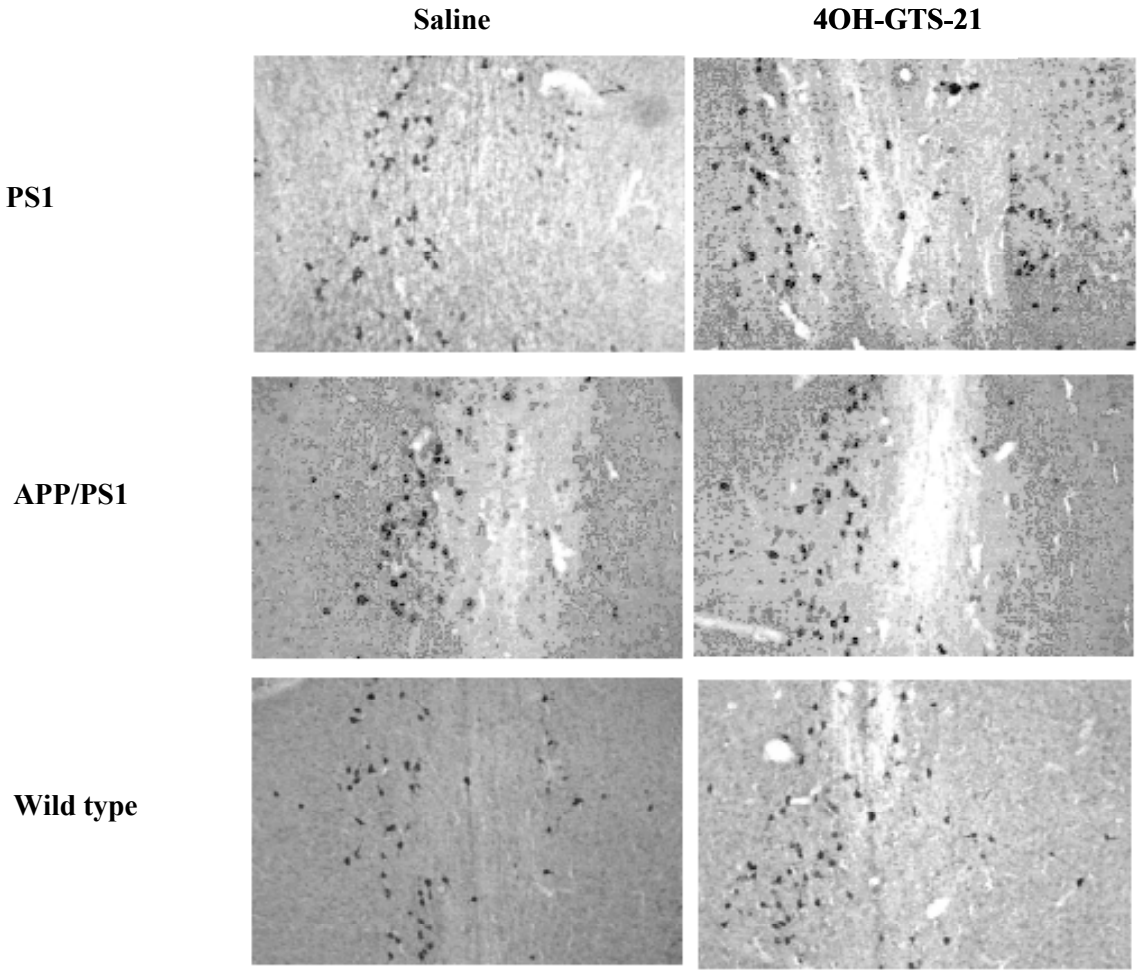

Figure 4-3. Septal ChAT-staining perilarya in 9 month old PS1, APP/PS1 and wild type C57/B16/J mice two weeks after unilateral aspirative FFX-lesions. Only the PS1 mice showed any neuroprotection with drug treatment.

The septal GABAergic neuron quantification was conducted by using parvalbumin immunohistochemisty that accounts for a major fraction of the GABAergic innervation to hippocampus (Figure 4-4). The immunohistochemistry staining is shown in Figure 4-5. The cell-counting data showed that no change affected the GABAergic neuron density.

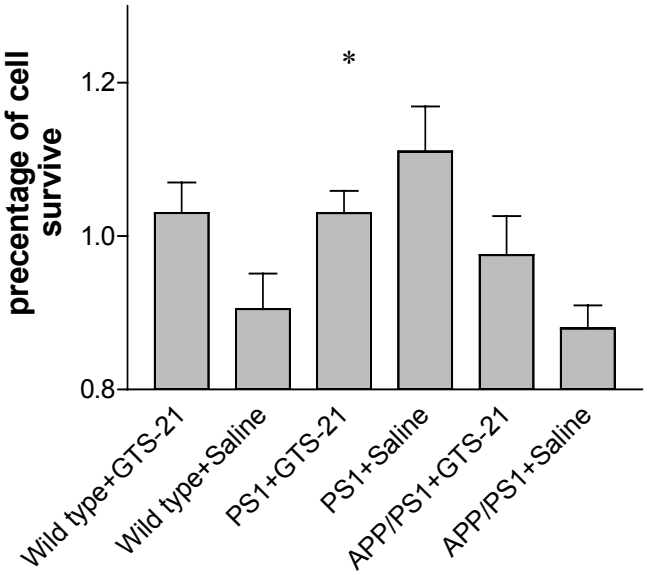

Figure 4-4. Septal GABAergic neuron staining in 9 month old mice. 4OH-GTS-21 was injected 2X daily (1 mg/kg IP) for 2 weeks. No change in septal GABAergic neurons staining in unilaterally lesioned mice. *$p<0.05$ compared to saline group (one way ANOVA).

.

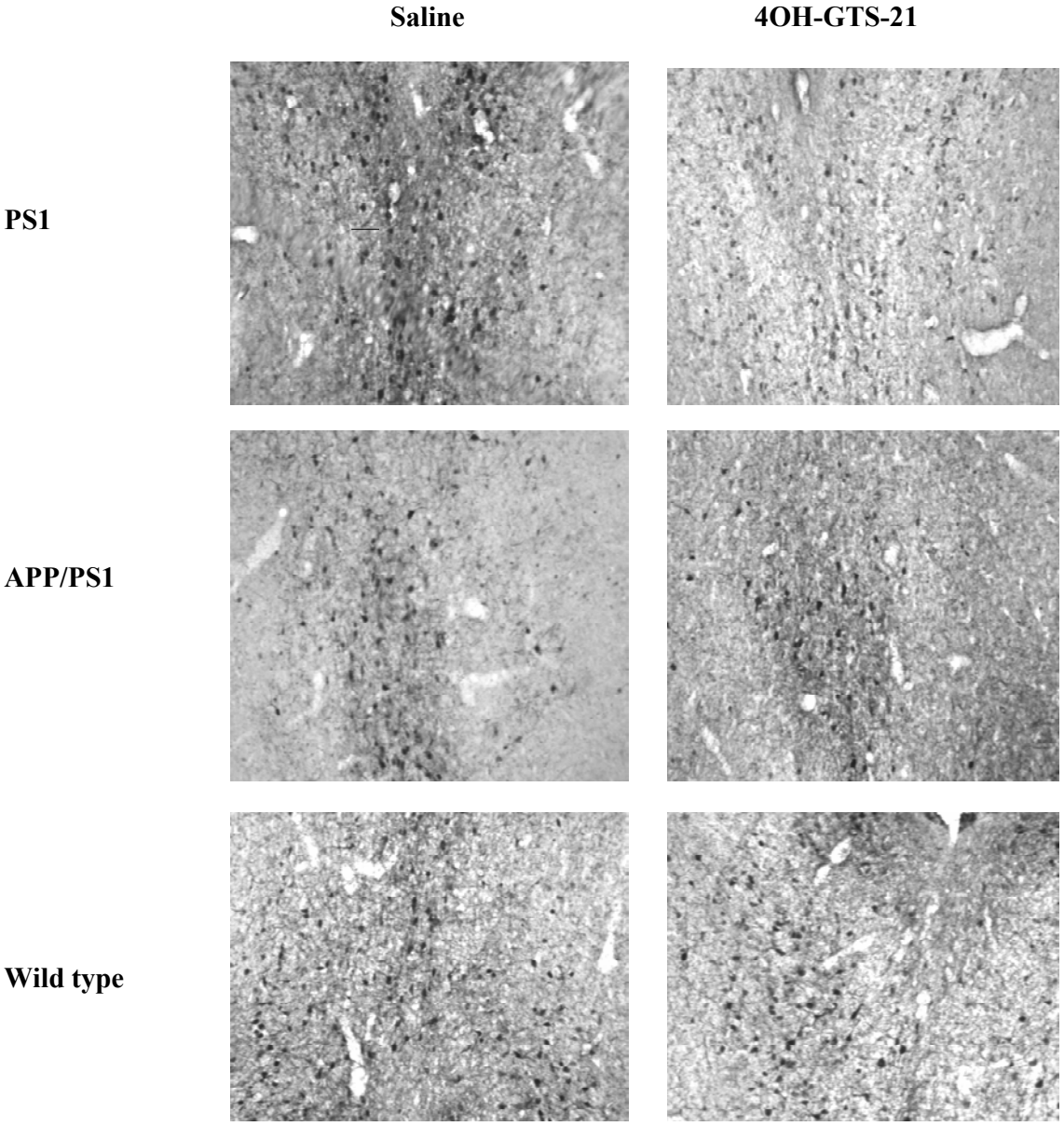

Figure 4-5. Septal GABAergic staining perilarya in 9 month old PS1, APP/PS1 and wild type C57/B16/J mice two weeks after unilateral aspirative FFX-lesions. No neuroprotection with drug treatment in these groups.

6E10 and thioflavine S staining were conduced in sections of these same 9-month-old APP/PS1 mice (Figure 4-6). APP/PS1 mice were treated with 4OH-GTS-21 or 0.9% saline vehicle IP for two weeks. The 4OH-GTS-21 + lesion groups had few plaques compared to saline group (Figure 4-7).

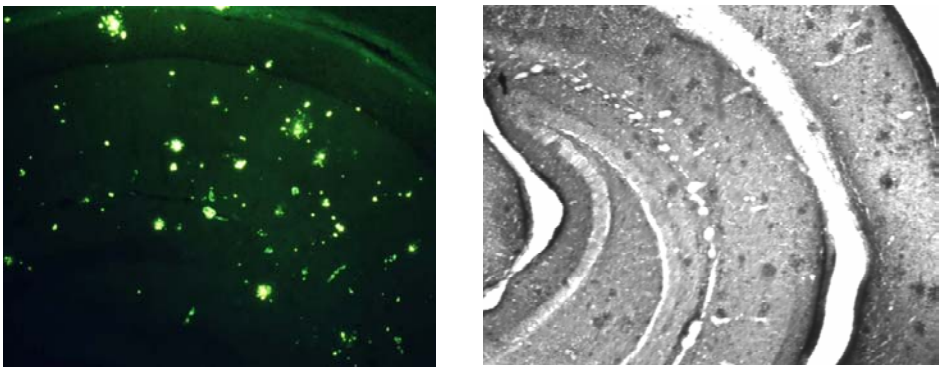

Figure 4-6. The thioflavine S and 6E10 staining in 9 month old APP/PS1 mice. Left pane: thioflavine S staining in hippocampus; Right panel: 6E10 staining in hippocampus and neocortex.

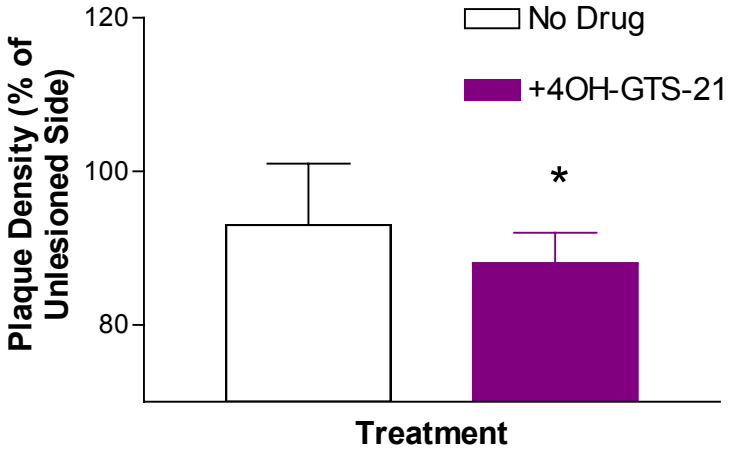

Figure 4-7. APP/PS1 mice (9 months old; N=4-5/gp) had lower hippocampal amyloid density stained with 6E10 antibody after a combination of fimbrial lesion and 4OH-GTS-21 IP X2 for 2 wks than either treatment alone. *p<0.05 compared to unlesioned side; there was no difference between drug treatment groups in absence of lesion.**Discussion**

This study investigated the α7 nicotinic receptor agonist effects on cholinergic and GABAergic neuron viability in wild type, APP/PS1 and PS1 mice receiving FFX-lesions. The aspirative FFX-lesions used in this study resulted in a substantial depletion of cholinergic markers in the mouse hippocampus though this depletion was less dramatic than reported previously, or than we saw based on AChE histochemistry, for rat. The extent of cholinergic depletion was the same for each group of saline-injected mice. Our data show that 4OH-GTS-21 could provide neuroprotection in PS1 lesioned mice, but no protection was observed in wild type or APP/PS1 lesioned mice treated with the drug. This difference may reflect additive or synergistic effects of PS1 and α7 nicotinic receptors.

Kang et.al show that presenilins play important roles in Akt/GSK signaling and tau phosphorylation (Kang *et al.*, 2005). The PS1 mutation was reported to enhance tau phosphorylation and reduces kinesin-based transport by increasing GSK-3 activity in primary neurons. However, the mechanism is not known for how the PS1 mutations could account for these effects. One factor may be the relative amount of PS1 vs. PS2 expression, since PS1 mutations led to a substantial reduction in PS2 fragment levels compared to wild type PS1. This could result in a corresponding decrease Akt and ERK activation by the PS1 mutation. Akbari et.al.(Akbari *et al.*, 2004) reported that PS1 mutations lead to increased intracellular stores and an attenuation of capacity calcium entry. Thus, α7 nicotinic receptor activations may have additive effects on intracellular calcium levels with PS1, which, as noted in Chapter 3, is important for neuroprotection. They also demonstrated that in the presence of APP overexpression, an inverse relationship exists between gamma-secretase activities. Since PS1 overexpressing mice

have increased levels of -Akt and ERK activation, both of which are important for α7 nicotinic receptor mediated neuroprotection, this may be another additive or synergistic interaction between these two systems. This may be the reason we saw the protection in cholinergic neurons in PS1 mice but not wild type mice.

For the APP/PS1 mice, both the APP and PS1 are overexpressed. However, APP has a high affinity for blocking α7 nicotinic receptors. This could interfere with 4OH-GTS-21 binding to α7 nicotinic receptors, attenuating the drug-induced protection in APP/PS1 mice. If so, higher doses of this partial agonist or the use of a more efficacious agonist than 4OH-GTS-21 might still be effective. Alternatively, the pharmacokinetic properties of the 4OH-GTS-21 could be considered more carefully in designing the dosing in order to optimize the amount of drug at receptors over more extended intervals. As noted in Chapter 1, 4OH-GTS-21 is a relatively short-life drug.

One interesting observation is that GABAergic neurons were not protected in the drug treatment group compared to the saline group. One factor is that the number of GABAergic neurons projecting to hippocampus is less than cholinergic neurons. Linke et al. showed that 38% of all retrograde labeled neurons were ChAT-positive whereas only 10% of all retrograde labeled cells were immunostained for parvalbumin (Linke *et al.*, 1994). This is support our hypothesis. Another possible reason is that the proportion of GABAergic neurons might have been underestimated because immunostaining for parvalbumin only labels a subpopulation of GABAergic neurons. Mechanistically, however, these data suggest that some factor activated by α7 nicotinic receptors is more effective in cholinergic than GABAergic neurons. This factor may be NGF, which as

noted above is protective for cholinergic but not GABA neurons in septum and which appears to be elevated by nicotine receptor activation.

Given the toxicity of aggregated Aβ to cells *in vitro*, it is perhaps surprising that even though Aβ aggregates have been abundant throughout the brains of APP/PS1 mice for most of their lives, there is little neurotoxicity. One possible explanation for the apparent lacks of overt Aβ toxicity in these mice involves the putative trophic effects of APP and PS1, which may counteract the degenerative effects of amyloid formation. Another explanation is that the effects of Aβ aggregation in plaques may be very local. It is hard to discern local degeneration of neurons in close to plaques (Hernandez *et al.*, 2001).

6E10 and thioflavine S staining were used to detect amyloid plaques in APP/PS1 mice with or without 4OH-GTS-21 treatments for two weeks. The density of plaques was slightly but significantly decreased in 4OH-GTS-21 treatment groups in the lesioned hemisphere compared to saline group's lesioned side, when both were normalized to the contralateral, unlesioned side. This normalization was necessary because of the wide inter-animal variability in plaque density, which was largely eliminated by this normalization. This result suggests that reducing septal input to the hippocampus combines with α7 nicotinic receptor activation to reduce plaque density. One hypothesis is that 4OH-GTS-21 treatments for 2 weeks may not be enough to decrease amyloid deposits as significantly as was reported for nicotine over a period of 3 months. We should also consider the alternative hypothesis that other nicotinic receptors are responsible for this action, either alone or in combination with α7 nicotinic receptors. A pharmacokinetic explanation is also possible; the short-term half-life of 4OH-GTS-21

may not have permitted it to exert the same anti-plaque action when injected 2 X per day that was possible when nicotine was administered in the water, the route used previously to reduce amyloid plaques.

CHAPTER 5
RAAV MEDIATED GENE TRANSFER *IN VITRO* AND *IN VIVO*

Introduction

Acetylcholine, acting through α7 nicotinic receptors, is an important modulator of electrical activity in the central nervous system and is involved in a variety of physiological processes and synaptic plasticity, including cognition and development (Volpicelli and Levey, 2004). The loss of cholinergic function has been implicated in AD. We already know that AChE inhibitors have in clinical studies shown palliative effects on symptoms and a trend to slow disease progression. But at the later stages of AD, the AChE inhibitors have little or no effect on AD. A consistent and significant loss of α7 nicotinic receptors has also been observed in neocortical autopsied brain tissue including hippocampus from AD patients compared to aged-matched healthy subjects. So the cholinergic receptors including α7 nicotinic receptors of the hippocampus are considered to be therapeutic targets for memory loss and dementia.

α7 nicotinic receptors are highly expressed in the hippocampus and neocortex. Functional α7 nicotinic receptors in the hippocampus are mostly located at the cell bodies of the mossy cells and interneurons of the dentate gyrus. There is also evidence for the α7 nicotinic receptors being expressed on the synaptic terminals of interneurons and dendrites of pyramidal cells.

This thesis tests whether increasing the density of α7 nicotinic receptors can be accomplished with gene delivery in a manner that is functional, long term, dose-

dependent, and non-toxic. This would be a potential alternative method to the classic, pharmacological approach of increasing α7 nicotinic receptor activities with higher agonists concentrations. In our previous study, we showed that a high, 50 μM concentration of the α7 nicotinic receptor selective agonist GTS-21 could cause cell toxicity *in vitro* (Li *et al.*, 1999b). Although similar toxicity *in vivo* has not been seen and may be unlikely because of the very rapid desensitization of these receptors at such high concentrations, this desensitization would also be expected to interfere with efforts to increase α7 receptors function through high dose agonist regimens. Therefore, increasing the density of α7 nicotinic receptors is another promising target for therapy of AD, schizophrenia, and other conditions associated with dysfunctional α7 receptors.

Despite pharmacological evidence that changes in α7-receptor activity affect behavior and cell survival, transgenic α7 knockout mice show few behavioral changes compared to wild type controls. One possible explanation of this observation involves compensatory processes to replace those normally mediated by the receptor. We have developed another approach to modify α7 receptors gene expression in adults, bypassing potential developmental compensatory processes, using the rAAV vector system.

In this study, the rAAV is used as a gene delivery vector due to its apparent non-toxicity, ability to transduce postmitotic neuron and long-term expression gene (Robbins *et al.*, 1998). A single injection into the hippocampus leads to widespread expression of transgene in interneurons and other neuronal types. The serotypes of rAAV2 and rAAV8/2 were compared in our study since little is known about the latter in brain and since it appears to be more effective with respect to spread of transgene in other tissues. The cells of the nervous system can be divided into two broad categories: neurons and a

variety of supporting neuroglial cells. rAAV2 has been the most widely studied of the serotypes in brain and its tropism is neuronal predominantly. The possible mechanism of this tropism is either receptor-mediated or promoter-dependent selectivity. Early studies showed that rAAV2 mediated transgene expression occurred in hippocampal interneurons, and less strongly in hippocampal CA1 pyramidal neurons or dentate gyrus granule neurons. In this study, the rAAV8/2 vectors were also studied to determine the distribution and spread of the vectors in hippocampus. The rAAV2 and rAAV8/2 vectors used here both contained the chicken beta actin promoter combined with CMV enhancer. This is an extensively used promoter system for gene transfer in brain because of its high activity for extended intervals (Klein *et al.*, 2002).

We tested the rAAV mediated α7 nicotinic receptor gene deliveries *in vitro* and *in vivo*. For *in vitro* studies, rat pituitary tumor derived cells (GH4C1) were chosen. These do not express endogenous α7 receptors but can express functional α7 receptors after transfection because they synthesize the chaperone protein RIC-3. For the *in vivo* studies, wild type C57/Bl/J mice and Sprague Dawley rats, as well as α7 KO mice (strain B6.129S7-Chrna7^{tm1Bay}) were used. The goal was to test the following hypotheses: 1) α7 nicotinic receptors could expressed *in vitro* and *in vivo* in a dose dependent and functional manner, with no greater toxicity observed than under normal conditions in the presence of an α7 agonist; 2) α7 nicotinic receptor gene transfer could restore function in KO mice; 3) different neuronal populations in the hippocampus are similarly able to express this transgenic receptor after transduction *in vivo*; and 4) α7 vector mediated gene transfer into hippocampus could improve memory related behavior analogous to agonist-treatment.

Results

The structures of the pUF12-rat α7-plasmid containing expression cassette are shown in Figure 5-1. The CBA promoter is the hybrid truncated CMV enhancer and chickenβ actin promoter. The size of the first plasmid from TR to TR was 5.1Kb that is slightly greater than the rAAV package size of 5 Kb. The pUF12-rat α7 plasmid without WPRE was used in subsequent parts of this study accordingly. The empty and GFP plasmids were controls as specified.

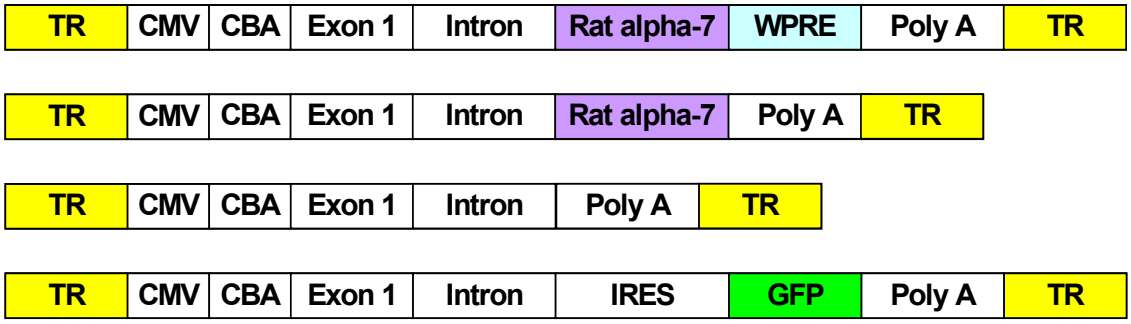

Figure 5-1. Schematic diagram of the expression cassettes.

To evaluate the ability of the plasmid constructs to code for rat α7 and GFP, GH4Cl cells were transfected with rAAV-rat α7 plasmid and pUF12 using a calcium phosphate method. GFP expression was observed 24 hours after transfection and around 15% of the cells expressed GFP at day 3. Rat α7 expressions was measured by ligand (MLA) binding assay at day 3 and found only in the α7 transfected cultures (Figure 5-2).

In order to determine whether the α7 gene delivery had any effect on cell viability, either by itself or in the presence of a toxic agent, some of the transfected GH4C1 cells were also exposured to 20 μM Abeta 25-35 for this 3 day interval. Cell viability was measured by cell counting using an NIH image system. GFP and α7 gene transfer alone had no effect on cell density, but 20 μM Abeta 25-35 caused significant cell loss. Cells

transfected with rat α7 receptors and then treated with Abeta 25-35 displayed no protection in total cell density, possibly because the transfection efficiency was too low and too few cells were protected overall in the culture. However, it appears that the few cells expressing these transgenic α7 receptors may have been protected. The α7 nicotinic receptor binding was 110± 15 fmol/mg in the non-Abeta treated cultures and 217± 20 fmol/mg in the Abeta 25-35 treated group (Figure 5-2). This increase in receptor density could reflect the relative sparing of cells expression α7 nicotinic receptors. Alternatively, the Abeta peptide may have acutely increased α7-receptor density by some other mechanism, though this has not been seen previously.

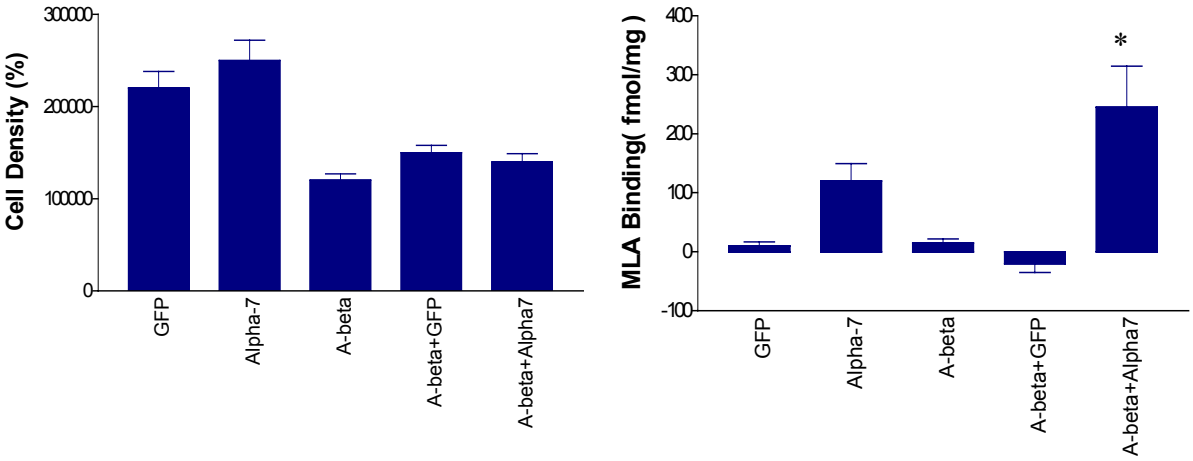

Figure 5-2. Transfection of GH4Cl cells with rat α7 nicotinic receptors:effect of Abeta 25-35 exposure on cell viability and receptor density. Cell viability was measured 72 hr later and expressed as the mean ± SEM of 6-8 plates per group by cell counting using an NIH image system. The high affinity MLA binding to α7 nicotinic receptors was conducted in membranes from the same cultures. *$p<0.05$ compare to other group (one way ANOVA).

The plasmids were packaged into rAAV2 and rAAV8/2 using the adenovirus-free method developed by Zolotukhin et al. (1999). The discontinuous iodixanol gradient was built (Figure 5-3A). After a two hour centrifugation, the rAAV distributed around the 40-60% density-interface (Figure 5-3B). A dot plot analysis was used to titer the number of

total genomic particles (Figure 5-3B). This method quantified viral DNA by hybridizing with a biotin probe of pUF12 and by comparing the intensity of labeling against known quantities of plasmid pUF12-rat α7. The first and second lanes were standard curves. The highest band had 5 ng/μl DNA with 1 ng = 4 x 10^{11} genomic particles/ml. The titer of rAAV2-rat α7 was 3 x 10^{12} genomic particles/ml. The titer of rAAV8/2-rat α7 was 4 x 10^{12} particles/ml. The titer of rAAV2-GFP was 1.5 x 10^{12} genomic particles/ml. The title of rAAV8/2 was 2x 10^{12} genomic particles/ml.

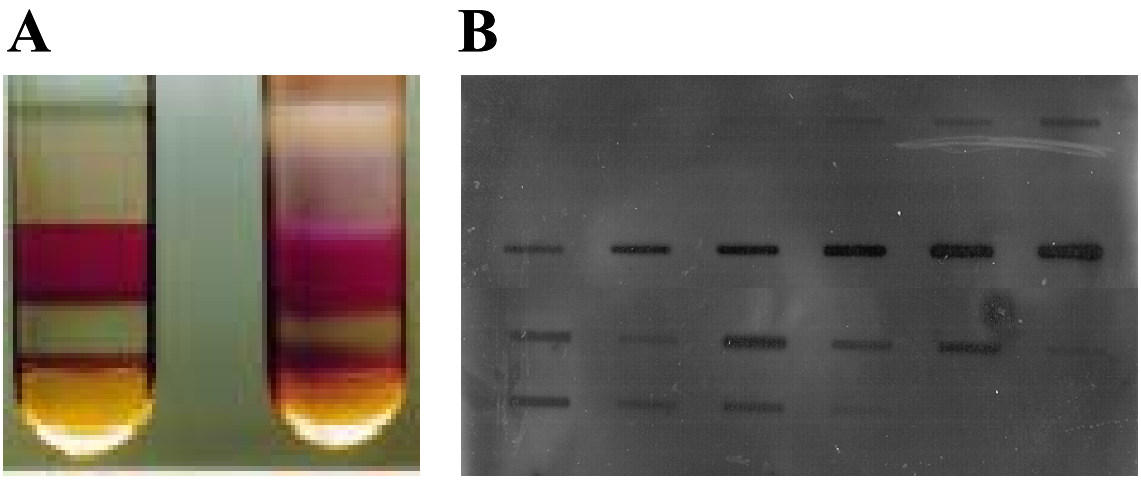

Figure 5-3. Iodixanol gradient for the purification of rAAV and dot plots for titer. (A). Preformed gradients shown before (left tube) and after (right tube) the 2 hour centrifugation. (B). The first and second lanes were standard curves. The third and fourth lanes were samples.

The different concentrations of rAAV2-rat α7 and rAAV2-GFP transductions of GH4C1 cells are shown in Figure 5-4. GFP expression was observed in culture within 24 hours. By day 5, over 90% of cell expressed GFP in the 30 x 10^{9} genomic particles/ml treatment group. Functional rat α7 receptors expressions were detected by the [^{3}H] MLA binding assay. Increasing the concentration of vector resulted in more α7 nicotinic receptor binding.

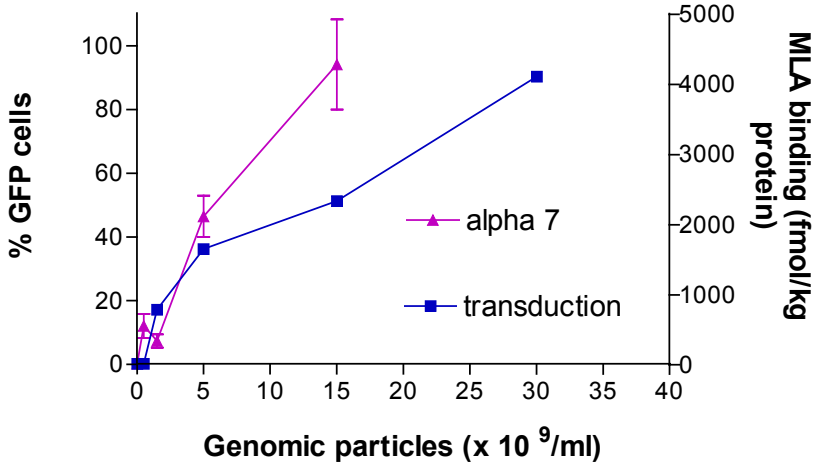

Figure 5-4. The dose response of rAAV2-rat α7 receptor and rAAV-GFP. Binding assay was measured 5-day later and 6-8 plates per group.

The expressions of α7 nicotinic receptors were compared among transduced GH4C1 cells and several other cell types using MLA binding. There were 960 fmol/mg protein expressed in rAAV2-rat α7 (5 x 10^9 genomic particles) transduced GH4C1 cells after 5 days (Figure 5-5). An α7 stable cell line (also GH4C1) had 750 fmol/mg protein expressed, while the PC12 cell line used for neuroprotection studies in Chapter 3 had 50 fmol/mg protein expression. There were approximately 100 fmol of receptor/mg protein expressed in pUF12-rat α7 plasmid transfected GH4C1 cells using the calcium phosphate method, although only a small fraction of these cells was transfected as noted above. This study demonstrated that the rAAV2-rat α7 was highly effective in increasing α7 nicotinic receptor expressions in GH4C1 cells.

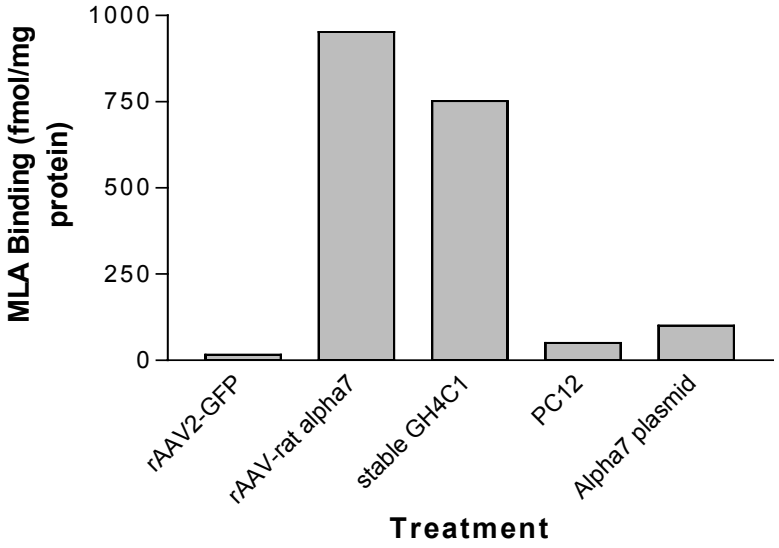

Figure 5-5. α7 receptor expression was measured in different populations of transiently transfected, stably transfected, transduced, and normally expressing cells. 1.5 x10 12 genomic particles of rAAV2- rat α7 and pUF12-rat α7 plasmid were used to introduce α7 receptors into GH4C1 cells. Binding assay were conducted 5-days after gene transfer. These receptor-binding values are compared to those of NGF-differentiated PC12 cells and stably transfected and selected GH4C1 cells. (N= 3 plates per group).

After showing that rAAV2-rat α7 vectors were able to increase the rat α7 receptors expressing *in vitro*, the next step was to test whether this increase the rat α7-receptor density could cause toxicity in the absence or presence of increase the concentration of GTS-21 (Figure 5-6). GH4C1 cells were transduced with $2X10^9$ genomic particles of rAAV2-rat a7 vectors and were exposed 5 days later to specified GTS-21 concentrations for another 3 days. PC12 cells were used as the positive control, though with much lower receptor density. GH4C1 cells transduced with rAAV2-GFP were used as the negative control. The binding assay was showed that PC12 had 50 fmol MLA binding/mg protein expressed. GH4C1 cells transduced with $2X10^9$ genomic particles of rAAV2-rat a7 vectors had 750 fmol MLA binding/mg protein. The cell density was determined and normalized to drug-free control values (N = 3 plates/group). Despite much higher

receptor binding density in transduced GH4C1 cells, there was no increase in agonist potency for toxicity. This suggests that toxicity depends on agonist concentration more than receptor density. It was previously established high agonist concentration were associated with much different receptor kinetics (i.e. peak + very rapid desensitization) than the low volume, steady state receptor activation caused by low agonist concentration. The present results indicate that the shape of this receptor response, which is agonist concentration dependent, is more important than the total number of receptors activated for affecting cell viability. Interestingly, GTS-21 appeared to increase cell density in GFP-transduced cells, though this effect did not reach significantly except at the lowest GTS-21 concentration. It may be that GTS-21 exerts an unknown action on these cells that is independent of α7 receptors.

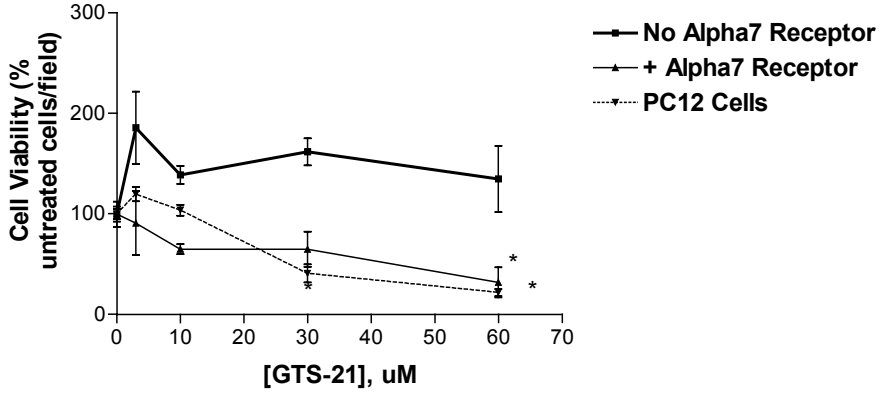

Figure 5-6. Effects of GTS-21 on the viability of PC12 cells and α7 transduced GH4C1 cells. The cell viability was measure after exposure to GTS-21 for three days. It showed that 60 μM GTS-21 could cause significant cell loss. The density of α7 receptor expression had no effect on cell viability. *$p < 0.05$ compared to same treatment with different concentration of GTS-21 (One-Way ANOVA).

In order to investigate the *in vivo* effects of α7-receptor gene delivery in brain, a very low dose of 4 x 10^5 genomic particles of rAAV2-rat α7 with WPRE vector was injected unilaterally into male adult Sprague Dawley (SD) rats (250 g) hippocampus CA1

region. Two weeks after injection, both sides of hippocampus were rapidly dissected from euthanized animals. The contralateral, uninjected side was the control. High affinity MLA binding increased in the hippocampus injected side compared to control (143 $\pm$ 13% of contralateral control binding) (Figure 5-7). This result demonstrated that near physiological increases in receptor density were feasible with this gene delivery system, using a very low vector dose.

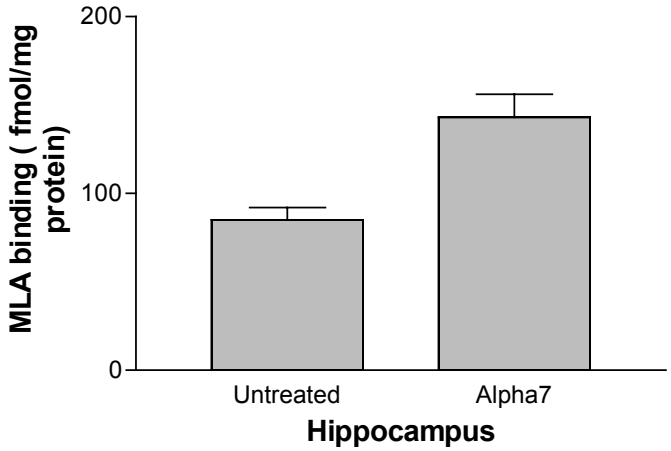

Figure 5-7. Low vector dose: in vivo transduction with α7 vectors in hippocampus. 4 x 105 genomic particles of rAAV2-rat a7 were injected into hippocampus. High affinity MLA binding increased in the hippocampus 2 weeks after transduction with the rAAV2-rat α7. All values are mean + SEM of 4 animals. *P<0.05 compared to untreated group (t-test).

Since one of my goals was to investigate the safety and function of α7 receptors *in vivo*, I next focused on the effects of high vector doses on this receptor expression. A higher dose of 5 x 10^9 genomic particles of rAAV2-rat α7 vectors without WPRE was injected unilaterally into male adult SD rat brain hippocampus CA1 region. Two weeks after injection, both sides of hippocampus were rapidly dissected from euthanized animals. The uninjected side was treated as the control for endogenous α7 receptors. MLA binding was dramatically increased in the injected side compared to controls

(Figure 5-8A). An equal dose of rAAV2-GFP was also injected in rat hippocampus to determine the transduction efficiency with this type of vector (Figure 5-8B).

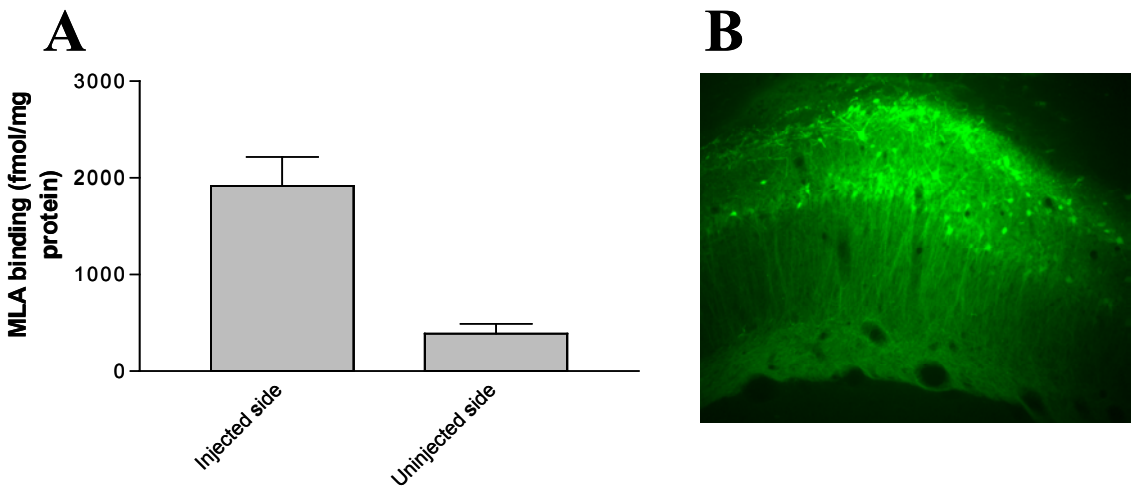

Figure 5-8. Effects of a higher vector dose on α7 nicotinic receptor exprrssion in hippocampus. A. 5x109 genomic particles of rAAV2- rat α7 were injected in the rat hippocampus. High affinity MLA binding increased in the injected side. B. rAAV2-GFP transduction was highly efficacious. *P<0.05 compared to untreated group (t-test).

In order to identify and study exogenous α7 gene expression in the absence of endogenous receptors, 1.5 x 10^{10} genomic particles of rAAV2-rat α7 were injected unilaterally into the hippocampal CA1 region of α7 nicotinic receptor knockout mice. Two weeks after injection, each side of hippocampus and neocortex was assayed for MLA binding. Knockout mice on the injected side had high α7-receptor expression (500 fmol/mg protein), but no measurable binding on the uninjected side (Figure 5-9A). The α7 heterozygous mice had 1200 fmol MLA binding/mg protein expression in the injected hippocampus, but no nicotine displaceable MLA binding on the control side. The neocortex had α7-receptor expression in both knockout and α7 +/- mice (Figure 5-9B). This study demonstrated that we could restore α7 receptors in knockout mice.

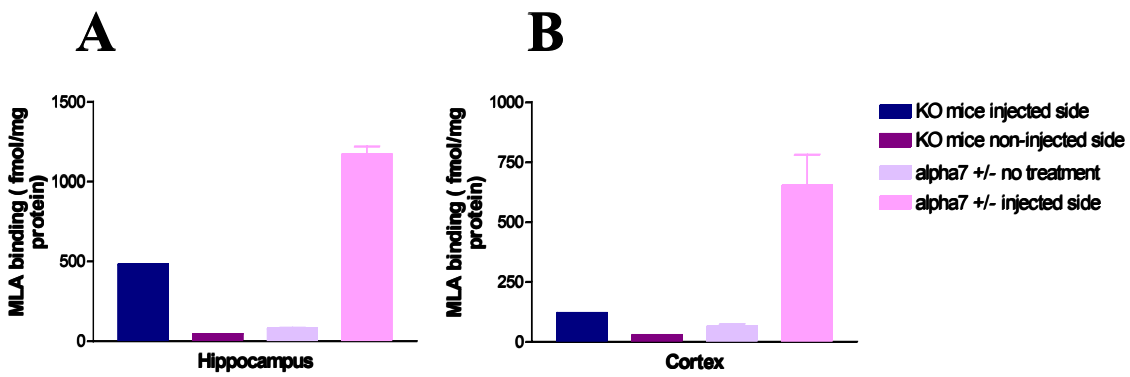

Figure 5-9. rAAV2-rat α7 vector gene transfer in α7 KO and α7 heterozygous (+/-) mice. 1.5 x 10^{10} genomic particles of rAAV2-rat α7 were injected into hippocampus of α7 KO or heterozygous mice. These results showed that the neuronal transgenic α7 receptor was expressed in hippocampus and, presumably through vector spread from the injection track through neocortex. * and #$p<0.05$ compare to same genotype untreated side (t-test).

Scatchard plots were used to calculate the Kd and Bmax values of MLA binding in the transduced hippocampus to determine whether there the binding properties of the transgenic receptors compared to endogenous receptors. 1.8 x10^{10} or 3.6 x10^{10} genomic particles were bilaterally injected into wild type mouse hippocampus. After two weeks, binding assays were conducted with varying concentrations of labeled MLA. The MLA Kd was found to range from 1.98~2.288 nM in these 3 treatments, indicating that the endogenous and transgenic receptors has similar MLA binding affinities (Table 5-1). The Bmax increased with the concentration of vector as expected.

Table 5-1. Scatchard analyses of MLA Kd and Bmax in mouse with or without α7 knockout mice gene transfer

Vector (genomic particles)	Kd (nM)	Bmax (fmol/mg protein)
0	2.228	23.24
1.8	2.062	855.5
3.6	1.98	926.4

Table 5-1. MLA Kd and Bmax. Each treatment had 5 mice/per group.

The immunohistochemistry of wild type rats, wild type mice and α7 KO mice hippocampus is shown in Figure 5-10. The left panel shows the wild type rat CA1 region. The middle panel shows the wild type mice CA1 region. The right panel shows the knockout mice hippocampus. This study demonstrated that no α7 receptors could be detected in knockout mice, while there was endogenous α7 receptor expression in wild type rat and mice.

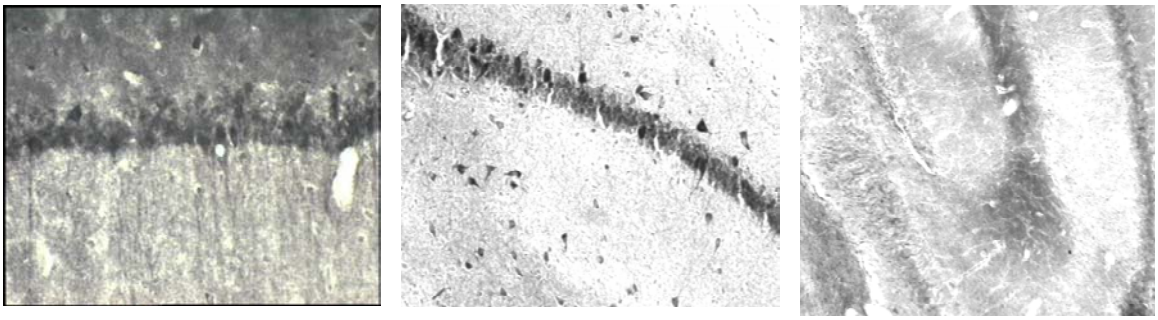

Figure 5-10. mAB 306 immunohistochemical staining of rat, mice and α7 KO mice.

1.8 x10^{10} genomic particle of rAAV2-rat α7 were unilaterally injected into knockout mice septum. Two weeks after injection, knockout mice were perfused and dissected and sections analyzed. Figure 5-11 shows the immunohistochemical staining of septum after injection.

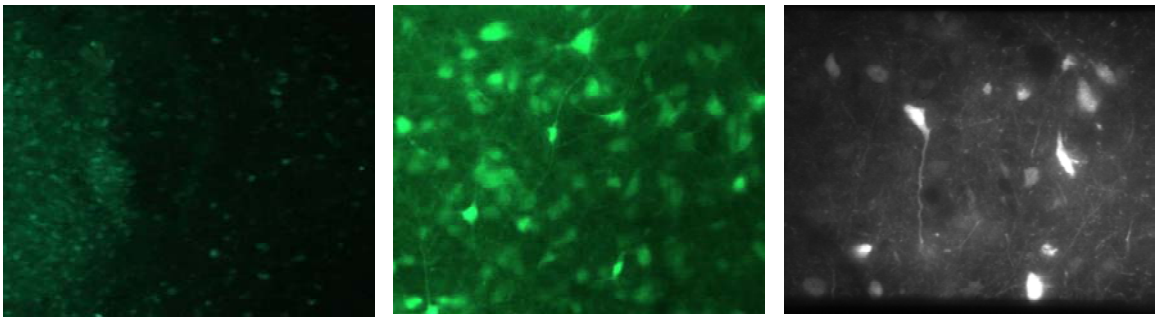

Figure 5-11. FITC-staining of knockout mouse septum after injection. The left panel shows that the injection side had α7 receptor expression. The middle panel is a high magnification of the injection side. The right panel is a cofocal image of injection side.

In order to increase vector spread in brain *in vivo*, an rAAV8/2-rat α7 was generated. As noted above, this vector was reported to have greater spread than rAAV2 in brain and some other tissues. It should be noted that in preliminary studies, we found it less effective *in vitro* than rAAV2, which is the reason that we continued using rAAV2 for those studies. Since little is known about rAAV8/2 mediated gene transfer in brain, rAAV8/2-GFP was first evaluated for neuron specificity (Figure 5-12). No colocalization of GFP and astrocytes stained with GFAP was observed, indicating that rAAV8/2 transduced neurons primarily. This agrees with the morphological assessment of the GFP expressing cells, which was exclusively neuronal in hippocampus and neocortex. However, this study did not eliminate the possibility that other brain glia (microglia, oligodendrocytes) may have been transduced as well.

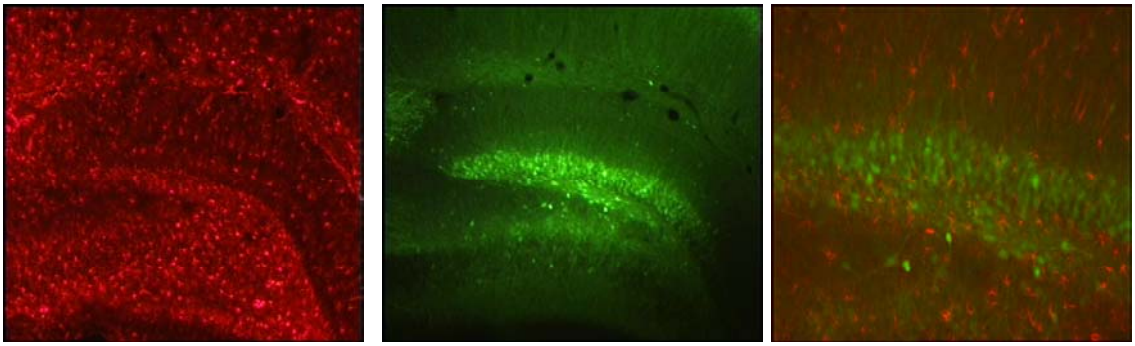

Figure 5-12. rAAV8/2 transduction in rat brain. The left panel was stained with GFAP (red). The middle panel is GFP expression. The right panel shows merged astrocytes (red) and GFP expressing cells.

In order to determine whether there was any toxicity caused by α7-receptor gene delivery into hippocampus, several measurements were used. First, fluorojade labeling of the hippocampus found no evidence of dying neurons two weeks following injection of a high dose of vector (3.6 x 10^{10} genomic particles of rAAV8/2-rat α7). Since α7 receptor binding density was very high at this 2 weeks interval, it is not likely that the receptor transduced neurons had already died. In another line of study, several animals transduced with this 1.8 or 3.6 x 10^{10} genomic particles of this vector (2 animals/dose) underwent Morris water task analyses and were found to be unaffected compared to control mice, indicating no apparent dysfunction in that complex spatial memory related behavior.

In order to determine if the increase in α7 nicotinic receptor bindings after gene transfer in hippocampus was functional, electrophysiological responses were used. 1.8 x 10^{10} genomic particles of rAAV8/2-rat α7 combined with 0.6 x 10^{10} genomic particles of rAAV8/2-GFP were injected together unilaterally into mouse hippocampus. The contralateral side received 0.6 x 10^{10} genomic particles of rAAV8/2-GFP only. Two weeks after injection, fresh hippocampus was rapidly removed and its single cell electrophysiological responses were measured. GFP-transduced cells were identified

with a fluorescence microscope. The whole-cell current in response to 1 mM acetylcholine was near 5,000pA in transduced cells on the injected side (Figure 5-13 B). GFP-transduced neurons in the contralateral hippocampus had a smaller, conventional α7 type current (Figure 5-13 A).

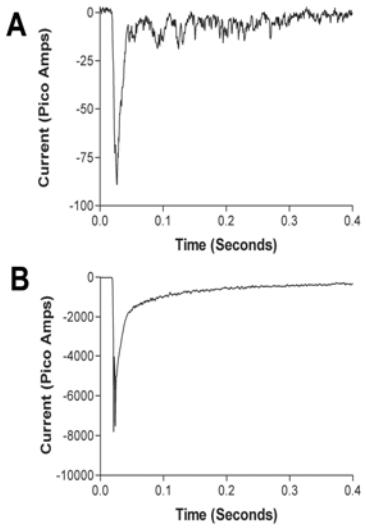

Figure 5-13. Electrophysiological responses in wild type mouse hippocampus following α7 gene delivery (A): 1 mM acetylcholine produces a typical α7 type current in a hippocampal stratum radiatum interneuron in control tissue. (B): A neuron located in the contralateral hippocampus, which received α7 gene delivery. The response is nearly 50 times greater in peak amplitude than that shown in A. The whole-cell current in response to acetylcholine is near 5000 pA.

The wild type mouse and rat hippocampus dentate granule cells normally do not express α7 receptors and typically have no response to 1 mM acetylcholine in this region (Figure 5-14 Cell 1). When 1 mM acetylcholine was added to the injected hippocampus, there was a significant response in dentate granule cells (Figure 5-14 Cell 2), indicating that this gene delivery was effective even in typically non-α7 receptor expressing neurons.

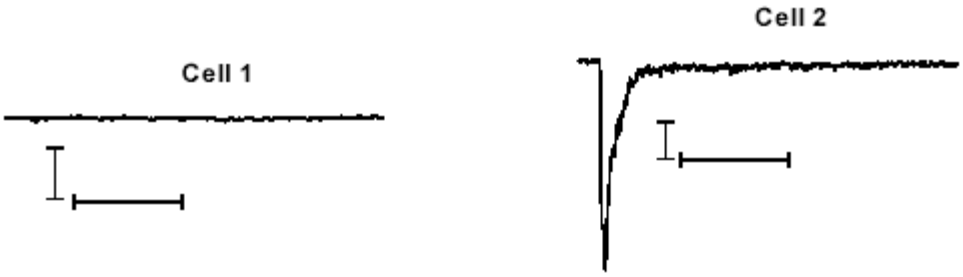

Figure 5-14. Electrophysiological responses in wild type dentate granule rat cells. Response to 1 mM ACh (scale bars: vertical 100pA/horizontal 100 ms). Cell 1 is from GFP-transduced hippocampus. Cell 2 is in α7 receptor transduced side.

In order to determine whether α7 gene delivery restored receptor function in α7 knockout mice, 2-month-old α7 knockout mice were injected with rAAV8/2-rat α7 (1.8 $x10^{10}$ genomic particles) combined with 0.6 x 10^{10} genomic particles of rAAV8/2-GFP in the hippocampus in order to detect likely transduced neurons. Rreceptor-transduced neurons from this region had evoked α7 nicotinic receptor responses in the presence of 1 mM acetylcholine, and this response was completely blocked with 50 nM MLA (Figure 5-15).

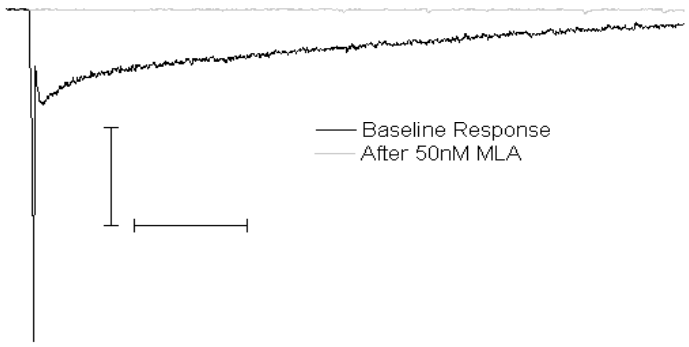

Figure 5-15. Evoked α7 nicotinic receptor responses in α7 knockout mice transduced with rat α7 nicotinic receptors. Recording from stratum radiatum interneuron, which had a response in the presence of 1 mM acetylcholine. This response was completely blocked with 50 nm MLA (scale bars 1 nA and 100 ms).

Dentate granule cells and pyramidal cells are populations of hippocampal neurons that do not normally produce functional α7 nicotinic receptors. Two-month-old mice were injected with 1.8 x 10^{10} genomic particles of rAAV8/2-rat α7 receptor together with 0.9 x10^{10} genomic particles of rAAV8/2-GFP, or with 0.9 x10^{10} genomic particles of rAAV8/2-GFP alone, in hippocampus. One week after injection, dentate granule cells expressed GFP (Figure 5-16). Typical α7 response kinetics was produced by somatic application of 1 mM ACh in these GFP-labeled neurons (Figure 5-16 middle panel). This response was blocked by 50 nM MLA, demonstrating α7 selectivities (Figure 5-16 right panel).

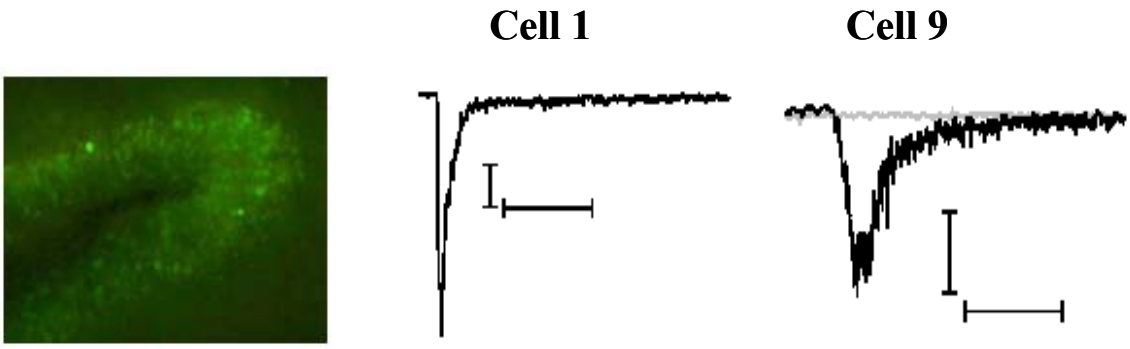

Figure 5-16. Histology following electrophysiological recording: 2 month old mice that received gene transfer with rAAV8/2 -rat α7 + rAAV8/2-GFP. 10X image of dentate granule cells expressing GFP/rat α7. Middle panel: typical α7 response kinetics produced by somatic application of 1 mM acetylcholine. Right panel: acetylcholine evoked response was blocked with 50 nm MLA (scale bars: 50pA and 100ms).

Similarly, three week old rats injected with 1.8 x 10^{10} genomic particles of rAAV8/2-rat α7 + 0.9 x10^{10} genomic particles rAAV8/2-GFP into hippocampus showed α7 functional responses in pyramidal cells. 300-micron sections were used for electrophysiological recordings. CA1 pyramidal layer cells expressing GFP were selected for recordings (Figure 5-17). 1 mM acetylcholine evoked somatic currents in

CA1 pyramidal cells that were blocked by 50 nm MLA (Figure 5-17).

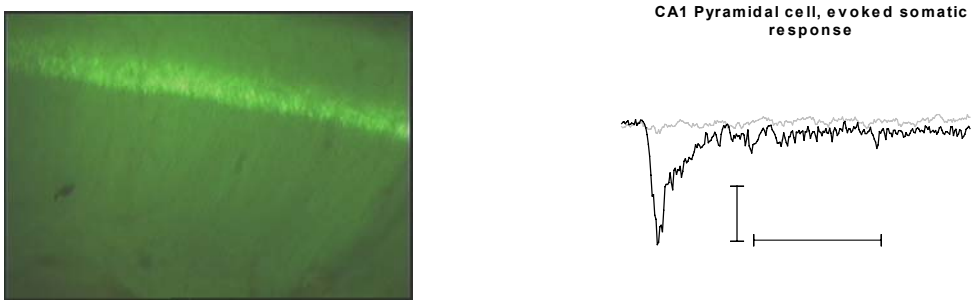

Figure 5-17. Electrophysiological recording of a CA1 pyramidal neuron in the hippocampus of a 3 week old α7 receptor-transduced mouse. Dark tracing: current in the presence of 1 mM acetylcholine. MLA (lighter tracing) blocked the current. Scale bars: 25 pA and 100 ms.

Discussion

The results of this study indicate for the first time that α7 nicotinic receptor expression and function can be modulated in a dose-dependent, non-toxic manner for extended intervals by gene delivery. Further, this gene delivery approach can restore α7 receptor function to brain neurons in receptor knockout animals deficient in their endogenous expression. It therefore appears that this approach may provide an alternative approach for treating conditions associated with dysfunction of the α7 nicotinic receptor system, including AD and schizophrenia.

There have been very few publications demonstrating the functional vector-mediated gene delivery of any plasma membrane receptors in brain *in vivo*, and none using rAAV. Bahi et al. (Bahi *et al.*, 2004) used lentivirus vector mediated gene transfer to express D3 dopamine receptors into the nucleus accumbens, with resultant changes in cocaine-induced locomotion. This work demonstrated that vector mediated gene transfer could be functional even in the complex and highly regulated milieu of the brain, at least

for some receptors. Our results indicate that this is likely to be true for α7 nicotinic receptors as well in multiple brain regions.

One of the advantages of using rAAV2 vectors for brain has been their selectivity for neurons, permitting selective genetic modification of that cell type. Since α7 nicotinic receptors are primarily neuronal under most conditions, this vector is appropriate for attempting to restore α7 receptor functions without unwanted expression other cell types. However, little is known about cell type selectivity for rAAV8/2 vectors in brain. The present data indicate that this novel hybrid serotype also has neurotropism in brain since glias were not transduced with GFP. Further, the spread of transgene expression with rAAV8/2 was greater than that with rAAV2 based on qualitative evaluations following hippocampal injections, so rAAV8/2 became the system of choice in later functional studies involving ligand binding, electrophysiology, and behavior.

One of the concerns about α7-receptor gene transfer into neurons has been the apparent requirement for the chaperone protein RIC-3 for functional expression of the receptor. RIC-3 is expressed by GH4C1 cells, unlike many other cell lines that do not normally synthesize α7 nicotinic receptors. This appears to account for the ability of these cells to express MLA-binding, plasma membrane associated, α7 receptors following gene transfer of the receptor, which is not seen in RIC-3 negative cells. Cell lines that intrinsically express α7 receptors (e.g., PC12 cells), also express RIC-3. Based on these observations, it was not clear whether α7 receptors would be expressed in neurons in which these receptors are not normally seen, such as hippocampal dentate gyrus or pyramidal neurons. Our observation that both of these cell types express

functional α7 receptors in the rat only after α7 gene transfer indicates that the rate limiting step in their production is not normally RIC-3 but the receptor itself.

Another concern about α7 gene transfer was whether it led to functional expression in adult knockout mice that had never expressed the receptor. Conceivably, these animals had developed compensatory processes that simultaneously interfered with ectopic receptor expression. The results of this study indicate that knockout mice could express ectopic α7 receptors at high levels after rAAV gene delivery. However, the level of this expression appeared to be lower than was seen in identically treated wild type mice. This reduction was seen in total hippocampal high affinity MLA binding levels, but was even more evident in single neuron electrophysiology, in which responses to acetylcholine by transduced KO mouse hippocampal interneurons were much less than those seen in wild type mice receiving the same α7 vector dose. While the mechanism underlying this differential level of functional α7 receptors is not clear, it may involve intrinsic modulatory factors recently found to affect these receptors.

The levels of transgenic α7 receptors binding in hippocampus were dependent on vector dose over a wide range. At the highest rAAV 8/2 vector doses used, which required vector high titers, there were large, 30-50 fold increases in receptor binding throughout the entire hippocampus and in electrophysiological responses of individual neurons that express the receptor intrinsically. This comparable increase in α7-receptor expression in individual neurons and throughout the hippocampus is consistent with the widespread distribution of the rAAV8/2 vector in this region seen using GFP-expression. A lower, more physiological level (40-50% over control values) of transgenic α7 receptor expression could also be produced in rat hippocampus, though this required a much lower

(10,000-fold) dose of vector. It should be noted that this lower expression of α7 receptors was seen using a different serotype (rAAV2) that also contained the WPRE insert to stabilize mRNA and potentially increase receptor expression. A comparable low, physiological level of α7 transgene expression has not been determined yet for rAAV8/2 because the focus of this project was to evaluate the efficacy and safety of the α7 receptor gene transfer under maximal expression conditions. This permits a more conservative determination of the safety than would be possible with much lower receptor expression, though both approaches will ultimately be important.

The α7-receptor MLA binding characteristics in hippocampus were comparable between rAAV8/2 transgenic and wild type α7 receptors. Despite the much higher Bmax values for the vector treated mice, the MLA-binding affinities (Kds) were similar between these groups. This is important because it indicates: 1) that the processing of the plasma membrane transgenic receptor is comparable to that of the wild type; and 2) the binding affinities of drugs for wild type receptors are likely to be predictive of their activities at the transgenic receptors. Therefore, differences in the dose-response characteristics to agonists between wild type and transgenic receptors will more likely reflect the different densities of the receptors. Since, as noted in Chapter 3, α7-receptor density can affect neuroprotection, this will be an important area for investigation *in vivo* following gene delivery leading to very high levels of the receptor expression.

The apparent non-toxicity of the gene transfer of α7 receptors was demonstrated in several manners. *In vitro*, overexpression of these receptors had no effect on the GTS-21 induced dose-response curve for acute toxicity. This result indicated that the dose-dependent agonist-receptor interactions were more important than the receptor density in

determining cell survival. *In vivo*, there was no apparent loss of α7 receptor binding density over several weeks, suggesting that the cells expressing these receptors were intact. Further, there was no fluorojade labeling of dying neurons following the high dose α7 receptor gene delivery. These results suggest that restoration of neuroprotection will be possible using α7 gene transfer under neurodegenerative conditions in which α7 receptors are low, without the toxicity or desensitization associated with high agonist concentrations.

The observation that receptor-mediated toxicity is agonist concentration dependent more than on receptor density is important for predicting the effects on cell survival of different approaches for increasing nicotinic receptor expression. For examples, it suggests that receptor modulator that are being developed commercially to increase α7 receptor function by increasing its opening time may be no more toxic when combined with an agonist than the agonist would be alone. Several agents have been found to increase α7-receptor function (e.g., 5-hydroxyindole) without being agonists themselves, and these may provide a future therapeutic approach without undue toxicity based on my results with gene transfer.

With respect to α7 receptor mediated neuroprotection following gene transfer, the increase in high affinity MLA binding expressed per mg protein in cells transfected with α7 receptors and treated with ABeta peptide vs. those not treated with Abeta is consistent with the receptor-mediated sparing of transfected cells. Selective protection of the α7-receptor expressing cells from Abeta would result in a higher receptor/total cell protein ratio. While there was no accompanying increase in cell density in this α7-receptor transgene treatment group, this may reflect the low transfection efficiency for these cells

(under 10%). An alternative explanation is that the α7-receptor density was elevated directly by Abeta peptide exposure. This possibility is supported by the observation that alpha7 receptor binding density is elevated in the brains of Abeta-overexpressing transgenic mice, at least for several months.

Unfortunately, it is difficult to use behavioral analyses such as the Morris water task for most purposes other than demonstrating a lack of toxicity relative to memory related behavior. This is because of several reasons. First, the α7 knockout mouse does not show deficits in this behavior, so a gene delivery approach to improve the behavior would be difficult to interpret. Even more difficult to interpret would be an analysis of the effects of α7 gene transfer into wild type animals, since this gene transfer increases receptor expression in neurons that do not normally synthesize the receptor. Since α7 receptors are activated by choline, which is ubiquitous in brain, any of these ectopic receptors could have effects on neuronal circuitry that affect memory. Therefore, it would be difficult to determine whether increased levels of normal transmission or to this abnormal transmission caused any improvement in behavior.

While these studies indicated that α7 nicotinic receptor genes could be functionally delivered into brain neurons using rAAV vectors, several important questions remain unanswered regarding their potential for therapeutic use. One issue is whether there may be toxicity over more extended intervals than those used here, up to 2 weeks posttransduction. Another is whether the α7-receptor gene transfer improves memory or is neuroprotective in impaired individuals. One way to do this study would be to investigate the effects of gene transfer into the APP/PS1 transgenic mice receiving fimbrial fornix lesions as described in Chapter 4. Since Dr. Meyer and his colleagues

recently demonstrated that lesions reduce α7-receptor function in hippocampus, it would be important to determine whether α7-receptor gene delivery could counteract this deficit, even in mice that have significant amyloid loads. A third issue about the use of gene therapy targeting α7 nicotinic receptors is whether there may be behavioral or physiological side effects caused by these receptors being expressed in excessively high levels or in neurons that do not normally express them. This possibility would require careful analyses of many potential behaviors and physiological processes. While this could be very much work, it is also possible that it could lead to new ways to modulate these other behaviors.

CHAPTER 6
CONCLUSIONS AND FUTURE STUDIES

Conclusions

The goal of this project was to improve our understanding of the mechanisms of the α7 nicotinic receptors mediated neuroprotection *in vitro* and *in vivo* and test whether the α7 nicotinic receptors gene delivery could become a potential approach to treat AD. This involved, testing several hypotheses: 1) that intracellular calcium, calcium channels, and several kinase-systems are necessary for α7 nicotinic receptor- mediated neuroprotection; 2) that an α7 nicotinic receptor agonist protected lesioned septal cholinergic neurons *in*

vivo; 3) that rAAV mediated α7 nicotinic receptor gene transfer was functional in a non-toxic manner *in vitro* and *in vivo*.

When α7 agonists bind to the α7 receptors, they trigger the calcium entry into cells. Calcium ion then can trigger PKC and PKA activation, as well as ERK1/2 phosphorylation. These processes were all found to be important for cytoprotection. PKC activation was necessary for protection in the NGF/serum-withdrawal model in PC12 cells but not in the Abeta 25-35 exposed SK N SH model. But the PKA activity was important in both models. ERK1/2 phosphorylation levels were increased when α7 receptors were activated. Neither p38 nor the JNK pathway was apparently activated by a protective concentration of α7 agonists.

Intracellular calcium ions were necessary for α7 nicotinic receptor mediated protection based on data that showed that intracellular calcium chelation BAPTA blocked GTS-21 induced protection. Our data showed that BAPTA exposure attenuated GTS-21 induced PKC activation. PKC activation was found to be essential for α7 mediated protection in this apoptotic model. Multiple channels modulate intracellular calcium levels. Our data showed that activations of the intracellular IP3 calcium channel and to a lesser extent the ryanodine receptor were necessary for complete α7 mediated protection. But the L-type calcium channels were not essential for α7 receptor mediated protection. One possible reason is that L-type channels may not be open long enough for neuroprotection as they close upon repolarization of the cell.

The effects of the α7 receptors selective agonist 4OH-GTS-21 on cholinergic and GABAergic neuron viability in wild type, APP/PS1 and PS1 mice receiving FFX-lesions were investigated. The data showed that 4OH-GTS-21 could provide cholinergic

neuroprotection in PS1 lesioned mice, but no protection was observed in wild type or APP/PS1 lesioned mice treated with the drug. Our hypothesis is that there may be additive effects of mutant PS1 overexpression and α7 nicotinic receptor activations. There are reports showing that overexpression of this PS1 mutation leads to increased intracellular calcium stores and an attenuation of capacity calcium entry, as well as ERK1/2 phosphorylation. Thus, α7 nicotinic receptors activation may have additive effects on intracellular calcium levels and kinase systems with PS1. These intracellular calcium levels are important for cell survival as noted above. We did not observe neuroprotection in APP/PS1 mice, perhaps because the APP-derived peptides have high affinity for blocking α7 nicotinic receptors and may therefore interfere with drug-induced protection.

GABAergic neurons were not protected in the drug treatment group compared to the saline group. This may be related to the small fractions of GABAergic neurons lost in the lesions, which in turn reflects the smaller percent of total septal GABAergic neurons projecting to hippocampus. One reason why activated α7 nicotinic receptors is more effective in cholinergic neurons than GABAergic neurons is that nicotinic receptor mediated increases in NGF release may be involved. As noted above, NGF is protective for cholinergic but not GABA neurons in septum and appears to be elevated by α7 nicotine receptor activation.

For the amyloid plaques, our data suggests that reducing septal input to the hippocampus combines with α7 nicotinic receptor activation to reduce plaque density, while neither one alone has this effect. Based on previous studies with nicotine showing amyloid reductions, this was a surprising result. One hypothesis is that 4OH-GTS-21

treatments for 2 weeks may not be long enough to decrease amyloid deposits in intact animals. An alternative hypothesis that other nicotinic receptors are responsible for this action, either alone or in combination with α7 nicotinic receptors. Why denervation of the hippocampus from septal projections would combine with α7 nicotinic receptors activation to reduce amyloid plaques is unclear. One possibility is that transmitters released from the septal projections (e.g., acetylcholine, GABA, neuropeptide transmitters) counteract the effects of the α7 nicotinic agonists, so that removal of this transmission permits the α7 agonists to be effective. If so, this observation would suggest that α7 nicotinic receptors activation would be particularly effective even in the early stages of AD when septal dysfunction is already observed.

One potential pathway of α7 nicotinic receptors mediated neuroprotection is described in Figure 6-1 based on the results in aim #1 and aim #2, as well as other data in the literature.

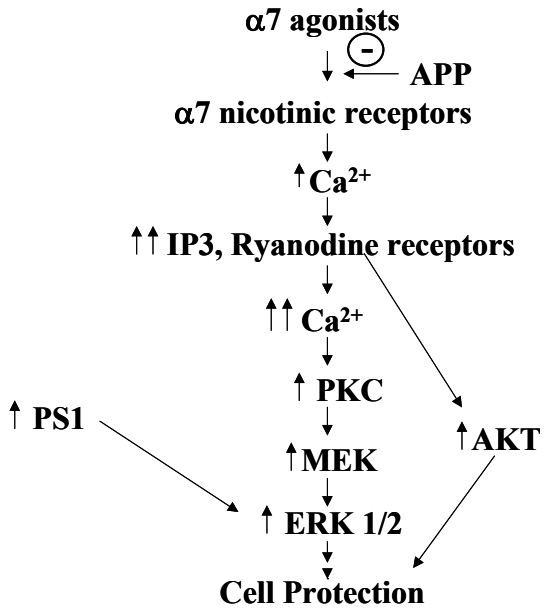

Figure 6-1. The potential pathway of α7 nicotinic receptors mediated neuroprotection.

This thesis also demonstrated for the first time that rAAV mediated gene transfer is a feasible way to deliver a plasma membrane receptor transgene into rat or mouse brain for long-term expression that can be modulated in a dose-dependent manner without producing degenerative neurons. Functional receptors were restored into the α7-knockout mouse using this vector approach as well. Therefore, it appears that this method may provide a way to treat deficits in α7 receptors. In my study, rAAV8/2 had greater spread than rAAV2, though both were neuron selective. The levels of α7 receptors expressed in hippocampus were dependent on the vector dose.

One of the interesting observations is that functional α7 nicotinic receptors were expressed after gene transfer in the hippocampal dentate gyrus or pyramidal neurons that normally do not have functional α7 nicotinic receptors. This result indicates that the rate-limiting step in α7 productions is not normally the RIC-3 chaperone or other potential factors necessary for receptor expression, but the receptor itself. This had been a matter of some speculation in the field.

No apparent toxicity due to the gene transfer of α7 receptors was observed *in vitro* or *in vivo*. *In vitro*, overexpression of these receptors had no effect on the GTS-21 induced dose-response curves for acute toxicity compared to those seen at physiological receptor levels. This result indicated that the dose-dependent agonist-receptor interactions were more important than the receptor density. *In vivo,* there was no fluorojade labeling of dying neurons after gene transfer 3 months after gene transfer.

Future Studies

More studies will be need to determine the complex relationship between APP and α7 receptors, and the functions of α7 receptors expressed after gene transfer in the α7-knockout mice, e.g., with respect to neuroprotection in the septum after FFX-lesions.

In chapter 4, we did not observe that 4OH-GTS-21 provided neuroprotection against FFX-lesioned APP/PS1 mice. Our hypothesis is that APP binding to the α7 receptors blocked the protection. In future studies, higher doses of the agonist could be injected to overcome this lack of protection or the rAAV-rat α7 vector could be injected to septum of APP/PS1 mice to increase drug-sensitivity relative to neuroprotection, receptor expression and behavior. The goals of this future study would be to test: 1) whether the septum cholinergic neurons are protected in this AD model; 2) whether the up-regulation of astrocyte α7 receptors in APP/PS1 mice is blocked by 4OH-GTS-21; 3) whether behavioral improvements are seen in the APP/PS1 mice following gene delivery; and 4) whether the amyloid plaques density could be reduced or prevented by the gene expression.

A novel way to test α7 receptors function is restore the α7 receptors back into the α7-knockout mouse hippocampus and septum. One important study would be to test whether restoring functional α7 receptors in the knockout mouse also restores the neuroprotective effects of 4OH-GTS-21 and this drug's effects on septal cholinergic neuron viability, and second messenger systems such as the ERK1/2, PHA and PKC pathways.

LIST OF REFERENCES

ADLER, L.E., OLINCY, A., WALDO, M., HARRIS, J.G., GRIFFITH, J., STEVENS, K., FLACH, K., NAGAMOTO, H., BICKFORD, P., LEONARD, S., and FREEDMAN, R. (1998). Schizophrenia, sensory gating, and nicotinic receptors. Schizophr. Bull. **24**, 189-202.

AKBARI, Y., HITT, B.D., MURPHY, M.P., DAGHER, N.N., TSENG, B.P., GREEN, K.N., GOLDE, T.E., and LAFERLA, F. (2004). Presenilin regulates capacitative calcium entry dependently and independently of gamma-secretase activity. Biochem. Biophys. Res. Commun. **322**, 1145-1152.

ALBUQUERQUE, E.X., ALKONDON, M., and PEREIRA, E.F.R. (1997). Properties of neuronal nicotinic acetylcholine receptors:pharmacological characterization and modulation of synaptic function. J. Pharmacol. Exp. Ther. **280**.

ALLSOP, D., TWYMAN, L.J., DAVIES, Y., MOORE, S., YORK, A., SWANSON, L., and SOUTAR, I. (2001). Modulation of beta-amyloid production and fibrillization. Biochem. Soc. Symp., 1-14.

ARENDASH, G.W., SENGSTOCK, G.J., SANBERG, P.R., and KEM, W.R. (1995). Improved learning and memory in aged rats with chronic administration of the nicotinic receptor agonist GTS-21. Brain Res. **674**, 252-259.

BAHI, A., BOYER, F., KAFRI, T., and DREYER, J.L. (2004). CD81-induced behavioural changes during chronic cocaine administration: in vivo gene delivery with regulatable lentivirus. Eur. J .Neurosci. **19**, 1621-1633.

BELL, K.A., O'RIORDAN, K.J., SWEATT, J.D., and DINELEY, K.T. (2004). MAPK recruitment by beta-amyloid in organotypic hippocampal slice cultures depends on physical state and exposure time. J. Neurochem. **91**, 349-361.

BERNS, K., and GIRAUD, C. (1996). Biology of adeno-associated virus. Curr. Top Microbiol. Immunol. **218**, 1-23.

BERRIDGE, M.J., LIPP, P., and BOOTMAN, M.D. (2000). The versatility and universality of calcium signalling. Nat. Rev. Mol. Cell Biol. **1**, 11-21.

BETTANY, J.H., and LEVIN, E.D. (2001). Ventral hippocampal alpha7 nicotinic receptor blockade and chronic nicotine effects on memory performance in the radial-arm maze. Pharmacol. Biochem. Behav. **70**, 467-474.

BICKLER, P.E., and FAHLMAN, C.S. (2004). Moderate increases in intracellular calcium activate neuroprotective signals in hippocampal neurons. Neuroscience **127**, 673-683.

BOUCHARD, R., PATTARINI, R., and GEIGER, J.D. (2003). Presence and functional significance of presynaptic ryanodine receptors. Prog. Neurobiol. **69**, 391-418.

BRIGGS, C.A., ANDERSON, D.J., BRIONI, J.D., BUCCAFUSCO, J.J., BUCKLEY, M.J., and AL., E. (1997). Functional characterization of the novel neuronal nicotinic acetylcholine receptor ligand GTS-21 in vitro and in vivo. Pharmacol. Biochem. Behav. **57**, 231-241.

BRONFMAN, F.C., MOECHARS, D., and VAN LEUVEN, F. (2000). Acetylcholinesterase-positive fiber deafferentation and cell shrinkage in the septohippocampal pathway of aged amyloid precursor protein london mutant transgenic mice. Neurobiol. Dis. **7**, 152-168.

BROWN, R.W., GONZALEZ, C.L., WHISHAW, I.Q., and KOLB, B. (2001). Nicotine improvement of Morris water task performance after fimbria-fornix lesion is blocked by mecamylamine. Behav. Brain. Res. **119**, 185-192.

COOPER, J.D., SALEHI, A., DELCROIX, J.D., HOWE, C.L., BELICHENKO, P.V., CHUA-COUZENS, J., KILBRIDGE, J.F., CARLSON, E.J., EPSTEIN, C.J., and MOBLEY, W.C. (2001). Failed retrograde transport of NGF in a mouse model of Down's syndrome: reversal of cholinergic neurodegenerative phenotypes following NGF infusion. Proc. Natl. Acad. Sci. USA **98**, 10439-10444.

DAJAS-BAILADOR, F., MOGG, A.J., and WONNACOTT, S. (2002a). Intracellular Ca^{2+} channels evoked by stimulation of nicotinic acetylcholine receptors in SH-SY5Y cells: contribution of voltage-operated Ca^{2+} channels and Ca^{2+} stores. J. Neurochem. **81**, 606-619.

DAJAS-BAILADOR, F.A., SOLIAKOV, L., and WONNACOTT, S. (2002b). Nicotine activates the extracellular signal regulated kinase 1/2 via the alpha7 nicotinic acetylcholine receptor and protein kinase A, in SH-SY5Y cells and hippocampal neurones. J. Neurochem. **80**, 520-530.

DAJAS-BAILADOR, F.A., SOLIAKOV, L., and WONNACOTT, S. (2002c). Nicotine activates the extracellular signal-regulated kinase 1/2 via the alpha7 nicotinic acetylcholine receptor and protein kinase A, in SH-SY5Y cells and hippocampal neurones. J. Neurochem. **80**, 520-530.

DE STROOPER, B., and ANNAERT, W. (2000). Proteolytic processing and cell biological functions of the amyloid precursor protein. J. Cell Sci. **113**, 1857-1870.

DONNELLY-ROBERTS, D.L., XUE, I.C., ARNERIC, S., and SULLIVAN, J. (1996). In vitro neuroprotective properties of the novel cholinergic channel activator (ChCA), ABT-418. Brain Res. **719**, 36-44.

EBERT, U., and KIRCH, W. (1998). Scopolamine model of dementia: electroencephalogram findings and cognitive performance. Eur. J. Clin. Invest. **28**.

EFTHIMIOPOULOS, S., VASSILACOPOULOU, D., RIPELLINO, J.A., TEZAPSIDIS, N., and ROBAKIS, N.K. (1996). Cholinergic agonists stimulate secretion of soluble full-length amyloid precursor protein in neuroendocrine cells. Proc. Natl. Acad. Sci. USA **93**, 8046-8050.

FAGNI, L., CHAVIS, P., ANGO, F., and BOCKAERT, J. (2000). Complex interactions between mGluRs, intracellular Ca^{2+} stores and ion channels in neurons. Trends Neurosci. **23**, 80-88.

GAFNI, J., MUNSCH, J.A., LAM, T.H., CATLIN, M.C., COSTA, L.G., MOLINSKI, T.F., and PESSAH, I.N. (1997). Xestospongins: potent membrane permeable blockers of the inositol 1,4,5-trisphosphate receptor. Neuron **19**, 723-733.

GUEORGUIEV, V.D., ZEMAN, R.J., HIREMAGALUR, B., MENEZES, A., and SABBAN, E.L. (1999). Differing temporal roles of Ca^{2+} and cAMP in nicotine-elicited elevation of tyrosine hydroxylase mRNA. Am. J. Physiol. **276**, C54-65.

GUEORGUIEV, V.D., ZEMAN, R.J., MEYER, E.M., and SABBAN, E., L. (2000). Involvement of alpha7 nicotinic acetylcholine receptors in activation of tyrosine hydroxylase and dopamine beta-hydroxylase gene expression in PC12 cells. J. Neurochem. **75**, 1997-2005.

HERNANDEZ, D., SUGAYA, K., QU, T., MCGOWAN, E., DUFF, K., and MCKINNEY, M. (2001). Survival and plasticity of basal forebrain cholinergic systems in mice transgenic for presenilin-1 and amyloid precursor protein mutant genes. Neuroreport **12**, 1377-1384.

HETMAN, M., and XIA, Z. (2000). Signaling pathways mediating anti-apoptotic action of neurotrophins. Acta. Neurobiol. Exp. (Wars) **60**, 531-545.

HOLCOMB, L., GORDON, M., MCGOWAN, E., YU , X., BENKOVIC, S., JANTZEN, P., WRIGHT, K., SAAD, I., MUELLER, R., MORGAN, D., SANDERS, S., ZEHR, C., O'CAMPO, K., HARDY, J., PRADA, C., ECKMAN, C., YOUNKIN, S., HSIAO, K., and DUFF, K. (1998). Accelerated Alzheimer-type phenotype in transgenic mice carrying both mutant amyloid precursor protein and presenilin 1 transgenes. Nat. Med. **4**, 97-100.

HSU, Y.L., KUO, P.L., LIN, L.T., and LIN, C.C. (2004). Asiatic acid, a triterpene, induces apoptosis and cell cycle arrest through activation of extracellular signal-regulated kinase and p38 mitogen-activated protein kinase pathways in human breast cancer cells. J. Pharmacol. Exp. Ther., Epub. ahead of print.

JOHNSTON, D., CHRISTIE, B., FRICK, A., GRAY, R., HOFFMAN, D., SCHEXNAYDER, L., WATANABE, S., and YUAN, L. (2003). Active

dendrites, potassium channels and synaptic plasticity. Philos. Trans. R. Soc. Lond B Biol. Sci.. **358**, 667-674.

JONASSON, Z., CAHILL, J.F., TOBEY, R.E., and BAXTER, M.G. (2004). Sexually dimorphic effects of hippocampal cholinergic deafferentation in rats. Eur. J. Neurosci. **20**, 3041-3053.

JONNALA, R.R., and BUCCAFUSCO, J.J. (2001). Relationship between the increased cell surface alpha7 nicotinic receptor expression and neuroprotection induced by several nicotinic receptor agonists. J. Neurosci. Res. **66**, 565-572.

KANG, D., YOON, I., REPETTO, E., BUSSE, T., YERMIAN, N., IE, L., and KOO, E. (2005). Presenilins mediate phosphatidylinositol 3-kinase/AKT and ERK activation via select signaling receptors. Selectivity of PS2 in platelet-derived growth factor signaling. J. Biol. Chem. **36**, 31537-31547.

KASA, P., RAKONCZAY, Z., and GULYA, K. (1997). The cholinergic system in Alzheimer's disease. Prog. Neurobiol. **52**, 511-535.

KEM, W.R. (2000). The brain alpha7 nicotinic receptor may be an important therapeutic target for the treatment of Alzheimer's disease: studies with DMXBA (GTS-21). Behav. Brain Res. **113**, 169-181.

KERWIN, J.M., MORRIS, C.M., PERRY, R.H., and PERRY, E.K. (1992). Hippocampal nerve growth factor receptor immunoreactivity in patients with Alzheimer's and Parkinson's disease. Neurosci. Lett. **143**, 101-104.

KIHARA, T., SHIMOHAMA, S., SAWADA, H., HONDA, K., NAKAMIZO, T., SHIBASAKI, H., KUME, T., and AKAIKE, A. (2001). alpha7 Nicotinic receptor transduces signals to phosphatidylinositol 3-kinase to block A beta-amyloid-induced neurotoxicity. J. Biol. Chem. **276**, 13541-13546.

KITAGAWA, H., TAKENOUCHI, T., AZUMA, R., WESNES, K.A., KRAMER, W.G., CLODY, D.E., and BURNETT, A.L. (2003). Safety, pharmacokinetics, and effects on cognitive function of multiple doses of GTS-21 in healthy, male volunteers. Neuropsychopharmacology **28**, 542-551.

KLEIN, R.L., HAMBY, M.E., GONG, Y., HIRKO, A.C., WANG, S., HUGHES, J.A., KING, M.A., and MEYER, E.M. (2002). Dose and promoter effects of adeno-associated viral vector for green fluorescent protein expression in the rat brain. Exp. Neurol. **176**, 66-74.

KOKOSKA, E., SMITH, G., WOLFF, A., DESHPANDE, Y., RIECKENBERG, C., BANAN, A., and MILLER, T. (1998). Role of calcium in adaptive cytoprotection and cell injury induced by deoxycholate in human gastic cells. Am J Physiol. **275**, G322-330.

KYOSSEVA, S.V. (2004). Mitogen-activated protein kinase signaling. Int. Rev. Neurobiol. **59**, 201-220.

LEOPOLD, P., FERRIS, B., GRINBERG, I., WORGALL, S., HACKETT, N., and CRYSTAL, R. (1998). Fluorescent virions: dynamic tracking of the pathway of adenoviral gene transfer vectors in living cells. Hum. Gene Ther. **9**, 367-378.

LI, Y., KING, M.A., GRIMES, J., SMITH, N., DE FIEBRE, C.M., and MEYER, E.M. (1999a). Alpha7 nicotinic receptor mediated protection against ethanol-induced cytotoxicity in PC12 cells. Brain Res. **816**, 225-228.

LI, Y., MEYER, E.M., WALKER, D.W., MILLARD, W.J., HE, Y.J., and KING, M.A. (2002). Alpha7 nicotinic receptor activation inhibits ethanol-induced mitochondrial dysfunction, cytochrome c release and neurotoxicity in primary rat hippocampal neuronal cultures. J. Neurochem. **81**, 853-858.

LI, Y., PAPKE, R.L., HE, Y., MILLARD, W., and MEYER, E.M. (1999b). Characterization of the neuroprotective and toxic effects of alpha7 nicotinic receptor activation in PC12 cells. Brain Res. **816**, 225-230.

LI, Y., PAPKE, R.L., MARTIN, E.J., HE, Y.-J., MILLARD, W.J., and MEYER, E.M. (1999c). Characterization of the neuroprotective and toxic effects of alpha7 nicotinic receptor activation in PC12 cells. Brain Res. **816**, 225-230.

LINKE, R., SCHWEGLER, H., and BOLDYREVA, M. (1994). Cholinergic and GABAergic septo-hippocampal projection neurons in mice: a retrograde tracing study combined with double immunocytochemistry for choline acetyltransferase and parvalbumin. Brain Res. **653**, 73-80.

LIU, Q., KAWAI, H., and BERG, D. (2001). beta -Amyloid peptide blocks the response of alpha 7-containing nicotinic receptors on hippocampal neurons. Proc. Natl. Acad. Sci. USA. **98**, 4734-4739.

LONDON, E.D., BALL, M.J., and WALLER, S.B. (1989). Nicotinic binding sites in cerebral cortex and hippocampus in Alzheimer's dementia. Neurochem. Res. **14**, 745-750.

MAJ, M., BRUNO, V., DRAGIC, Z., YAMAMOTO, R., BATTAGLIA, G., INDERBITZIN, W., STOEHR, N., STEIN, T., GASPARINI, F., VRANESIC, I., KUHN, R., NICOLETTI, F., and FLOR, P. (2003). (-)-PHCCC, a postive allosteric modulator of mGluR4: characterization, mechanism of action, and neuroprotection. Neuropharmacology **45**, 895-906.

MANN, D.M. (1991). The topographic distribution of brain atrophy in Alzeimer's disease. Acta. Neuropathol. **83**.

MCGOWAN, E., SANDERS, S., IWATSUBO, T., TAKEUCHI, A., SAIDO, T., ZEHR, C., YU, X., ULJON, S., WANG, R., MANN, D., DICKSON, D., and DUFF, K.

(1999). Amyloid phenotype characterization of transgenic mice overexpressing both mutant amyloid precursor protein and mutant presenilin 1 transgenes. Neurobiol. Dis. **6**, 231-244.

MCLAUGHLIN, S., COLLIS, P., HERMONAT, P., and MUZYCZKA, N. (1998). Adeno-associated virus general transduction vectors: analysis of proviral structures. J. Virol. **62**, 1963-1973.

MCNAMARA, R.K., and SKELTON, R.W. (1993). The neuropharmacological and neurochemical basis of place learning in the Morris water maze. Brain Res. Brain Res. Rev. **18**, 33-49.

MESULAM, M. (1995). Cholinergic pathways and the ascending reticular activating system of the human brain. Ann. NY. Acad. Sci. **757**, 169-179.

MEYER, E.M., KURYATOV, A., GERZANICH, V., LINDSTROM, J., and PAPKE, R.L. (1998a). Analysis of 3-(4-hydroxy, 2-Methoxybenzylidene)anabaseine selectivity and activity at human and rat alpha-7 nicotinic receptors. J. Pharmacol. Exp. Ther. **287**, 918-925.

MEYER, E.M., MEYERS, C., and KING, M.A. (1998b). The selective alpha7 nicotinic receptor agonist DMXB protects against neocortical neuron loss after nucleus basalis lesions. Brain Res. **786**, 152-154.

MEYER, E.M., TAY, E.T., PAPKE, R.L., MEYERS, C., HUANG, G., and DE FIEBRE, C. (1997). 3-[2,4-Dimethoxybenzylidene] anabaseine (DMXB) selectively activates rat alpha7 receptors and improvees memory-related behaviors in a mecamylamine-sensitive manner. Brain Res. **768**, 49-56.

MIAO, C., OHASHI, K., PATIJN, G., MEUSE, L., YE, X., THOMPSON, A., and KAY, M. (2000). Inclusion of the hepatic locus control region, an intron, and untranslated region increases and stabilizes hepatic factor IX gene expression in vivo but not in vitro. Mol. Ther. **1**, 522-532.

MORRIS, M. (2003). Homocysteine and Alzheimer's disease. Lancet. Neurol. **2**, 425-428.

MUZYCZKA, N., SAMBAMURTI, R.J., HERMONAT, P., SRIVASTAVA, A., and BERNS, K.I. (1984). The genetics of adeno-associated virus. Adv. Exp. Med. Biol. **179**, 151-161.

NORDBERG, A. (1994). Human nicotinic receptors--their role in aging and dementia. Neurochem. Int. **25**, 93-97.

NORDBERG, A., HELLSTROM-LINDAHL, E., LEE, M., JOHNSON, M., MOUSAVI, M., HALL, R., PERRY, E.K., BEDNAR, I., and COURT, J. (2002). Chronic nicotine treatment reduces beta-amyloidosis in the brain of a mouse model of Alzheimer's disease (APPsw). J. Neurochem. **81**, 655-658.

NORDBERG, A., and SVENSSON, A.L. (1998). Cholinesterase inhibitors in the treatment of Alzheimer's disease: a comparison of tolerability and pharmacology. Drug Saf. **19**, 465-480.

O'NEILL, M.J., MURRAY, T.K., LAKICS, V., VISABJI, N.P., and DUTY, S. (2002). The role of neuronal nicotinic acetylcholine receptors in acute and chronic neurodegeneration. Curr. Drug Target CNS Neurol. Disord. **4**, 399-411.

ORR-URTREGER, A., GOLDNER, F.M., SAEKI, M., LORENZO, I., GOLDBERG, L., DE BIASI, M., DANI, J.A., PATRICK, J.W., and BEAUDET, A.L. (1997). Mice deficient in the alpha7 neuronal nicotinic acetylcholine receptor lack alpha-bungarotoxin binding sites and hippocampal fast nicotinic currents. J. Neurosci. **17**, 9165-9171.

PAPKE, R.L., MEYER, E.M., NUTTER, T., and UTESHEV, V.V. (2000). Alpha7-selective agonists and models of alpha7 rreceptor activation. Eur. J. Pharmacol. **393**, 179-195.

PERRY, G., RODER, H., NUNOMURA, A., TAKEDA, A., FRIEDLICH, A., ZHU, X., RAINA, A., HOLBROOK, N., SIEDLAK, S., HARRIS, P., and SMITH, M. (1999). Activation of neuronal extracellular receptor kinase (ERK) in Alzheimer disease links oxidative stress to abnormal phosphorylation. Neuroreport **10**, 2411-2415.

ROBBINS, P.D., TAHARA, H., and GHIVIZZANI, S.C. (1998). Viral vectors for gene therapy. Trends Biotechnol. **16**, 35-40.

SALEHI, A., DELCROIX, J.D., and SWAAB, D.F. (2004). Alzheimer's disease and NGF signaling. J. Neural. Transm. **111**, 323-345.

SARTER, M., and BRUNO, J.P. (2002). The neglected constituent of the basal forebrain corticopetal projection system: GABAergic projections. Eur. J. Neurosci. **15**, 1867-1873.

SCOTT, S.A., MUFSON, E.J., WEINGARTNER, J.A., SKAU, K.A., and CRUTCHER, K.A. (1995). Nerve growth factor in Alzheimer's disease: increased levels throughout the brain coupled with declines in nucleus basalis. J. Neurosci. **15**, 6213-6221.

SEGUELA, P., WADICHE, J., DINELEY-MILLER, K., DANI, J.A., and PATRICK, J.W. (1993). Molecular cloning, functional properties, and distribution of rat brain alpha 7: a nicotinic cation channel highly permeable to calcium. J. Neurosci. **13**, 596-604.

SHIMOHAMA, S., GREENWALD, D.L., SHAFRON, D.H., AKAIKA, A., MAEDA, T., KANEKO, S., KIMURA, J., SIMPKINS, C.E., DAY, A.L., and MEYER, E.M. (1998). Nicotinic alpha 7 receptors protect against glutamate neurotoxicity and neuronal ischemic damage. Brain Res. **779**, 359-363.

SHIMOHAMA, S., and KIHARA, T. (2001). Nicotinic receptor-mediated protection against beta-amyloid neurotoxicity. Biol. Psychiatry. **49**, 233-239.

SHOOP, R.R., CHANG, K.T., ELLISMAN, M.H., and BERG, D.K. (2001). Synaptically driven calcium transients via nicotinic receptors on somatic spiness. J. Neurosci. **21**, 771-781.

SIMOSKY, J.K., STEVENS, K.E., KEM, W.R., and FREEDMAN, R. (2001). Intragastric DMXB-A, an alpha7 nicotinic agonist, improves deficient sensory inhibition in DBA/2 mice. Biol. Psychiatry. **50**, 493-500.

SOCCI, D.J., and ARENDASH, G.W. (1996). Chronic nicotine treatment prevents neuronal loss in neocortex resulting from nucleus basalis lesions in young adult and aged rats. Mo.l Chem. Neuropathol. **27**, 285-305.

SPERINDE, G., and NUGENT, M. (1998). Heparan sulfate proteoglycans control intracellular processing of bFGF in vascular smooth muscle cells. Biochemistry **37**, 13153-13164.

SUMMERFORD, C., BARTLETT, J., and SAMULSKI, R. (1999). AlphaVbeta5 integrin: a co-receptor for adeno-associated virus type 2 infection. Nat. Med. **5**, 78-82.

TAKAHASHI, T., YAMASHITA, H., NAKAMURA, S., ISHIGURO, H., NAGATSU, T., and KAWAKAMI, H. (1999). Effects of nerve growth factor and nicotine on the expression of nicotinic acetylcholine receptor subunits in PC12 cell. Neurosci Res. **35**, 175-181.

TALESA, V.N. (2001). Acetylcholinesterase in Alzeimer's disease. Mech. Aging Devel. **122**, 1961-1969.

TERRY, A.V., JR., and BUCCAFUSCO, J.J. (2003). The cholinergic hypothesis of age and Alzheimer's disease-related cognitive deficits: recent challenges and their implications for novel drug development. J. Pharmacol. Exp. Ther. **306**, 821-827.

TERRY, R.D., and KATZMAN, R. (1983). Senile dementia of the Alzheimer type. Ann. Neurol. **14**.

THINSCHMIDT, J., CJ, F., MA, K., EM, M., and RL, P. (2005). Septal innervation regulates the function of alpha7 nicotinic receptors in CA1 hippocampal interneurons. Exp. Neurol. **195**, 342-352.

TULLY, K., and TREISTMAN, S.N. (2004). Distinct intracellular calcium profiles following influx through N- versus L-type calcium channels: role of Ca^{2+}-induced Ca^{2+} release. J. Neurophysiol. **92**, 135-143.

UTSUKI, T., SHOAIB, M., HOLLOWAY, H., INGRAM, D., WALLACE, W., HAROUTUNIAN, V., SAMBAMURTI, K., LAHIRI, D., and GREIG, N. (2002).

Nicotine lowers the secretion of the Alzheimer's amyloid beta-protein precursor that contains amyloid beta-peptide in rat. J. Alzheimers Dis. **4**, 405-415.

VAUCHER, E., FLUIT, P., CHISHTI, M.A., WESTAWAY, D., MOUNT, H.T., and KAR, S. (2002). Object recognition memory and cholinergic parameters in mice expressing human presenilin 1 transgenes. Exp. Neurol. **175**, 398-406.

VIJAYARAGHAVAN, S., PUGH, P.C., ZHANG, Z.W., RATHOUZ, M.M., and BERG, D.K. (1992). Nicotinic receptors that bind alpha-bungarotoxin on neuerons raise intracellular free Ca^{2+}. Neuron **8**, 353-362.

VOLPICELLI, L.A., and LEVEY, A.I. (2004). Muscarinic acetylcholine receptor subtypes in cerebral cortex and hippocampus. Prog. Brain Res. **145**, 59-66.

W., X. (2001). Amyloid metabolism and secretases in Alzheimer's disease. Curr. Neurol. Neurosci. Rep. **1**, 422-427.

WARPMAN, U., and NORDBERG, A. (1995). Epibatidine and ABT 418 reveal selective losses of alpha 4 beta 2 nicotinic receptors in Alzheimer brains. Neurorepor. **6**, 2419-2423.

WONG, T.P., DEBEIR, T., DUFF, K., and CUELLO, A.C. (1999). Reorganization of cholinergic terminals in the cerebral cortex and hippocampus in transgenic mice carrying mutated presenilin-1 and amyloid precursor protein transgenes. J. Neurosci. **19**, 2706-2716.

WOODRUFF-PAK, D.S. (2003). Mecamylamine reversal by nicotine and by a partial alpha7 nicotinic acetylcholine receptor agonist (GTS-21) in rabbits tested with delay eyeblink classical conditioning. Behav. Brain Res. **143**, 159-167.

YAMAUCHI, T., KASHII, S., YASUYOSHI, H., ZHANG, S., HONDA, Y., and AKAIKE, A. (2003). Mitochondrial ATP-sensitive potassium channel: a novel site for neuroprotection. Invest Ophthalmol Vis Sci. **44**, 2750-2756.

YODER, R.M., and PANG, K.C. (2005). Involvement of GABAergic and cholinergic medial septal neurons in hippocampal theta rhythm. Hippocampus **15**, 381-392.

ZOLOTUKHIN, S., BYRNE, B.J., MASON, E., ZOLOTUKHIN, I., POTTER, M., CHESNUT, K., SUMMERFORD, C., SAMULSKI, R.J., and MUZYCZKA, N. (1999). Recombinant adeno-associated virus purification using novel methods improves infectious titer and yield. Gene Ther. **6**, 973-985.

BIOGRAPHICAL SKETCH

Ms. Ke Ren received her Doctor of Medicine at Zunyi Medical University in July 1994. And later Ke became a clinical doctor/researcher in ophthalmology in Guiyang Medical School Hospital for four years. Ke then joined the graduate program in the Department of Pharmaceutics, College of Pharmacy, University of Florida, Gainesville, Florida, in Jan. 2002. She finished her Ph.D. in pharmaceutics in Dec. 2004 under supervision of Dr. Jeffery Hughes.